GEOLOGY AND MINERALISATION OF THE WHITE DEVIL DEPOSIT, TENNANT CREEK, NORTHERN TERRITORY. AUSTRALIA

BY

Gregory J. Cozens BSc Hons

This thesis is submitted as a partial fulfilment of the requirement for Master of Economic Geology at the University of Tasmania Centre for Ore Deposit and Exploration Studies, Hobart, Tasmania, Australia.

July 1992

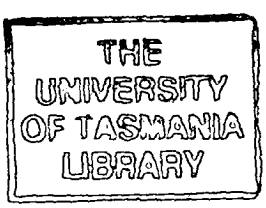

CONTENTS

		Page
	ABSTRACT	
	ACKNOWLEDGEMENTS	
1.	**INTRODUCTION**	1
2.	**REGIONAL GEOLOGY**	2
3.	**DEPOSIT GEOLOGY**	4
4.	**IRONSTONES**	8
	4.1 DESCRIPTION OF IRONSTONES	8
	4.2 IRONSTONE TEXTURE AND MINERALOGY	11
	4.2.1 Northern, Lensoidal Ironstone	11
	4.2.2 Other minerals in the Ironstone	14
	4.2.3 Southern Tabular Ironstone	16
	4.2.4 Stringer Zone	17
	4.3 SUMMARY	18
5.	**OREBODIES**	19
	5.1 MAIN ZONE	19
	5.2 DEEPS OREBODY	20
	5.3 OTHER MINERALISATION	23
	5.4 SUMMARY	25
	5.5 CONTROLS ON MINERALISATION	26
	5.6 METAL ZONATION	28
	5.6.1 Main Zone Metal Distribution	30

Page

6. CHLORITE 32

6.1 INTRODUCTION 32

6.2 PETROGRAPHY 33

6.3 MICROPROBE STUDY 37

7. PARAGENESIS AND MODEL 48

7.1 IRONSTONE FORMATION 48

7.2 MINERALISING STAGE 49

8. EXPLORATION IMPLICATIONS 52

9. CONCLUSIONS AND SUMMARY 53

10. REFERENCES 54

APPENDIX 1

FIGURES

FIGURE 1: Location Map

FIGURE 2: Regional Geology

FIGURE 3: White Devil Surface Geology and Long Section

FIGURE 4: Geological Cross Sections

FIGURE 5: Geological Level Plans. In pocket at rear.

FIGURE 6: Morphology of the Ironstones

FIGURE 7: fO2 - pH Diagram for Deposit Model

FIGURE 8: Gold-Bismuth-Copper Distribution across Deposit

FIGURE 9: Metal Distribution within Main Zone Orebody

FIGURE 10a: Plots of showing relationships between Si, Al, Mg and Fe

FIGURE 10b: Hay diagram showing composition of the chlorites analysed

FIGURE 11: Detailed Fe vs Mg plot of the chlorite analyses

FIGURE 12: Si, Al, Mg and Fe plot showing variations in composition of chlorite within and beside a vein

FIGURE 13: Plots of Temperature vs Si, Al, Fe and Mg.

FIGURE 14: Detailed Al(iv) vs T ^{o}C plot showing distribution of different chlorites

FIGURE 15: Cross sections showing distribution of Fe/Mg ratio within the deposit

PLATES

PLATE 1: Eastern end of outcropping hematite-quartz-magnetite ironstone.

PLATE 2: Eastern end of outcropping ironstone, showing fracture pattern.

PLATE 3: Core from Pinter Ironstone showing "birdsfoot" and "globular" magnetite in quartz and minor pyrite.

PLATE 4: Magnetite laths within quartz.

PLATE 5: Magnetite laths etched with HBr acid.

PLATE 6: Close up of large lath in Plate 4. HBr acid etching has highlighted the different magnetite grains and also the `clean' primary magnetite which grew into cavities during and following the replacement process.

PLATE 7: Dendritic magnetite growth within talc.

PLATE 8a: Open magnetite lath texture within Deeps ironstone.

PLATE 8b: Spherulitic magnetite growth, replaced hematite, surrounded by chlorite.

PLATE 8c: Skeletal/spongy texture of the Deeps ironstone. The replacement process has retained the primary hematite texture.

PLATE 9: Magnetite chlorite-altered sediment rock. Clasts of mildly chloritic sediments are surrounded by magnetite stringers in chlorite.

PLATE 10a: Selective martitisation of magnetite. Replacement of single grains around cavities and edge of lath.

PLATE 10b: Martitisation along grain boundaries. The alteration highlights the irregular magnetite grains forming the lath.

PLATE 10c: Approaching complete martitisation of magnetite and the growth of hematite laths within a cavity.

PLATE 11: Pyrite, fractured, intergrown with magnetite and quartz.

PLATE 12: Remnant chlorite within magnetite-quartz of the Pinter ironstone. The chlorite occurs along the boundaries of several quartz grains and appears to have been replaced by the quartz.

PLATE 13a: Coarse grained chlorite infilling the gaps between magnetite in magnetite chlorite rock.

PLATE 13b: Magnetite lath within coarse grained chlorite. The chlorite also occurs within the lath.

PLATE 14a: Magnetite-talc-chlorite rock.

PLATE 14b: Coarse grained chlorite being altered to talc, with the talc retaining the chlorite texture.

PLATE 14c: Chlorite completely altered to talc. The talc still retains the coarse chlorite texture.

PLATE 15: Fractured magnetite stringer within fine grained chloritic sediment.

PLATE 16: Open space quartz and chlorite growth within fractured magnetite stringer in magnetite chlorite-altered sediment rock within the Deeps ore zone.

PLATE 17: Fractured magnetite stringer within fine grained chloritic altered sediment. The fractures have been filled with coarse grained unfoliated chlorite.

PLATE 18a: Gold grain within magnetite lath in Lower Main Zone orebody.

PLATE 18b: Gold and bismuth sulphosalt grains within coarse grained chlorite in Main Zone orebody.

PLATE 19a: Gold grains in magnetite and coarse grained chlorite in Deeps orebody (north lens).

PLATE 19b: Gold filling vug and fracture in magnetite lath, south lens Deeps orebody.

PLATE 20a: Gold and bismuthinite within skeletal magnetite in Deeps orebody.

PLATE 20b: Intergrowth of gold and bismuth sulphosalt with magnetite and chlorite in north lens of Deep orebody.

PLATE 20c: Intergrowth of gold, bismuthinite, chalcopyrite and pyrite, from Deeps orebody.

PLATE 21a: Intergrowth of chalcopyrite and bismuthinite in magnetite adjacent to Deeps orebody.

PLATE 21b: Bismuth sulphosalt and chalcopyrite within "sigmoidal" tension cracks in magnetite.

PLATE 21c: Myrmekitic intergrowth of bismuthinite and emplectite.

PLATE 22: Skeletal pyrite intergrown with chalcopyrite and overgrown on magnetite, adjacent to Deeps orebody.

PLATE 23: Chalcopyrite with rim of chalcocite and bornite.

PLATE 24: Colour differences, under normal light, between the early and late chlorites.

PLATE 25: Partial alteration of chlorite to talc in Pinter Ironstone.

PLATE 26: Coarse grained chlorite amongst magnetite adjacent to fine grained altered sediment.

PLATE 27: Subhedral primary magnetite grains in coarse chlorite, grading to finer chlorite.

PLATE 28: Chloritic sediment and coarse chlorite vein.

PLATE 29a: Start of ironstone. Single and interlocking laths within altered sediments. The original hematite grew within the sediments and was later altered to magnetite.

PLATE 29b: Skeletal/spongy texture developed in interlocking laths within altered sediments

PLATE 29c: Skeletal/spongy ironstone with similar textures to the larger ironstones. The ironstone retains a very high porosity.

APPENDICES

APPENDIX 1: Microprobe analyses of chlorite, talc, biotite and sample descriptions.

ABSTRACT

Investigations into the textures in the ironstones, relationships between Au-Bi-Cu mineralisation and associated chlorite, metal zonation and distribution and paragenesis have been made on the White Devil Deposit in the Proterozoic Tennant Creek district of the Northern Territory. The textures within the ironstone revealed that they consist of intergrown and interlocking masses of magnetite laths pseudomorphed after hematite. The consistent textures and overgrowth of primary magnetite on the laths and in fractures indicates the ironstones existed in entirety and were deformed prior to magnetite alteration. The open porous lath texture of the ironstones has implications for ore deposition.

The mineralising stage was accompanied by the deposition of chlorite. The gold, bismuth sulphosalts and chalcopyrite are intergrown with coarse grained chlorite in the spaces between the magnetite laths and around magnetite stringers.

The chlorite associated with ore and altered sediments ranges from low temperature green Mg-rich pycnochlorite to high temperature blue Fe-rich ripidolite. Geothermometry has shown that the chlorite has a temperature range from 230 to 330^{o}C. Talc alteration of Mg chlorite occurred during the waning stage of the hydrothermal event.

The metal zonation within the deposit is not clear, even within the orebodies studied.

The initial hematite ironstone formed in chloritic sediments within the shear. The fluids became more reduced and interacted with the hematite, altering it to magnetite. The mineralising stage saw the introduction of higher temperature fluids which interacted with the magnetite causing the deposition of gold and chlorite followed by bismuth and copper with associated chlorite at higher temperatures. As the fluids cooled, alteration of Mg chlorite to talc, martitisation and quartz flooding of the Pinter Ironstone occurred.

ACKNOWLEDGEMENTS

I wish to acknowledge the support and financial assistance of Poseidon Gold and Poseidon Exploration throughout the course and in the preparation of the thesis.

I wish to thank my supervisor, Dr David Huston, for his assistance, encouragement and discussions throughout the project. I would like to acknowledge the following people: Simon Booth for editing drafts of chapters and stimulating discussions, Cathy Hooper and Paul Hunter at White Devil for assistance with information, Wayne Parsons for drafting the figures and all those who have assisted me along the way. Finally, to my wife, Heather, to whom I am especially thankful, for support and encouragement.

1 INTRODUCTION

The White Devil Gold Mine is located in the Tennant Creek Mineral Field, approximately 40 km northwest of Tennant Creek Township (Figure 1).

The gold-bismuth-copper mineralisation is intimately associated with and occurs in magnetite-chlorite-hematite-quartz ironstones and magnetite stringers within a highly chloritic shear zone.

The aim of this project is to study the geology and mineralisation at White Devil, focussing on the

- textures and mineralogy of the ironstones to determine their paragenesis,
- mineralisation and host rocks to the orebodies,
- controls on the mineralisation and metal zonation within the orebodies,
- chlorite composition and relationship to mineralisation.

The study also aims to develop a paragenetic model for the ironstones, mineralisation and chlorite and determine criteria which have implications for exploration.

The deposit contains features different from other Tennant Creek style deposits, in that it is hosted within a shear zone and contains two styles of mineralisation.

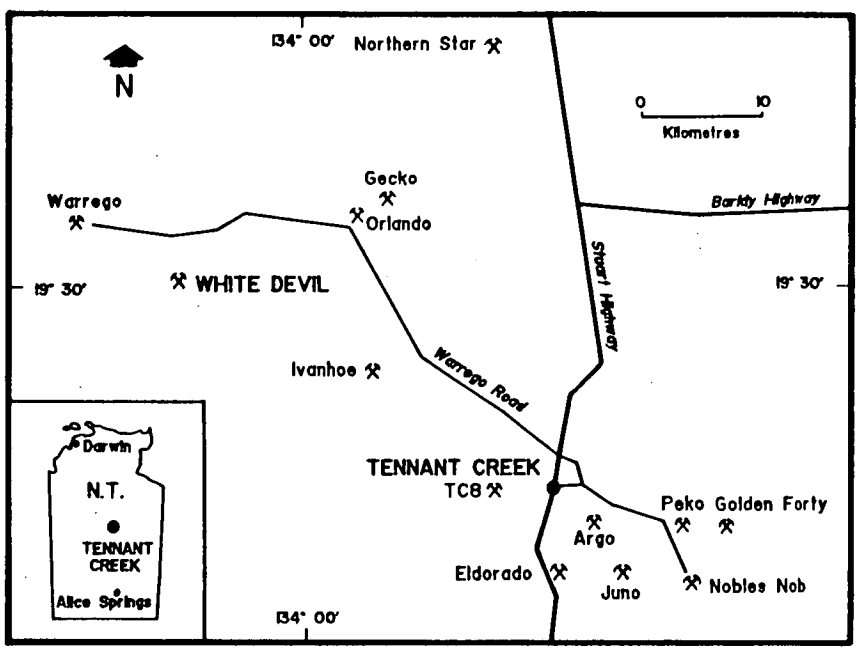

Locality map, White Devil Mine

Figure 1

2 REGIONAL GEOLOGY

The gold-bismuth-copper mineralisation in the Tennant Creek mineral field is hosted by the Lower Proterozoic Warramunga Group, which occupies an area of approximately 2000 sq km, Figure 2. To the north the Warramunga Group is bounded by the overlying arenites of the Tomkinson Creek beds and to the south by the Hatches Creek Group (Williams 1987, Le Messurier et al. 1990).

The Warramunga Group consists of dominantly felsic volcanic derived turbiditic shales, siltstone and greywacke, minor BIF lenses and hematite shales and stratiform porphyry bodies, which Large (1975) termed the Carraman Formation. The Warramunga Group also includes tuffaceous acid volcanics of the Bernborough Formation (Le Messurier et al 1990) and the shallow water siliclastic Whippet Sandstone. A maximun thickness of 6000m is indicated (Le Messurier et al 1990).

Quartz feldspar porphyries within the sequence have been interpreted as sills intruding poorly consolidated wet sediments and inferred to be comagmatic with the Tennant Creek Granite (McPhie in prep).

The Tennant Creek Granite is a 1870+\- 20 Ma old magnetite series granite (Black 1974) which intruded into the centre of the field. The Warrego Granite (1660+\- 20Ma) and Red Bluff Granite (1640+\- 50Ma) are ilmenite series batholiths intruded into the western portion of the field (Black 1984). The Red Bluff Granite is located 3 to 5 km south of the White Devil deposit. The age dating of the Tennant Creek rocks is currently being re-evaluated by D. Compston (PhD project, ANU).

Within the Carraman Formation an iron-rich magnetic unit has been defined as the Black Eye Member (Magnetite Facies, Large 1975) using aerial magnetic imagery. The member contains all the hematite shales, most of the porphyries and all of the ironstone-hosted mineralisation (Le Messurier et al, 1990).

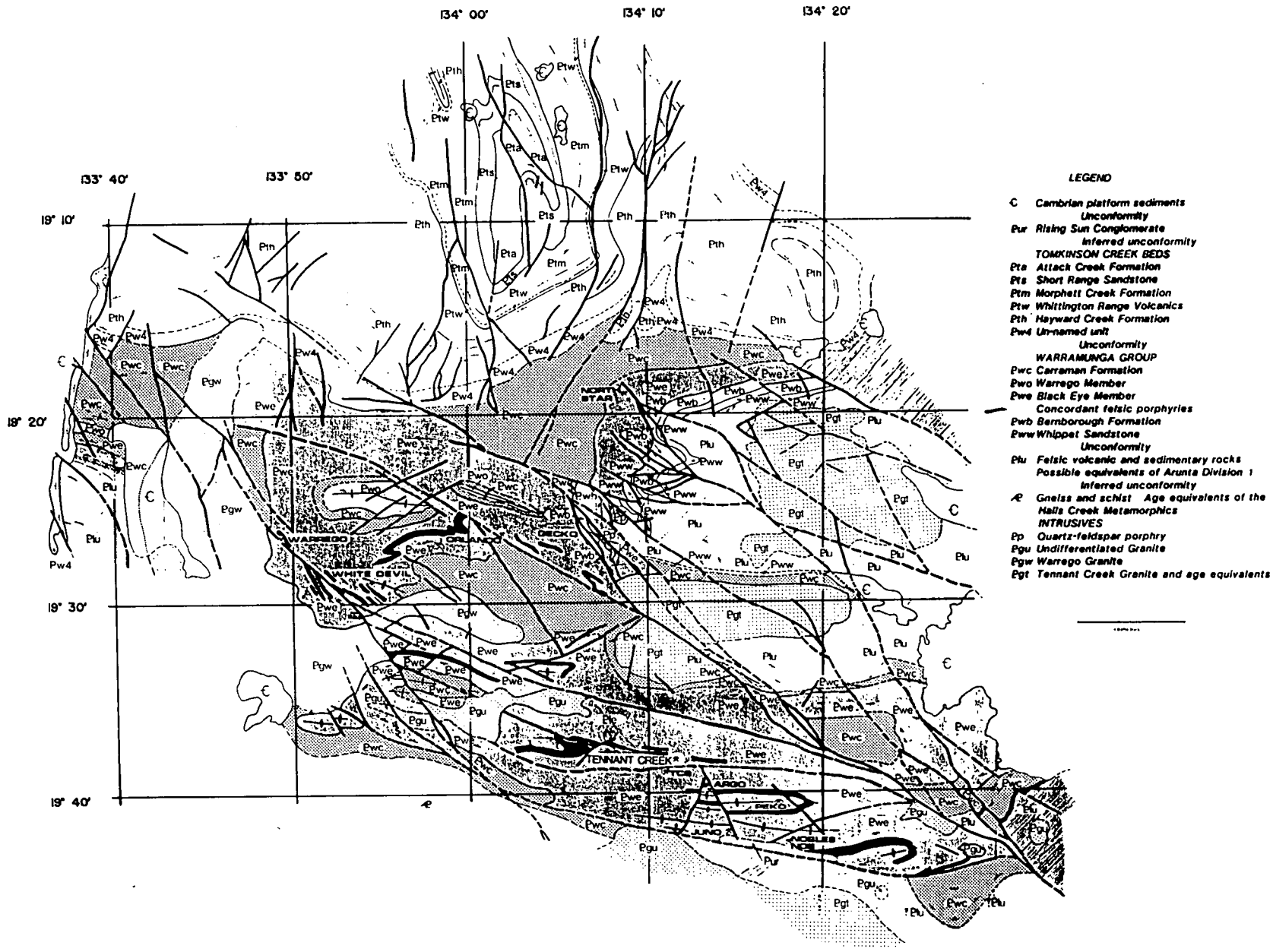

Figure 2 — Regional Geology
(LeMessurier et al 1990)

The Warramunga Group underwent major E-W folding and lower greenschist facies metamorphism which produced a strong slatey cleavage. Rattenbury (1990a) proposed a fold-thrust model for the deformation, with anticlinal structures propogated from the blind thrust tips. Several major E to ESE trending shear zones occur in the field (eg Mary Lane Shear), which are interpreted to be the surface expressions of the thrusts. The magnetite-quartz-hematite bodies (ironstones) are localised within or near the hinge zones of the anticlinal structures.

The gold-copper-bismuth mineralisation is associated with these ironstone bodies and their envelope of chlorite alteration. The field is characterised by relatively small, but very high grade deposits such as Nobles Nob - 1 mt @ 19.7 g/t Au, Juno - 0.45mt @ 57 g/t Au (Large 1975) and Warrego - 5mt @ 7 g/t Au, 2.6% Cu and 0.3% Bi (Wedekind & Love 1990).

3 DEPOSIT GEOLOGY.

The White Devil deposit consists of several Au-Bi-Cu orebodies within a highly chloritic shear zone (D2) developed near the hinge of an east-west anticline (D1). The deposit is cut by three quartz-feldspar porphyry dykes which have divided the deposit into three segments, from west to east: West Lodes, Main Zone/ East Lodes and Pinter Lodes (Figure 3).

Stratigraphy

White Devil is hosted by greywacke, siltstone and sandstone of the Carraman Formation (Large 1975) of the Warramunga Group sediments. Bedding thickness varies from a fine parallel lamination in shale (1 to 5 mm), to thick, massive beds in sandstone and greywacke (0.5 to 3m). Primary sedimentary structures are well developed in both weathered outcrop and fresh rocks and include graded bedding, cross bedding, soft sediment slump structures, load casts and cross laminations, consistent with the waning flow regime of a turbidity current (Edwards et al 1990).

Structure

The White Devil deposit is located within a shear zone that strikes 070^{o} which was developed during the regional deformation (D1) and remained active during the second phase of deformation (D2).

The initial deformation, D1, produced the regional E - W folds and axial plane slatey cleavage, S1, striking between 060^{o} and 080^{o} and dipping between 70^{o} south and vertical (Edwards et al 1990, Nguyen et al 1989).

The second progressive deformation (shearing) produced a discrete schistosity trending from 050^{o} to 100^{o}, which dips vertically to steeply north or south. The shearing produced a slickenside fibre lineation plunging between 30^{o} west and vertical (Nguyen et al 1989). Underground mapping and drill core examination indicate a vertical - oblique displacement on the shear with north block westwardly downthrown and the south block eastwardly upthrown, giving rise to the wide dilation zone between

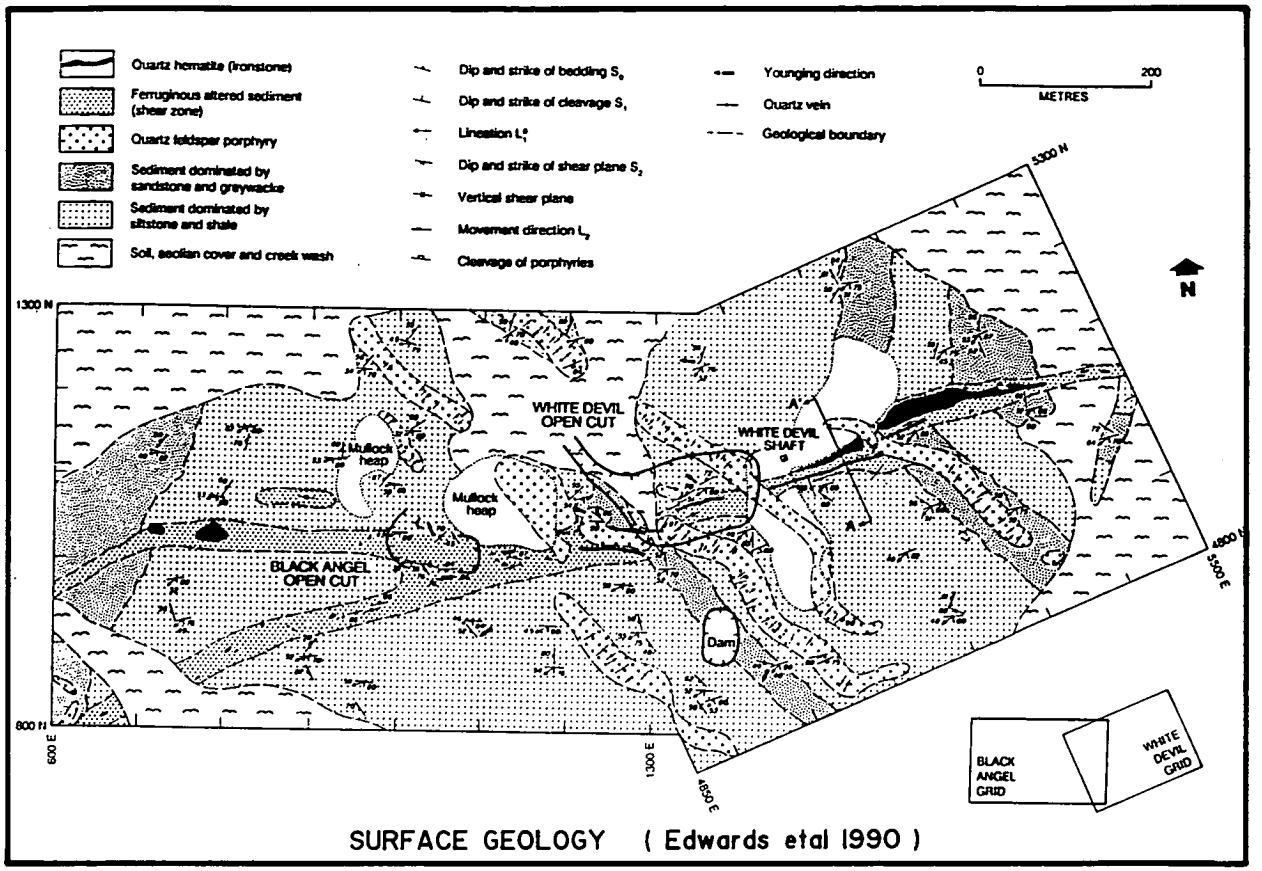

SURFACE GEOLOGY (Edwards etal 1990)

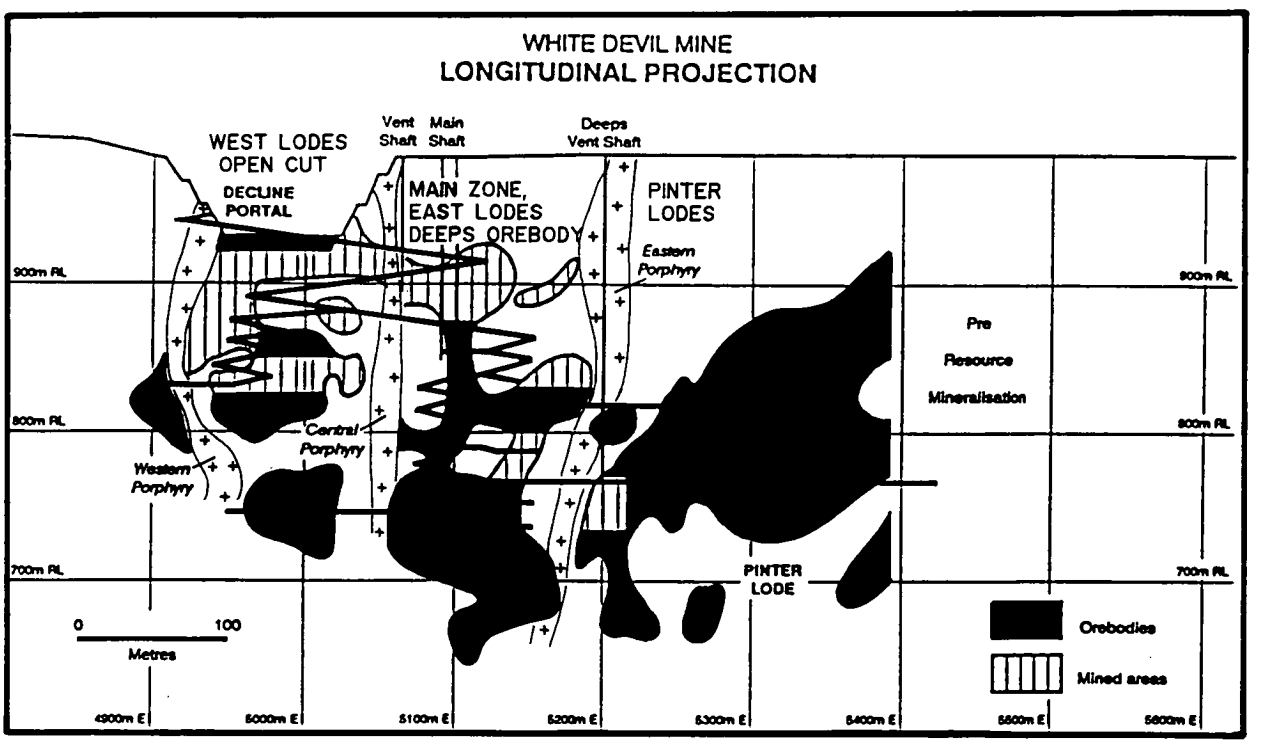

Figure 3 - SURFACE GEOLOGY & LONG SECTION

5050N and 5100N (Nguyen et al 1989; Hy 1988). Recent work by P. Hunter, Mine Geologist (pers comm) has confirmed the earlier work of Nguyen et al (1989) and Hy (1988) that the White Devil deposit formed in the dilational part, primary riedel, of the shear zone. The change in orientation of the shear both east and west of the deposit confirms this, Figure 3. Further evidence of this is that at the Black Angel and Crusader prospects to the West of the deposit, only small magnetite stringers have been observed within a narrow, 1 - 2m chlorite shear zone.

The cross sections in Figure 4 and level plans in Figure 5(pocket), show the geology of the deposit and the location of the orebodies.

Ironstones consisting of magnetite, quartz, lesser chlorite and hematite occur as subvertical lensoidal or tabular bodies that are oriented parallel to the shear and crosscut the stratigraphy.

A thin tabular ironstone marks the southern edge of the shear and the intense chlorite alteration, and occurs along the length of the deposit, unless disrupted by the porphyries. In the upper West Lodes, 830RL and above the tabular ironstone thickens to between 5 and 10 m.

A larger more massive ironstone occurs in the eastern portion of the deposit and marks the northern extent of the shear zone. The large ironstone plunges steeply west and quickly tapers off approaching the central porphyry. Minor faults displace the ironstone east of the Eastern Porphyry.

Both the tabular and large ironstone contain a set of north dipping, east-west striking reverse faults. The faults dip at approximately 30^{o} and have displacements up to 30 cm and the fault surfaces are highly polished. The ironstones also contain tension gashes filled with quartz, chlorite and sulphides.

Between the two ironstones, in the middle of the shear, are zones of highly chloritically altered sediments with magnetite stringers, that are typically 20mm wide, 150mm long and orientated parallel to cleavage. The stringer ironstones acted as rigid bodies within the shear and were deformed brittly, with extension fractures developing

WHITE DEVIL MINE

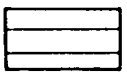

Massive magnetite ± hematite & chlorite
- C – Magnetite chlorite
- T – Magnetite talc
- AS – Magnetite + highly chloritic altered sediment

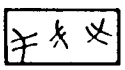

Stringer magnetite in highly chloritic sediment

Highly chloritic sediment
- T + Talc

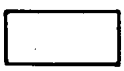

Unaltered or slightly chloritic sediment

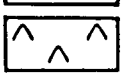

Quartz feldspar porphyry

Orebody

POSEIDON GOLD LIMITED

KEY TO FIGURE 4

Compiled by G.J.COZENS - May, 1992

SECTION 4945E

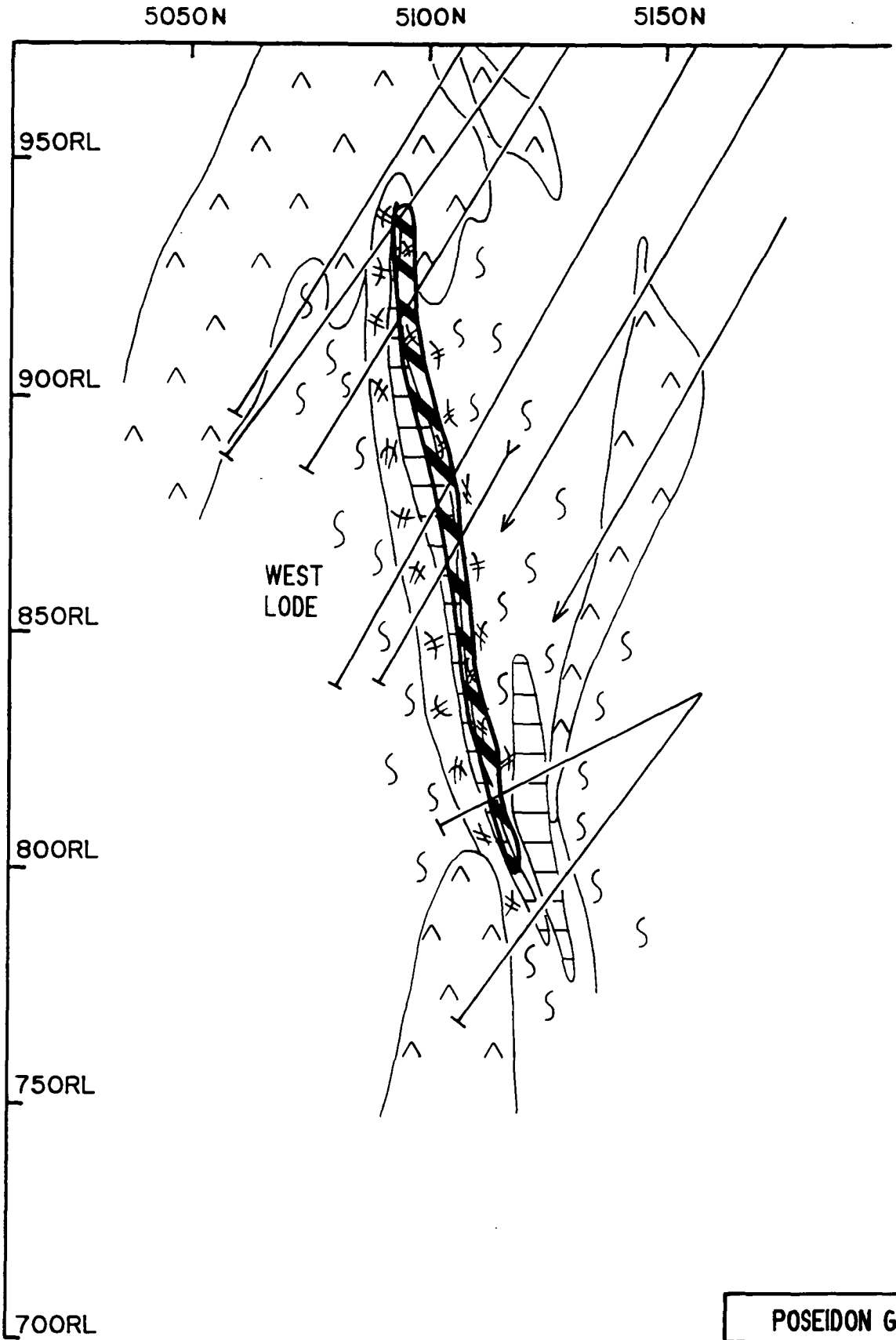

POSEIDON GOLD LIMITED

WHITE DEVIL MINE
TENNANT CREEK - N.T.
SECTION 4945E

Compiled by G.J.COZENS - April, 1992
Drawn by W.S.P. - Scale 1 : 1250

Figure 4 (i)

WHITE DEVIL MINE

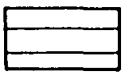

Massive magnetite ± hematite & chlorite
- C – Magnetite chlorite
- T – Magnetite talc
- AS – Magnetite + highly chloritic altered sediment

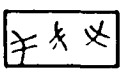

Stringer magnetite in highly chloritic sediment

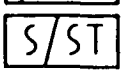

Highly chloritic sediment
T + Talc

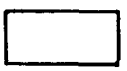

Unaltered or slightly chloritic sediment

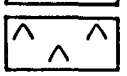

Quartz feldspar porphyry

Orebody

POSEIDON GOLD LIMITED
KEY TO FIGURE 4
Compiled by G.J.COZENS - May, 1992

SECTION 4995E

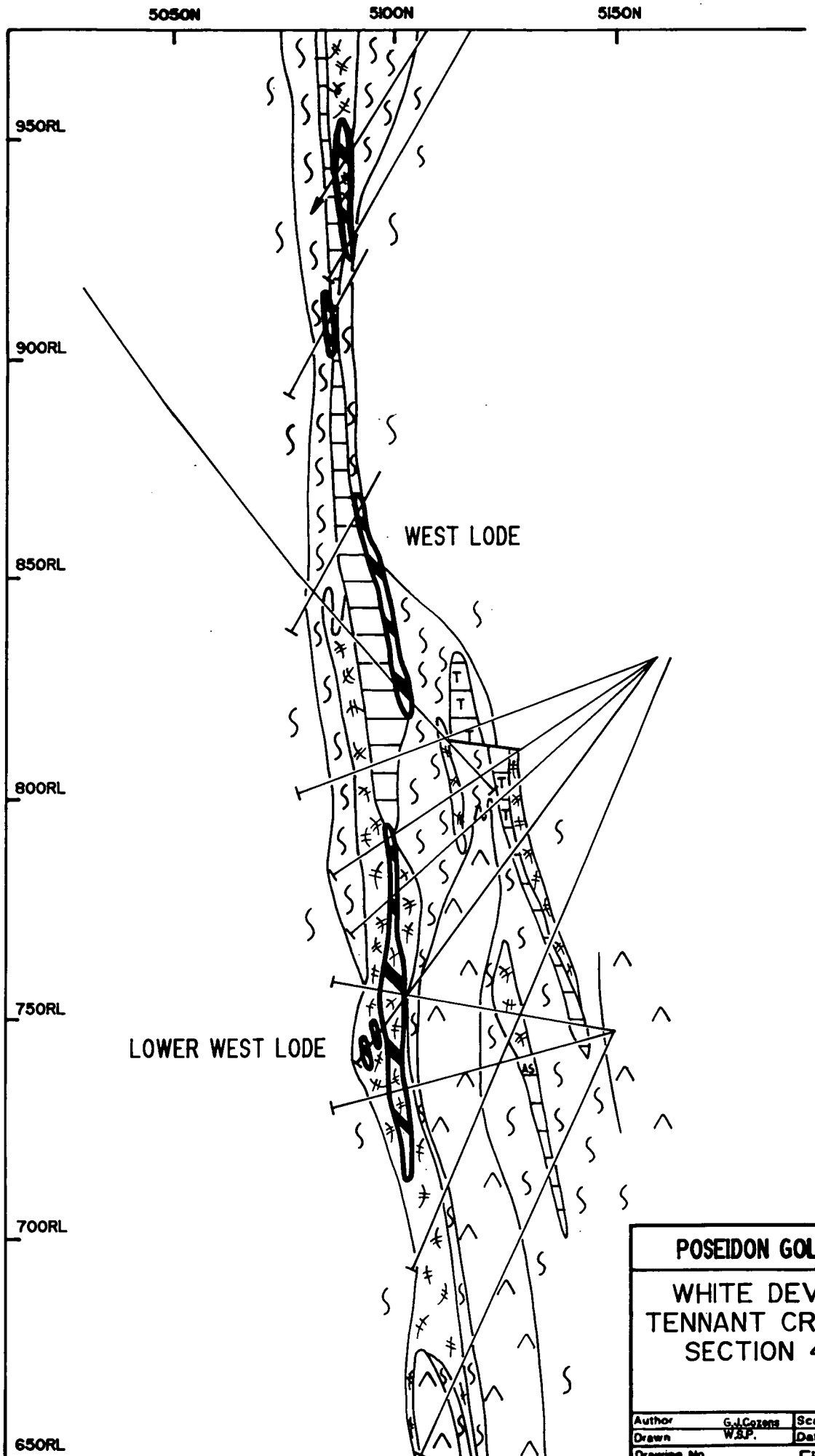

POSEIDON GOLD LIMITED

WHITE DEVIL MINE
TENNANT CREEK - N.T.
SECTION 4995E

Author	G.J.Cozens	Scale	1 : 1250
Drawn	W.S.P.	Date	Feb. 1992
Drawing No			Figure 4 (ii)

WHITE DEVIL MINE

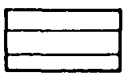

Massive magnetite ± hematite & chlorite
- C – Magnetite chlorite
- T – Magnetite talc
- AS – Magnetite + highly chloritic altered sediment

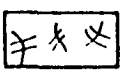

Stringer magnetite in highly chloritic sediment

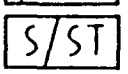

Highly chloritic sediment
T + Talc

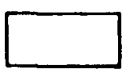

Unaltered or slightly chloritic sediment

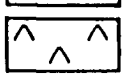

Quartz feldspar porphyry

Orebody

POSEIDON GOLD LIMITED

KEY TO FIGURE 4

Compiled by G.J.COZENS - May, 1992

SECTION 5095E

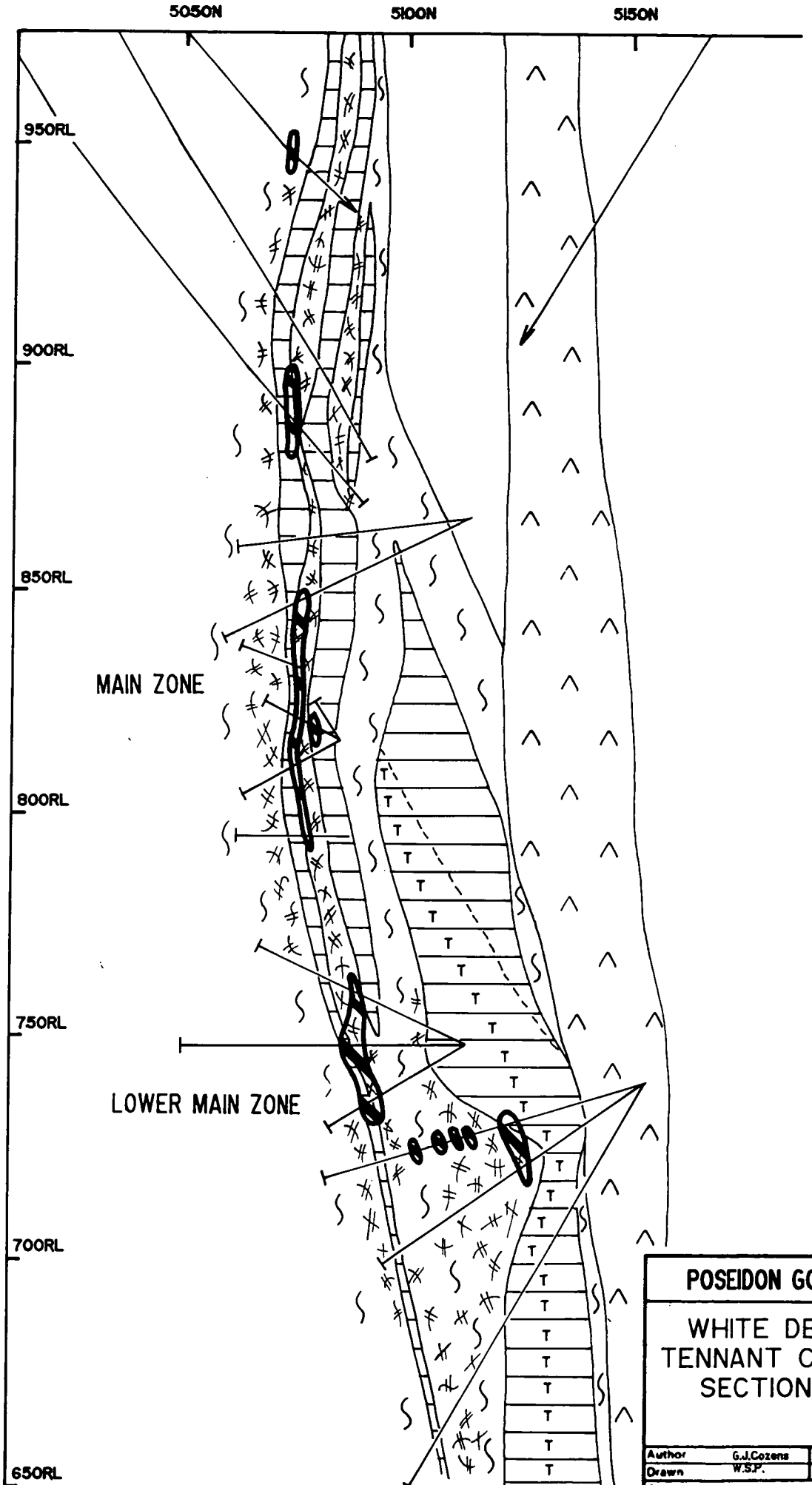

POSEIDON GOLD LIMITED

WHITE DEVIL MINE
TENNANT CREEK - N.T.
SECTION 5095E

Author	G.J.Cozens	Scale	1 : 1250
Drawn	W.S.P.	Date	Feb. 1992
Drawing No			

Figure 4 (iii)

WHITE DEVIL MINE

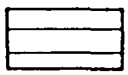

Massive magnetite ± hematite & chlorite
- C – Magnetite chlorite
- T – Magnetite talc
- AS – Magnetite + highly chloritic altered sediment

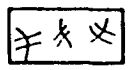

Stringer magnetite in highly chloritic sediment

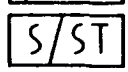

Highly chloritic sediment
- T + Talc

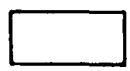

Unaltered or slightly chloritic sediment

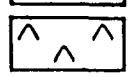

Quartz feldspar porphyry

Orebody

POSEIDON GOLD LIMITED

KEY TO FIGURE 4

Compiled by G.J.COZENS - May, 1992

SECTION 5135E

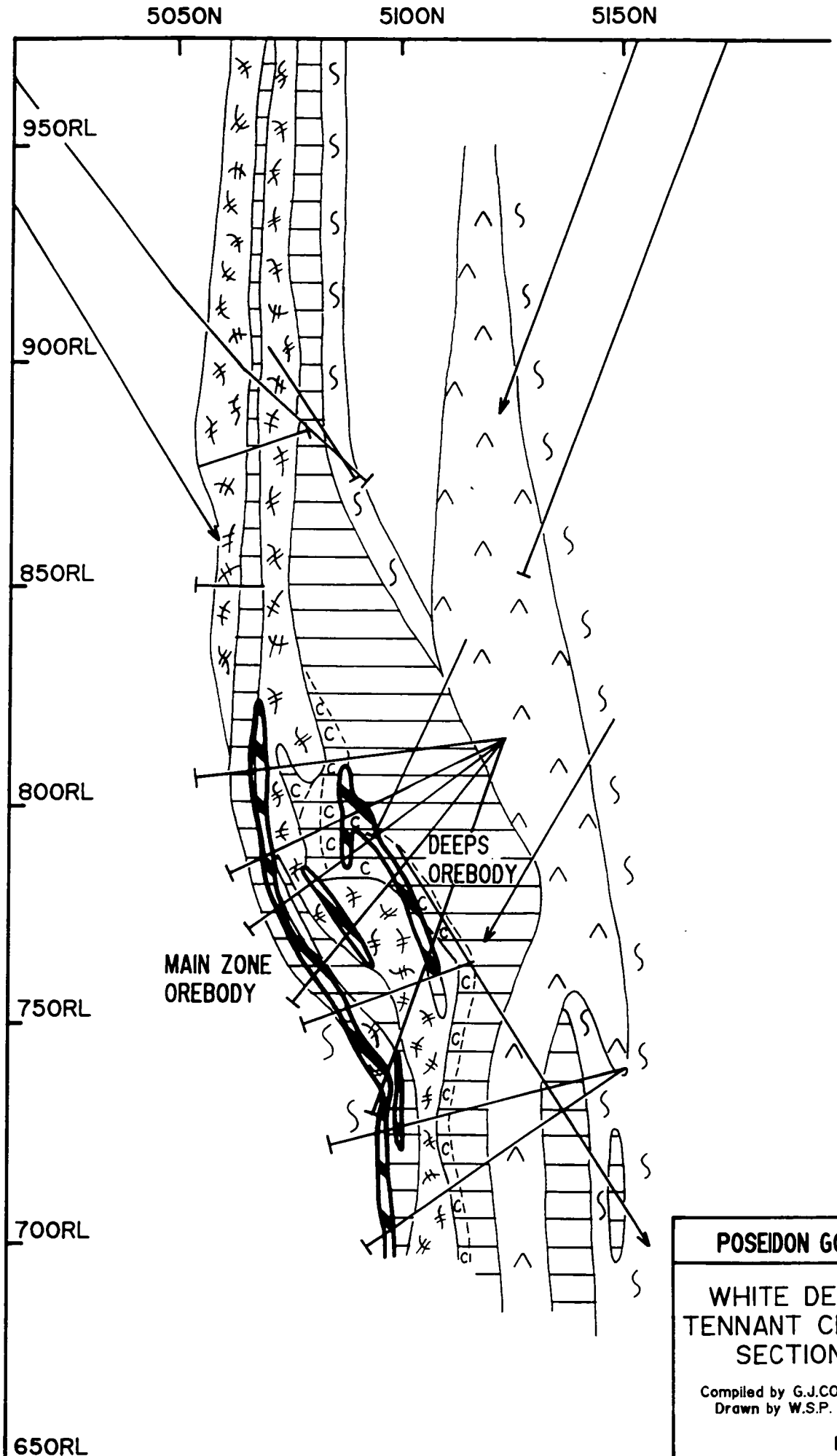

POSEIDON GOLD LIMITED

WHITE DEVIL MINE
TENNANT CREEK - N.T.
SECTION 5135E

Compiled by G.J.COZENS - April, 1992
Drawn by W.S.P. - Scale 1 : 1250

Figure 4 (iv)

WHITE DEVIL MINE

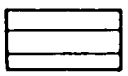

Massive magnetite ± hematite & chlorite
- C – Magnetite chlorite
- T – Magnetite talc
- AS – Magnetite + highly chloritic altered sediment

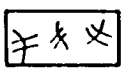

Stringer magnetite in highly chloritic sediment

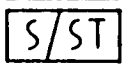

Highly chloritic sediment
- T + Talc

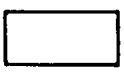

Unaltered or slightly chloritic sediment

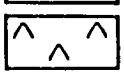

Quartz feldspar porphyry

Orebody

POSEIDON GOLD LIMITED

KEY TO FIGURE 4

Compiled by G.J.COZENS - May, 1992

SECTION 5155E

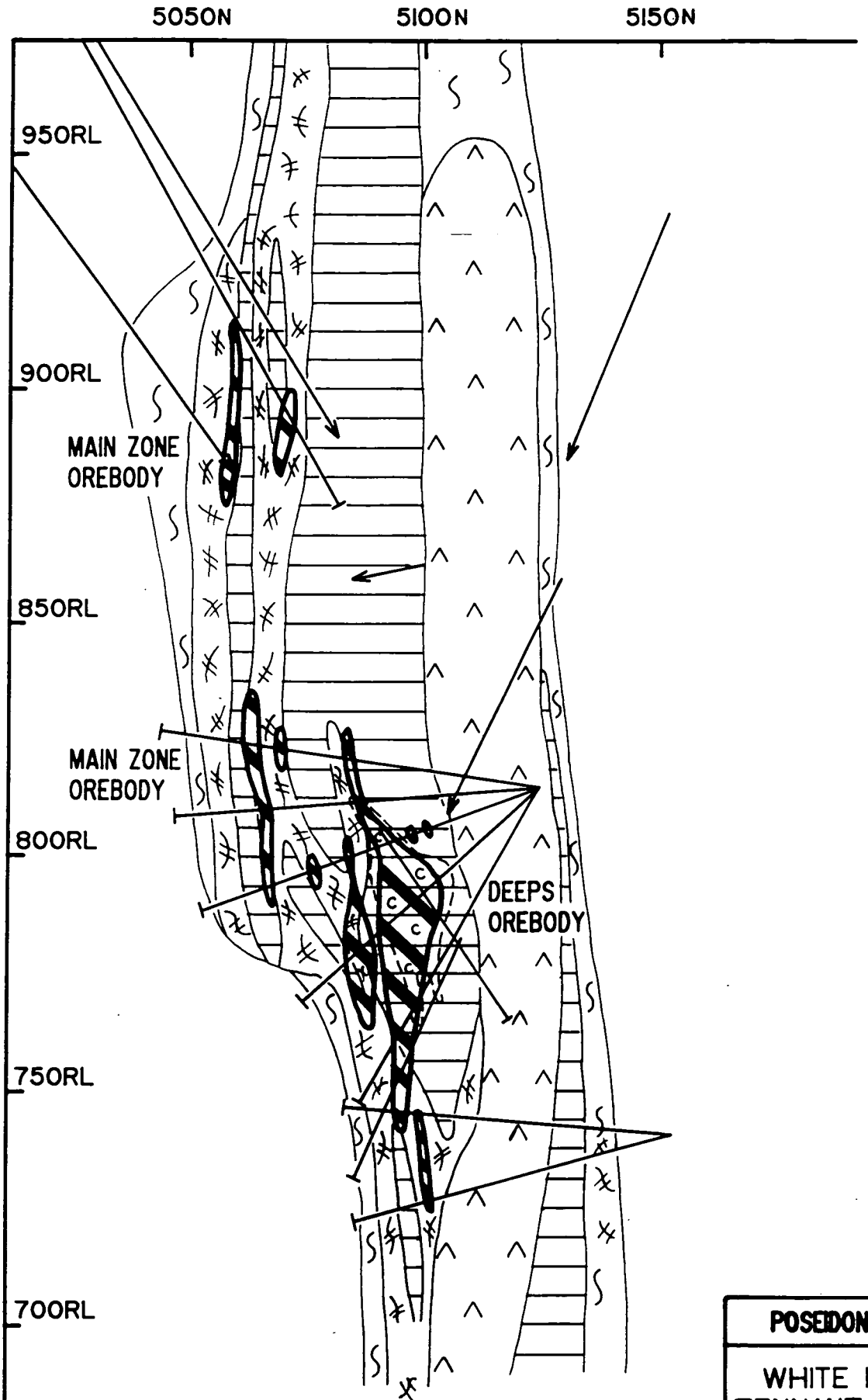

POSEIDON GOLD LIMITED

WHITE DEVIL MINE
TENNANT CREEK - N.T.
SECTION 5155E

Compiled by G.J.COZENS - April, 1992
Drawn by W.S.P. - Scale 1 : 1250

Figure 4 (v)

WHITE DEVIL MINE

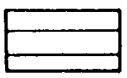

Massive magnetite ± hematite & chlorite
- C – Magnetite chlorite
- T – Magnetite talc
- AS – Magnetite + highly chloritic altered sediment

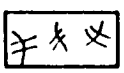

Stringer magnetite in highly chloritic sediment

Highly chloritic sediment
- T + Talc

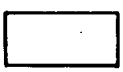

Unaltered or slightly chloritic sediment

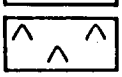

Quartz feldspar porphyry

Orebody

POSEIDON GOLD LIMITED
KEY TO FIGURE 4
Compiled by G.J.COZENS - May, 1992

SECTION 5235E

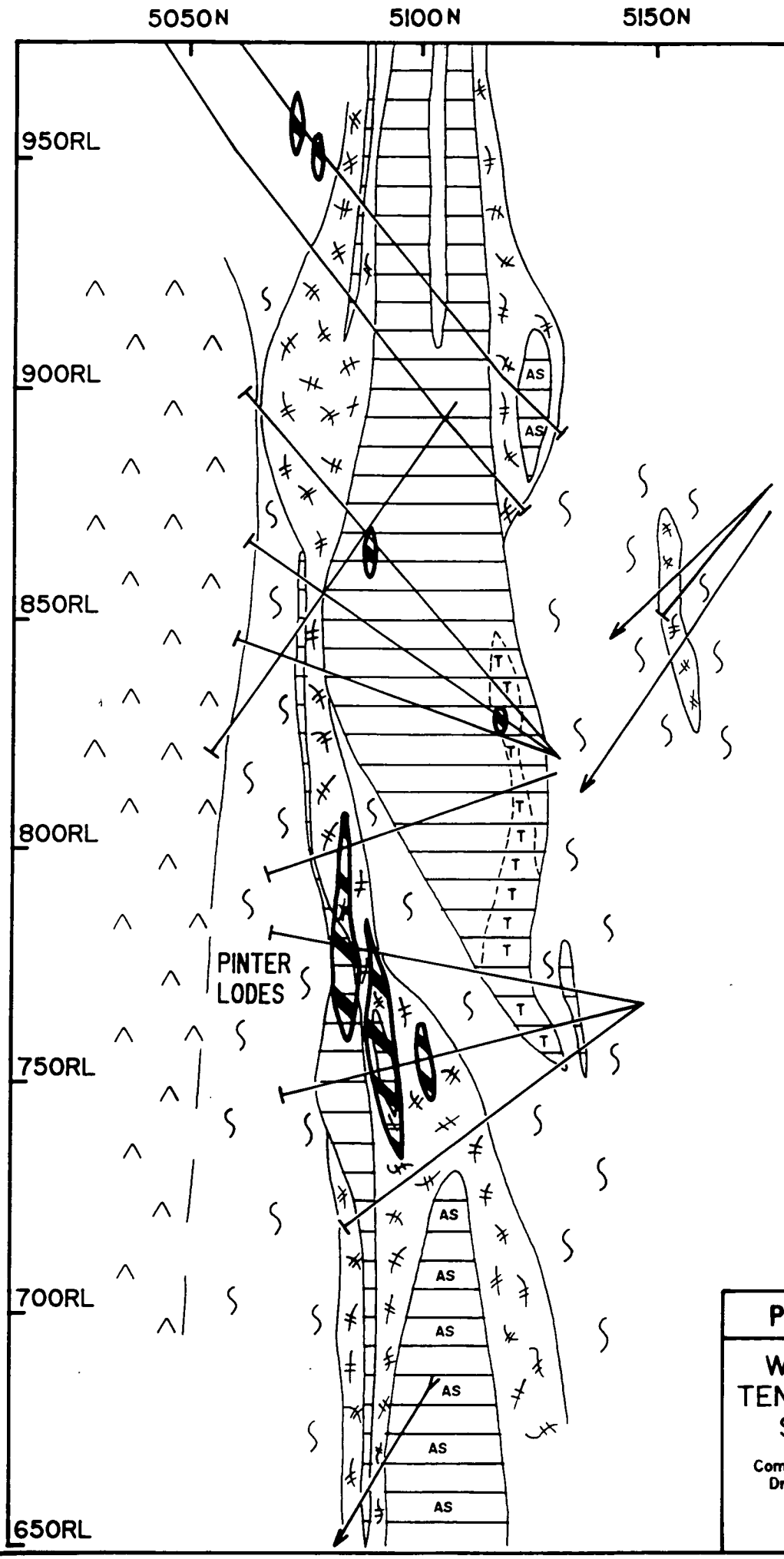

POSEIDON GOLD LIMITED

WHITE DEVIL MINE
TENNANT CREEK - N.T.
SECTION 5235E

Compiled by G.J.COZENS - April, 1992
Drawn by W.S.P. - Scale 1 : 1250

Figure 4 (vi)

WHITE DEVIL MINE

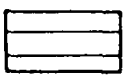

Massive magnetite ± hematite & chlorite
- C – Magnetite chlorite
- T – Magnetite talc
- AS – Magnetite + highly chloritic altered sediment

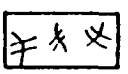

Stringer magnetite in highly chloritic sediment

Highly chloritic sediment
- T + Talc

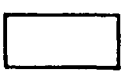

Unaltered or slightly chloritic sediment

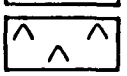

Quartz feldspar porphyry

Orebody

POSEIDON GOLD LIMITED

KEY TO FIGURE 4

Compiled by G.J.COZENS - May, 1992

SECTION 5265E

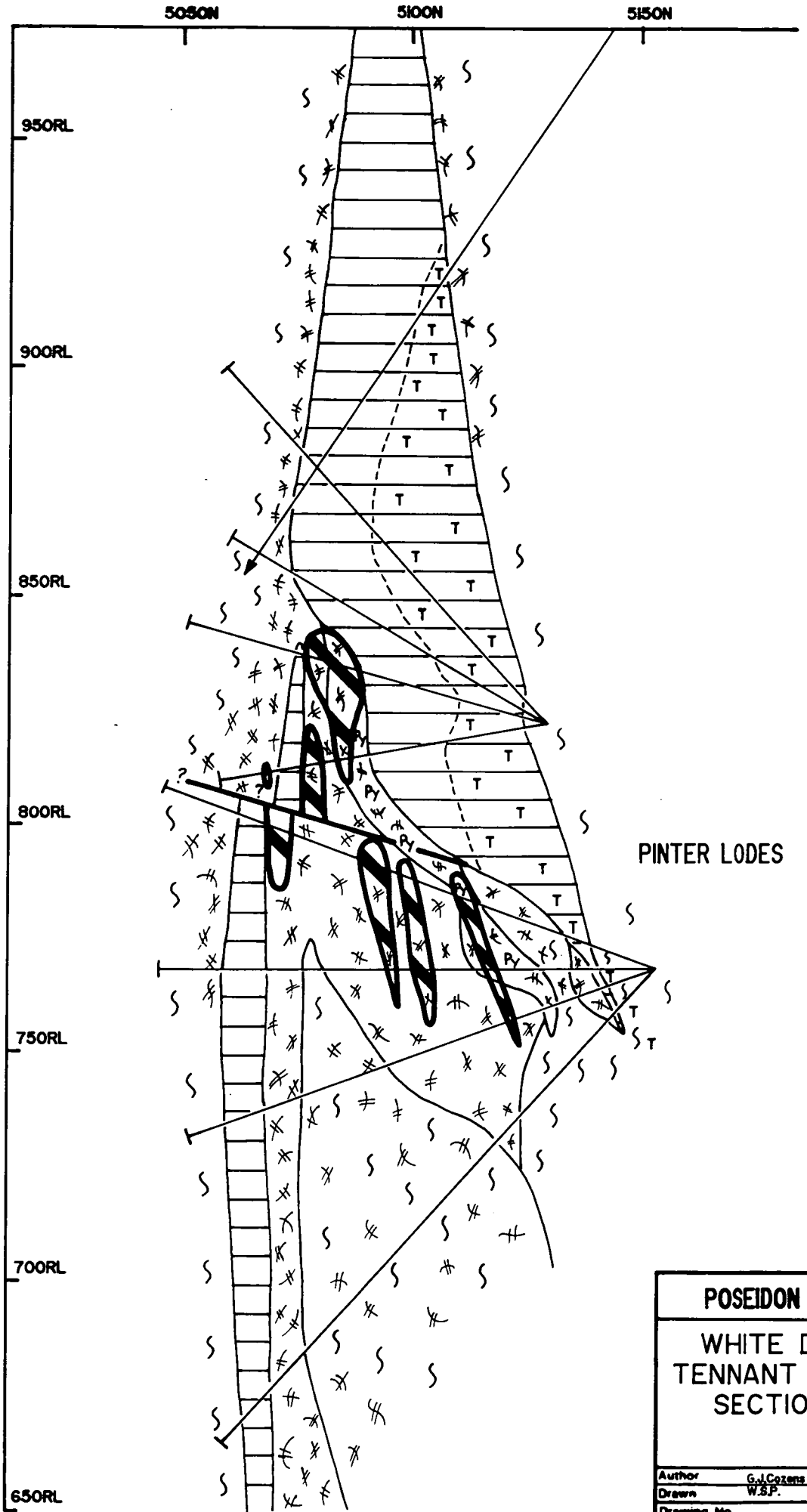

POSEIDON GOLD LIMITED			
WHITE DEVIL MINE TENNANT CREEK - N.T. SECTION 5265E			
Author	G.J.Cozens	Scale	1 : 1250
Drawn	W.S.P.	Date	Feb. 1992
Drawing No		Figure 4 (vii)	

in the shear direction. The width of the zone varies from very wide at 5265E to just a few metres in the west.

Chlorite is the dominant alteration mineral within the deposit. The country rocks in contact with the shear zone have been pervasively chloritised for approximately 15 to 20 m. On sections 5095, 5235 and 5265 (Figure 4) the shear contains zones of mildly chloritic, partly silicified, bleached sediments which contain no or minor magnetite. These zones can be seen on the level plans (Figure 5) and their size appears to increase with depth.

The level plans show the irregularity of the rock units within the shear. The shear is widest between the Central and Eastern Porphyries and east of 5240E, and thins towards the west.

Zones of talc and carbonate alteration occur within and around the ironstones and in the stringer zone. This alteration is particularly strong at the base of the Pinter ironstone. The alteration pattern has similarities to the zoning modelled for the Juno deposit by Large (1975), except that in the Pinter ironstone the zoning is upside down.

Hematite alteration of the magnetite has occurred throughout the ironstone, even below the level of weathering (95 to 100m). The extent of alteration varies from minor alteration along grain boundaries to almost complete replacement of all magnetite. Hematite alteration is most intense on the north side of the massive ironstone, near the contact with the porphyry between 5100 and 5125E.

Within the deposit there are two styles of mineralisation, both associated with magnetite ironstones, Figure 4. The Deeps orebody typifies the classical Tennant Creek model of Au and Bi mineralisation hosted within a large massive magnetite-hematite-chlorite ironstone. The gold-bismuth mineralisation occurs within a pod of magnetite-chlorite near the base of the ironstone. The Main Zone orebodies are associated with the thin (0.5 to 2m thick) tabular magnetite - hematite ironstone occurs along the southern margin of the shear zone. The mineralisation occurs in highly chloritic altered sediments containing small lenticular magnetite stringers on the

hanging wall side of the ironstone. The Main Zone orebodies vary between 0.5 and 7m thick and are bounded by a strong hanging wall shear.

The three rhyolitic quartz feldspar dykes which crosscut the deposit consist of coarse euhedral to subhedral quartz, k-feldspar and plagioclase crystals within a fine glassy matrix (McPhie in press).

The Eastern Porphyry separates the Eastern Main Zone and Deeps Lodes from the Pinter Lodes and appears to cut the large ironstone, Figure 5. The Deeps orebody terminates against the porphyry. The Central Porphyry diagonally cuts across the shear and separates the Eastern Main Zone and the West Lodes. Nguyen et al (1989) suggest that the Central Porphyry intruded later than the Eastern and Western Porphyries. The porphyries have been intensely chloritised and slickensided contacts and the porphyries themselves are chloritically altered throughout (Huston and Cozens in prep); near the Deep Orebody the core of the porphyry is sericitised. The Western Porphyry marks the western limit of economic mineralisation and the available drill data indicates the porphyry is a large stock rather than a dyke like the Eastern and Central porphyries. Several small porphyry stocks occur throughout the shear.

The timing of intrusion of the porphyries has been the subject of much conjecture (Hy 1988, Nguyen 1989, Huston and Cozens in prep). The porphyries appear to cut the ironstone (Figure 5) and studies by Huston and Cozens (in prep) supports the hypothesis of Nguyen et al (1989) that the porphyries intruded post ironstone formation and pre-mineralisation. Within the porphyry are small veinlets containing chalcopyrite, bismuthinite and pyrite indicating it was intruded prior to mineralisation (Huston and Cozens, in prep).

The deposit resource (including production) is 0.9mt at 21.2 g/t Au. The Deeps orebody had a reserve of 77,000 t @ 34g/t Au and the individual Main Zone orebodies average 20 - 30,000 t @ 15 - 25 g/t Au.

4 IRONSTONES

The ironstones, which are an integral part of the deposit, are described in this chapter, in particular their textures, mineralogy and associated alteration styles.

The ironstones crop out as a low semi-continuous ridge within a zone of iron oxide rich sediments along the axis of a west plunging anticline (Plate 1).

At surface the ironstone consists of hematite, quartz and magnetite. Much of the hematite is a weathering product of magnetite, and the ironstones are strongly magnetic in places. The ironstones are very resistant to weathering and retain much of the character observed at depth. Weathering has accentuated the brittle fracture pattern of the ironstone (Plate 2). The two parallel fractures running along the ironstone are sub parallel to the shear direction and the shorter fractures are sub perpendicular to this direction. This fracture pattern is consistent throughout the ironstone. A third fracture set strikes east- west and dips between 25 and 40^{o} north.

4.1 DESCRIPTION OF IRONSTONES

The ironstones consist of magnetite, hematite, quartz, chlorite, talc and carbonate in varying proportions.

Figure 6 illustrates the distribution of the ironstones on cross sections 5265E, 5235E, 5155E and 5135E. The different rock types within the ironstones are described below.

Altered Sediments(AS) refers to intensely chloritised sediments.

Magnetite + Altered Sediments(MAS) consists of magnetite containing fragments of altered sediments.

Magnetite Chlorite-Altered Sediments(MCAS) refers to the above unit except that the magnetite contains chlorite in fractures and vugs.

Magnetite Chlorite(MC) refers to a rock consisting of magnetite and chlorite associated with the mineralising phase. The chlorite occurs interstitially between the magnetite (Plate 13).

Magnetite-Minor Chlorite (M/c) is similar to the above unit except the chlorite is only a minor constituent.

Magnetite-Quartz to Magnetite(MQ,M/q,M) refers to a rock containing a varying quartz content from zero to 50%. Quartz infills the spaces between the skeletal magnetite (Plates 3&4).

5265E.

This section contains two different ironstones, a large lensoidal and a deeper tabular ironstone.

The tabular ironstone has a core of magnetite-quartz to magnetite only with magnetite-altered sediments on the edges. At 750RL a zone of hematite alteration occurs. The upper part of the ironstone is offset by a shallow dipping fault. The fault is inferred to dip north as this is the dominant fault direction.

The core of the large ironstone has been altered to a magnetite-talc rock. Carbonate alteration wraps around the lower portion of the ironstone. The existence of carbonate alteration at depth is opposite to the zonation sequence observed by Large (1975) at the Juno Mine.

To the south of the central magnetite-talc zone, towards the shear, is a zone of magnetite-quartz and magnetite, which is flanked by magnetite with minor chlorite and then by magnetite-altered sediments next to the highly sheared altered sediments. The northern edge of the ironstone consists of magnetite-altered sediments which have been extensively altered to hematite. The ironstone tapers off very quickly approaching 760RL but is continuous to surface.

5235E.

The ironstones on this section are very similar to those on 5265E, although this portion of the ironstone contains much less talc.

The large ironstone extends from surface to 750RL where it quickly tapers off. Between the two sections the depth extent of the ironstone has not changed, indicating that the ironstone does not plunging or continue below 750RL. However 750RL was the limit of drilling at the time the sections were produced. The ironstone is mostly magnetite-quartz to magnetite with minor pyrite. The quartz content varies from nil to more than 50%. At 900RL there is a small patch of magnetite-minor chlorite and talc. Towards the centre of the shear the ironstone changes from magnetite-quartz to magnetite-minor chlorite, magnetite-altered sediments and magnetite-quartz. Magnetite has been extensively altered to hematite next to the shear.

The lower portion of the ironstone is similar to 5265E, being magnetite-talc, but without carbonates. The carbonate and talc content of the ironstone increases to the east. The talc zone extends up into the core of the ironstone and may extend up as far as 900RL.

A small tabular ironstone occurs on the southern margin of the shear but is pinched out along bends in the southern wall of the shear. The upper portion is magnetite-quartz and the lower portion is magnetite-altered sediment and magnetite quartz, with extensive hematite alteration on the outer, southern edge of the ironstone.

5155E.

This section contains both tabular and large lensoidal ironstones.

The tabular ironstone is footwall to the Main Zone mineralisation above 780RL. Below this level it is pinched out by a bend in the shear. Below this bend the tabular ironstone continues at depth. This ironstone has a core of magnetite with minor chlorite surrounded by magnetite chlorite-altered sediments and minor magnetite-quartz.

PLATE 1

Eastern end of outcropping hematite-quartz-magnetite ironstone. Ironstone forms prominent ridge along crest of hill. Looking west.

PLATE 2

Eastern end of outcropping ironstone, showing fracture pattern. Fractures both parallel and perpendicular to shear which runs lower left to upper right.

PLATE 1

PLATE 2

GEOLOGICAL KEY

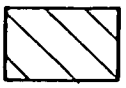

Magnetite - variable quartz to 50%

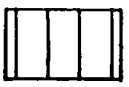

Magnetic chlorite

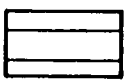

Magnetite - altered sediments

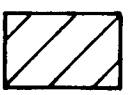

Magnetite - minor chlorite

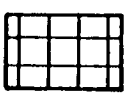

Magnetite chlorite - altered sediments

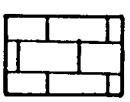

Carbonate, dolomite

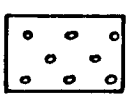

Magnetite talc

T Minor talc

H Hematite alteration

h Minor hematite alteration

POSEIDON GOLD LIMITED	
KEY TO FIGURE 6	
Author G.J.COZENS	Scale
Drawn W.S.P.	Date APRIL, 1992
Drawing No	Fig. No

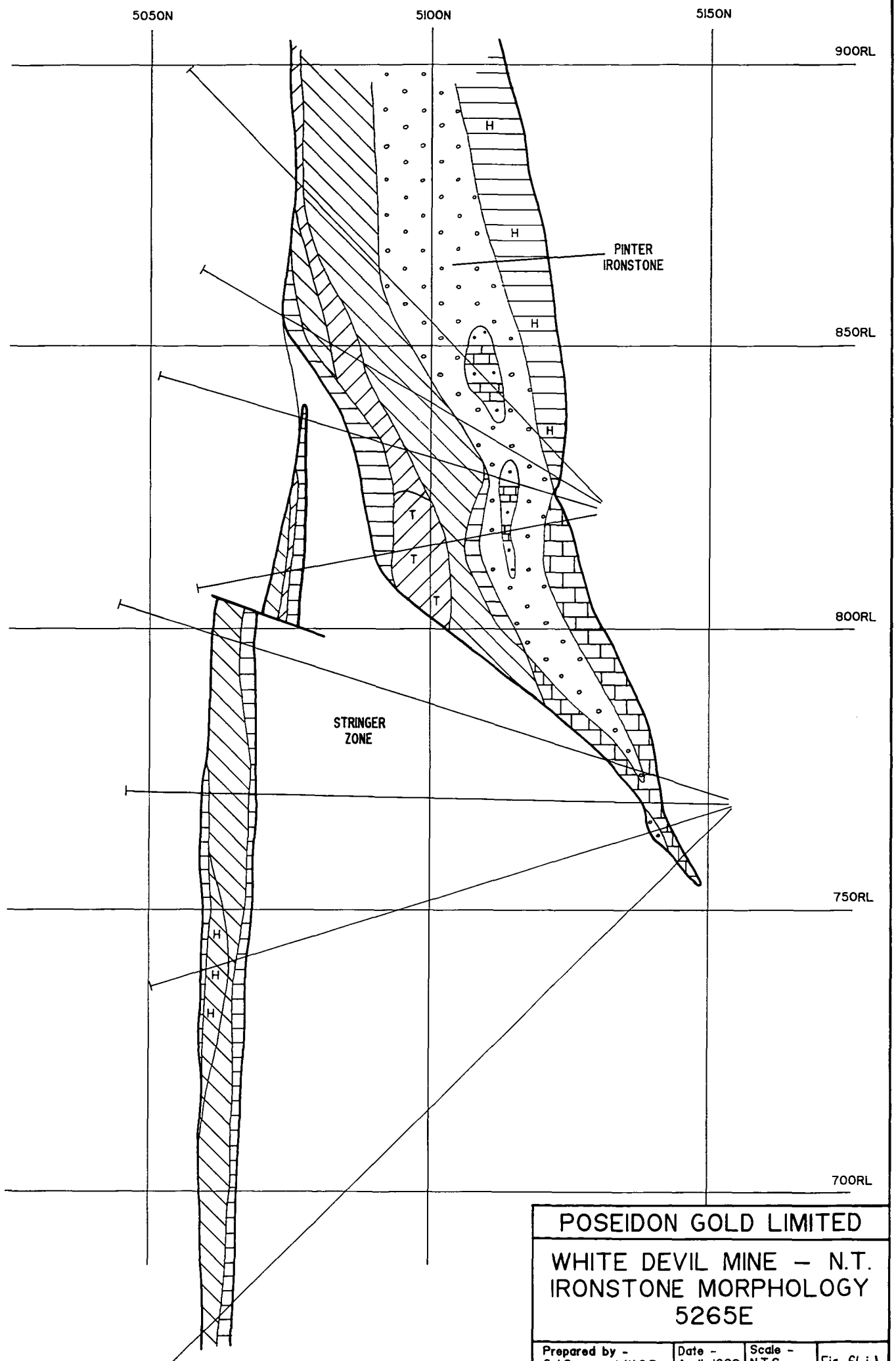

POSEIDON GOLD LIMITED

WHITE DEVIL MINE – N.T.
IRONSTONE MORPHOLOGY
5265E

Prepared by -	Date -	Scale -	Fig. 6(i)
G.J.Cozens / W.S.P.	April, 1992	N.T.S.	

GEOLOGICAL KEY

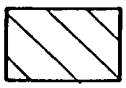

Magnetite - variable quartz to 50%

Magnetic chlorite

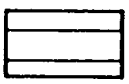

Magnetite - altered sediments

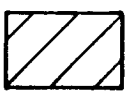

Magnetite - minor chlorite

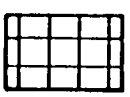

Magnetite chlorite - altered sediments

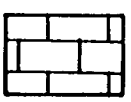

Carbonate, dolomite

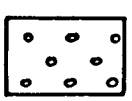

Magnetite talc

T Minor talc

H Hematite alteration

h Minor hematite alteration

POSEIDON GOLD LIMITED	
KEY TO FIGURE 6	
Author G.J.COZENS	Scale
Drawn W.S.P.	Date APRIL, 1992
Drawing No	Fig. No

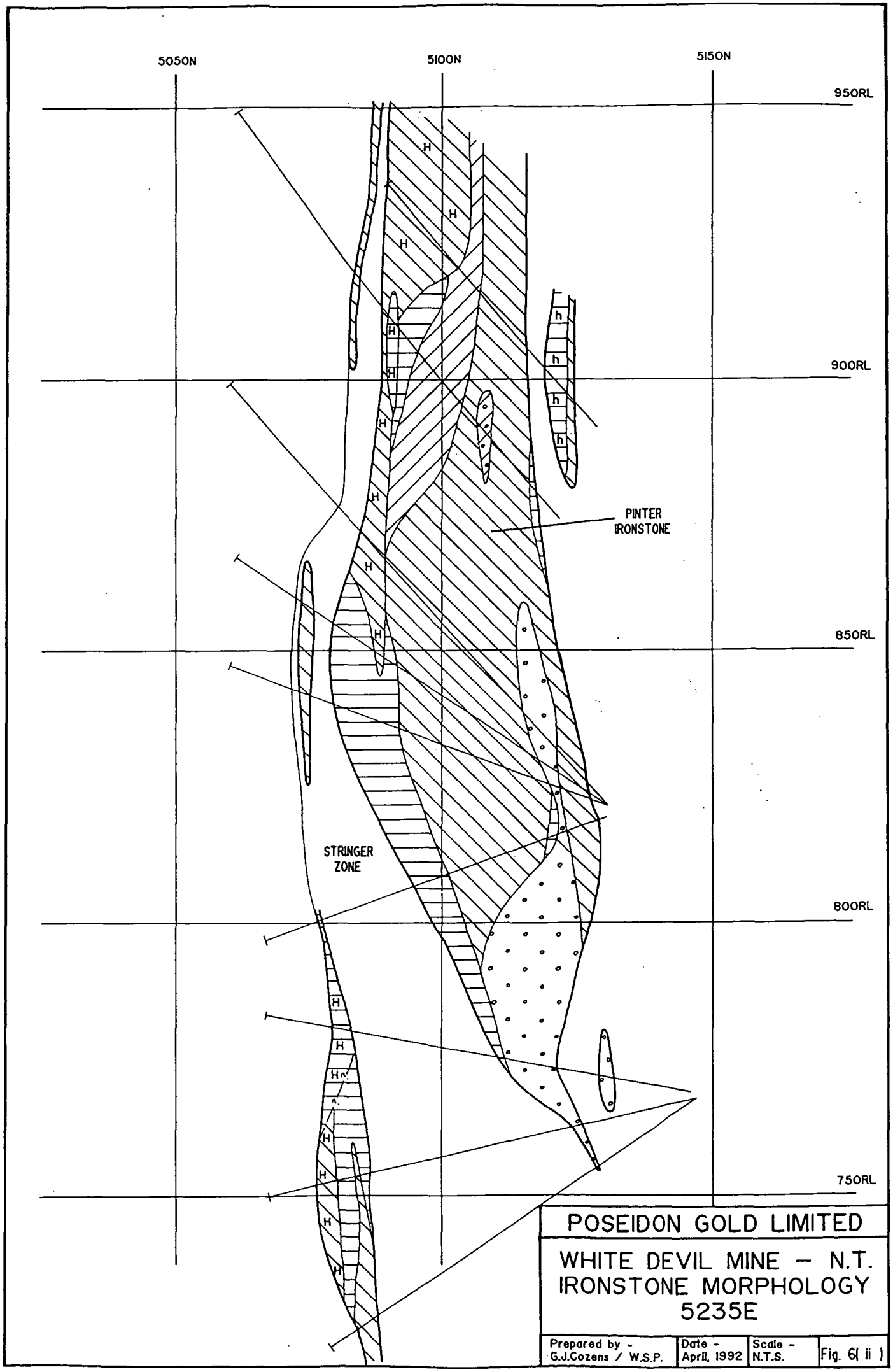

POSEIDON GOLD LIMITED

WHITE DEVIL MINE – N.T.
IRONSTONE MORPHOLOGY
5235E

Prepared by -	Date -	Scale -	Fig. 6(ii)
G.J.Cozens / W.S.P.	April, 1992	N.T.S.	

GEOLOGICAL KEY

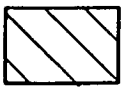

Magnetite - variable quartz to 50%

Magnetic chlorite

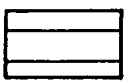

Magnetite - altered sediments

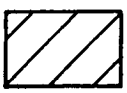

Magnetite - minor chlorite

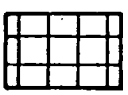

Magnetite chlorite - altered sediments

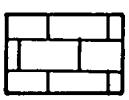

Carbonate, dolomite

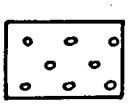

Magnetite talc

T Minor talc

H Hematite alteration

h Minor hematite alteration

POSEIDON GOLD LIMITED	
KEY TO FIGURE 6	
Author G.J.COZENS	Scale
Drawn W.S.P.	Date APRIL, 1992
Drawing No	Fig. No

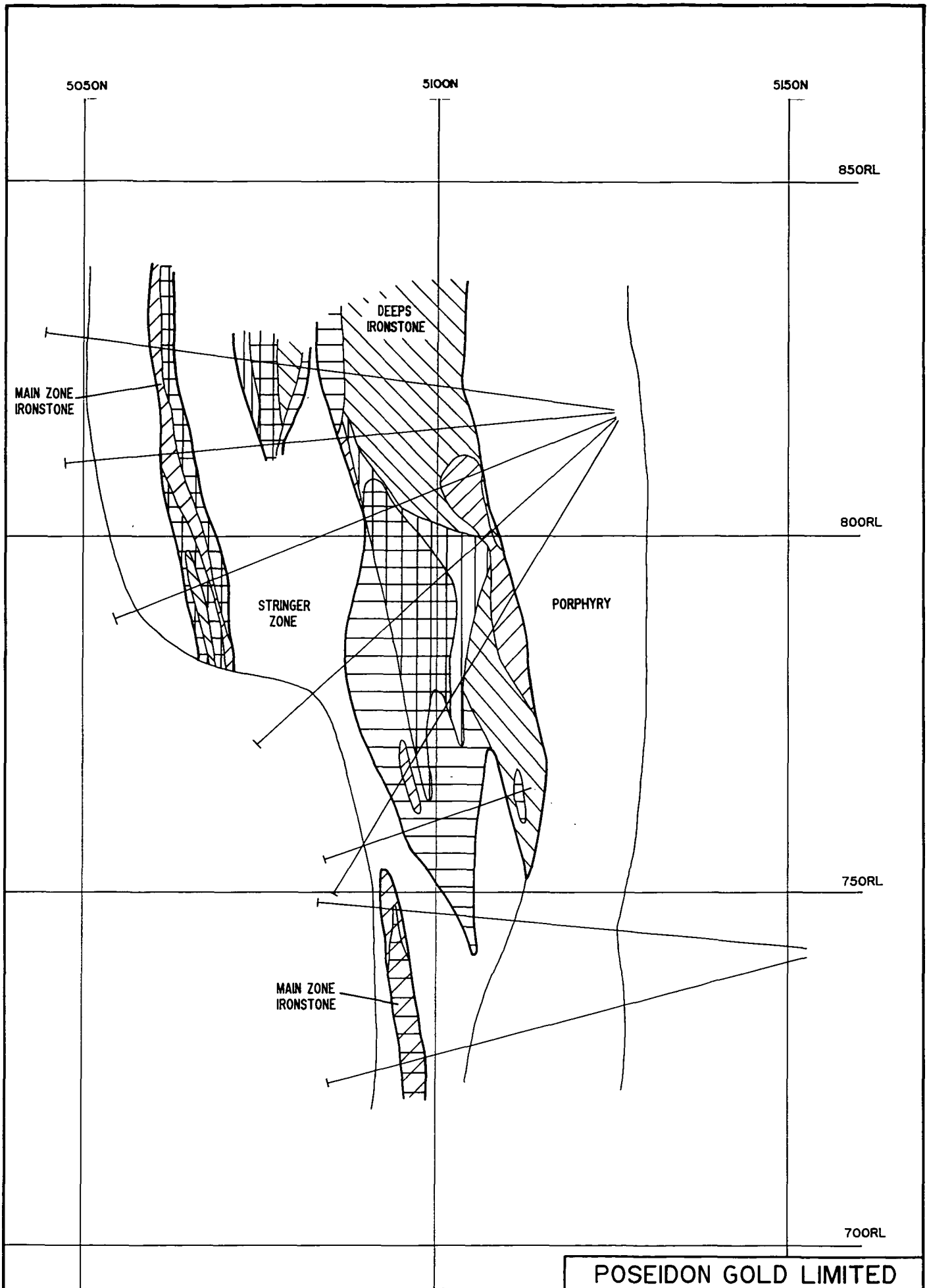

POSEIDON GOLD LIMITED

WHITE DEVIL MINE – N.T.
IRONSTONE MORPHOLOGY
5155E

Prepared by -	Date -	Scale -	Fig. 6(iii)
G.J.Cozens / W.S.P.	April, 1992.	1 : 1250	

GEOLOGICAL KEY

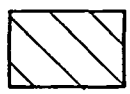

Magnetite - variable quartz to 50%

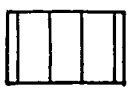

Magnetic chlorite

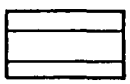

Magnetite - altered sediments

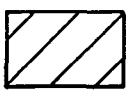

Magnetite - minor chlorite

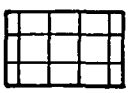

Magnetite chlorite - altered sediments

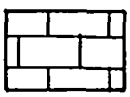

Carbonate, dolomite

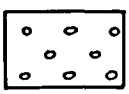

Magnetite talc

T Minor talc

H Hematite alteration

h Minor hematite alteration

POSEIDON GOLD LIMITED	
KEY TO FIGURE 6	
Author G.J.COZENS	Scale
Drawn W.S.P.	Date APRIL, 1992
Drawing No	Fig. No

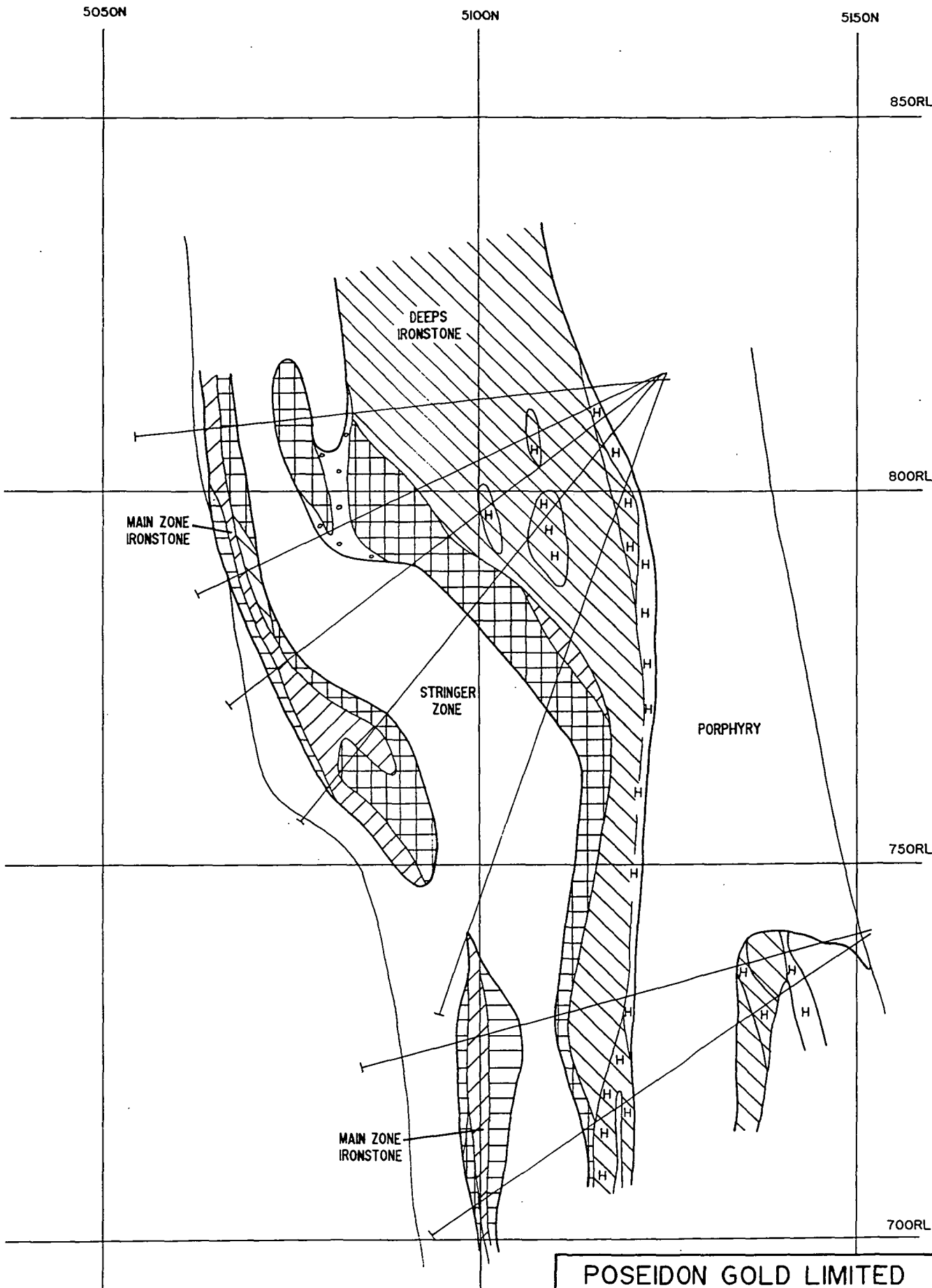

POSEIDON GOLD LIMITED

WHITE DEVIL MINE – N.T.
IRONSTONE MORPHOLOGY
5135E

Prepared by –	Date –	Scale –	Fig. 6(iv)
G.J.Cozens / W.S.P.	April, 1992	1 : 1250	

The large lensoidal ironstone consists of magnetite-quartz to magnetite and magnetite-minor chlorite in its upper portions and northern side. The southern margin of the ironstone, is magnetite-altered sediments, magnetite chlorite and magnetite chlorite-altered sediments which hosts the Deeps mineralisation. This portion of the ironstone does not contain any talc or carbonate alteration.

5135E.

Both types of ironstone are present on this section, and both associated with mineralisation.

Thin tabular ironstone occurs almost over the vertical extent of the section. Just below 750RL, the tabular ironstone pinches out as the result of D2 shearing. The ironstone has a core of magnetite-minor chlorite, with magnetite-altered sediments towards the south and magnetite chlorite-altered sediments towards the north.

The large lensoidal ironstone extends to depths below 700RL and is thickest between 830 and 780RL. The ironstone is predominantly magnetite-quartz to magnetite, with zones of intense hematite alteration within magnetite-quartz and along the porphyry contact. Towards the shear the ironstone is a mixture of magnetite-chlorite and magnetite-altered sediments, which hosts the mineralisation. A small zone of magnetite-talc occurs around 800RL, between two pods of magnetite chlorite-altered sediments. The talc zone may define the final fluid path through the shear.

4.2 IRONSTONE TEXTURES AND MINERALOGY

4.2.1 Northern, Lensoidal Ironstone

While working at White Devil Mine unusual textures within the magnetite quartz-minor pyrite Pinter ironstone were observed. The core contained magnetite needles, lacework and `birdsfoot' textures within quartz. The lacework and birdsfoot textures are shown in Plate 3. Lacework texture consists of an open network of interlocking or intergrown laths of magnetite which gives the rock a lace-like

appearance. Birdsfoot texture refers to two or three coarse magnetite laths radiating from a common point. There are also elongate globular shaped growths of magnetite intergrown with the needle and lacework magnetite. The pyrite is intergrown with the magnetite and quartz and the quartz appears to be in equilibrium with both.

These textures spurred the author to investigate the textures and formation of the ironstones. Thin sections were cut from the Pinter, Deeps and Main Zone ironstones.

The magnetite-quartz-pyrite of the Pinter ironstone, in thin section, consisted of radiating and intergrown/ intermeshed laths of magnetite within quartz (TS M7559, 60,61). Similar textures were observed by Large (1975) from the Juno ironstone and by Wall and Valenta (1990) at White Devil.

The magnetite laths have what appear to be corroded boundaries and many show signs of having had a hollow core (Plate 4). The shape of the laths does not correspond to the form of magnetite, rather that of hematite, suggesting the magnetite has replaced an earlier iron oxide mineral.

Ramdohr (1980) states that pseudomorphing of hematite by magnetite occurs due to a change in oxygen pressure or the action of reducing solutions without a temperature increase. The products of the pseudomorphing has been referred to by the superfluous name of "mushketoffite" (Ramdohr, 1980).

To test this thin section M7561 was etched with hydrobromic acid. The etching showed that the magnetite laths are composed of numerous irregular shaped, rough edged magnetite grains (Plate 5) and the corroded texture is due to non perfect pseudomorphing of the original lath.

The HBr etching has highlighted the irregular grain boundaries and also two textural forms of magnetite (Plate 6). The `dirty', pitted magnetite composing the laths is earlier than the cleaner, subhedral grains which occur as overgrowths on the laths. This shows that magnetite continued to precipitate following the replacement of the hematite. This feature was observed throughout the ironstones.

Thin section M7558 (5235E), of magnetite-quartz-talc, has a very open lath texture similar to other portions of the ironstone. Near the middle of the thin section is a zone of dendritic magnetite growths (Plate 7), which are orientated in the same direction.

Dendritic growth generally indicates rapid deposition or crystallisation. The magnetite growths appear to be in equilibrium with the surrounding quartz.

At the El Laco Magnetite flows in Chile (Henriquez & Martin, 1978) dendritic growth of magnetite was observed in the walls adjacent to gas escape tubes and vesicles and near the uppermost parts of slabs of magnetite flows. The magnetite growth was orientated perpendicular to the channelway. Spherulitic growths were also common. The Kiirunavaara Magnetite Iron Ore deposit in Norway (Nystrom & Henriquez, 1989) also contains dendritic growths of magnetite.

Clumps of radiating crystals also occur near the middle of the thin section. Spherulitic growths of magnetite are common throughout all the ironstones.

The dendritic magnetite is primary and probably formed during or post replacement of the hematite laths. Minor pyrite is intergrown with the magnetite and quartz.

Where there is a high proportion of magnetite in the ironstone the magnetite laths have formed a skeletal or spongy texture, which can increase in intensity until the ironstone has the appearance of a coalesced mass of laths (massive ironstone). This texture is widespread in the Deeps and Main Zone ironstones.

Plate 8 shows some of the textures within the Deeps ironstone (TS M7539 & 41, 5155E). The photos show individual lath like, radiating and spherulitic growths and the coalesced randomly orientated texture. An important feature displayed by the photos is the open texture of the ironstones.

The magnetite-chlorite zone of the Deeps ironstone, which hosts the mineralisation, has a similar spongy magnetite texture to the remainder of the ironstone. The spaces between the magnetite now contains coarse laths of chlorite and trace quartz. The chlorite is coarse and unfoliated suggesting it formed in an open

PLATE 3

Core from Pinter Ironstone showing "birdsfoot" and "globular" magnetite in quartz and minor pyrite.
Drillhole: WDD495, 60.7m, section 5265E.

PLATE 4

Magnetite laths (light grey) within quartz. Note: corroded edges of laths and dark strip in the middle of the laths.
Thin section: M7561, WDUD 487, 6.6m, 5235E,
FOV= 6.9mm

PLATE 3

PLATE 4

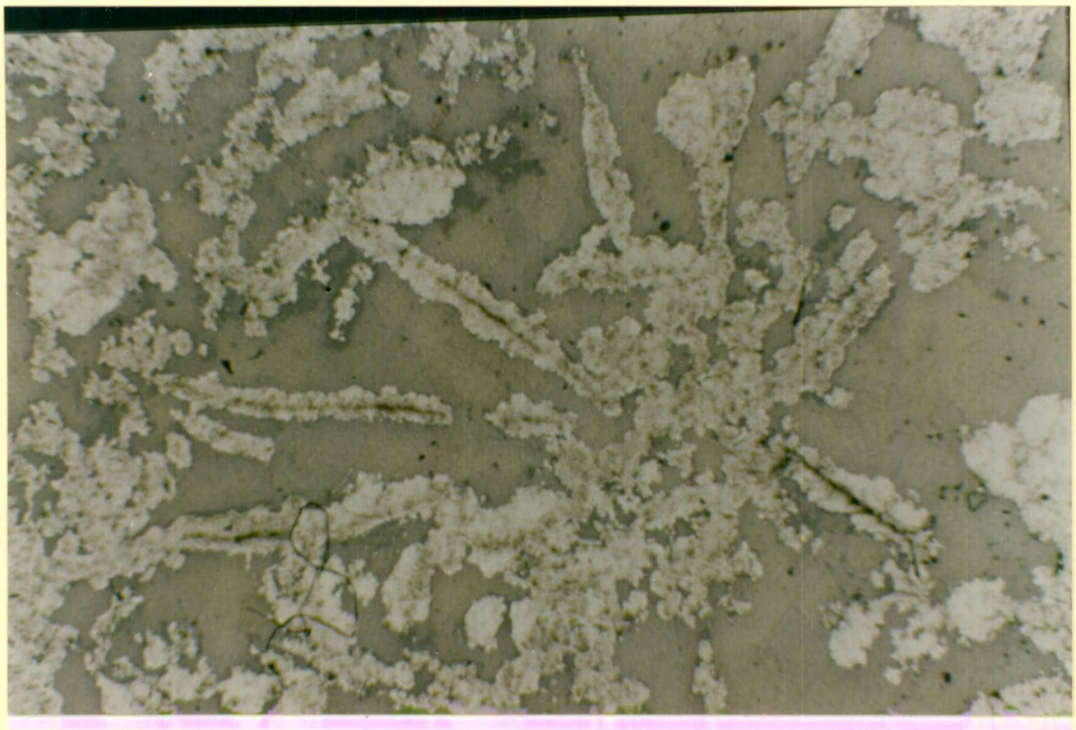

PLATE 5

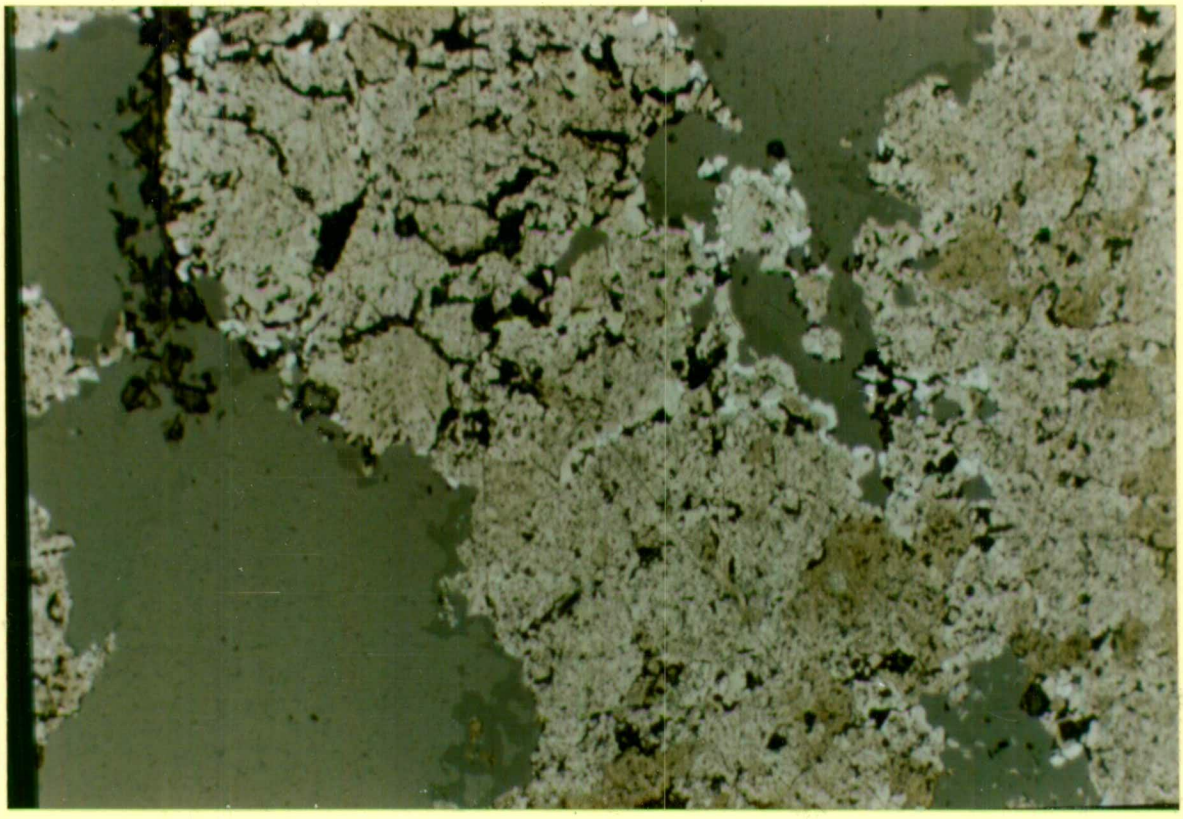

PLATE 6

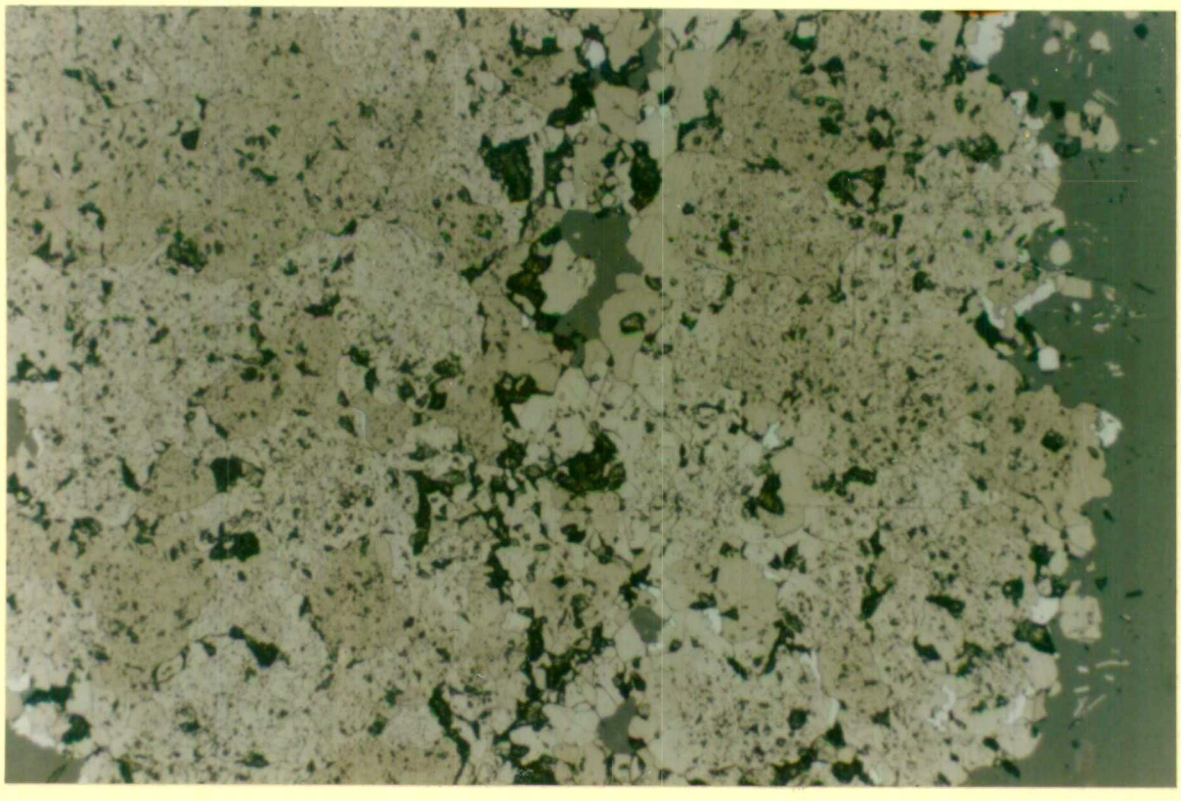

PLATE 5

Magnetite laths etched with HBr acid. Mottling is due to different etching rates of the magnetite grains. Etching showed that the laths are composed of subrounded, rough edged magnetite grains.
Thin section: M7561, WDUD 487, 6.6m, 5235E
FOV= 1.7mm

PLATE 6

Close up of large lath in Plate 4. HBr acid etching has highlighted the different magnetite grains and also the `clean' primary magnetite which grew into cavities during and following the replacement process. The `clean' magnetite in the centre of the photo corresponds to the dark strip in the middle of the lath in Plate 4. The light grey is hematite alteration.
Thin section: M7561, WDUD 487, 6.6m, 5235E
FOV= .87mm

PLATE 7

Dendritic magnetite growth within talc (dark grey). These growths are primary magnetite and occur within a talc zone in the magnetite-quartz ironstone.
Thin section: M7558, WDUD 487, 8m, 5235E
FOV = 3.5mm

PLATE 8a

Open magnetite lath texture within Deeps ironstone. Light grey - bismuthinite, dark grey - chlorite
Thin section: M7541, WDUD 285, 54m, 5155E
FOV = 1.7mm

PLATE 7

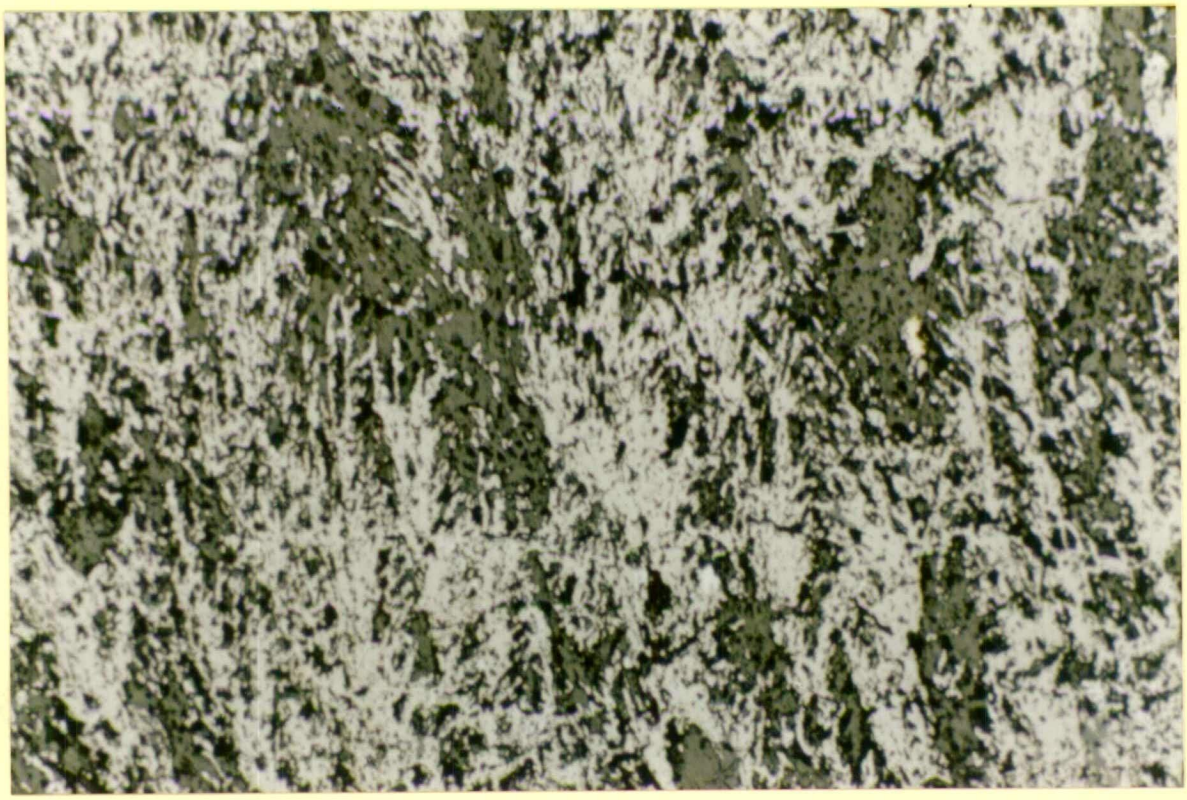

PLATE 8a

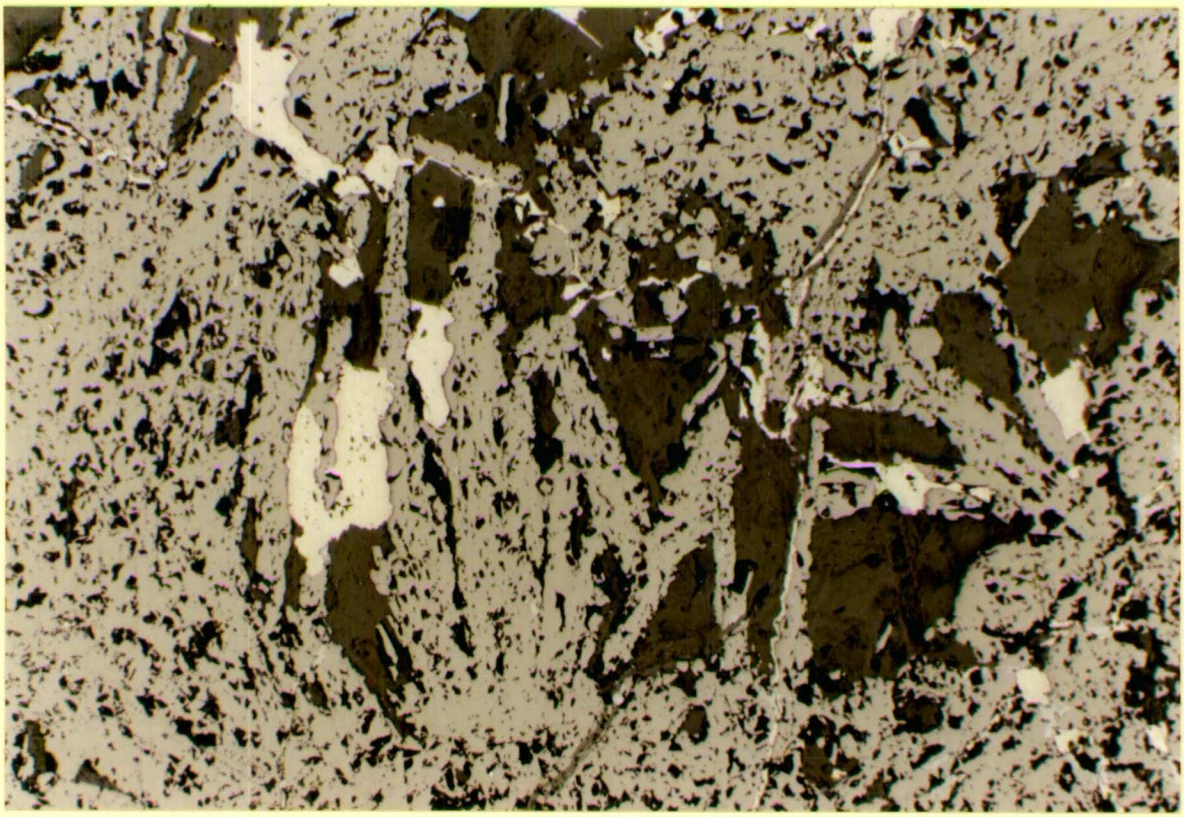

PLATE 8b

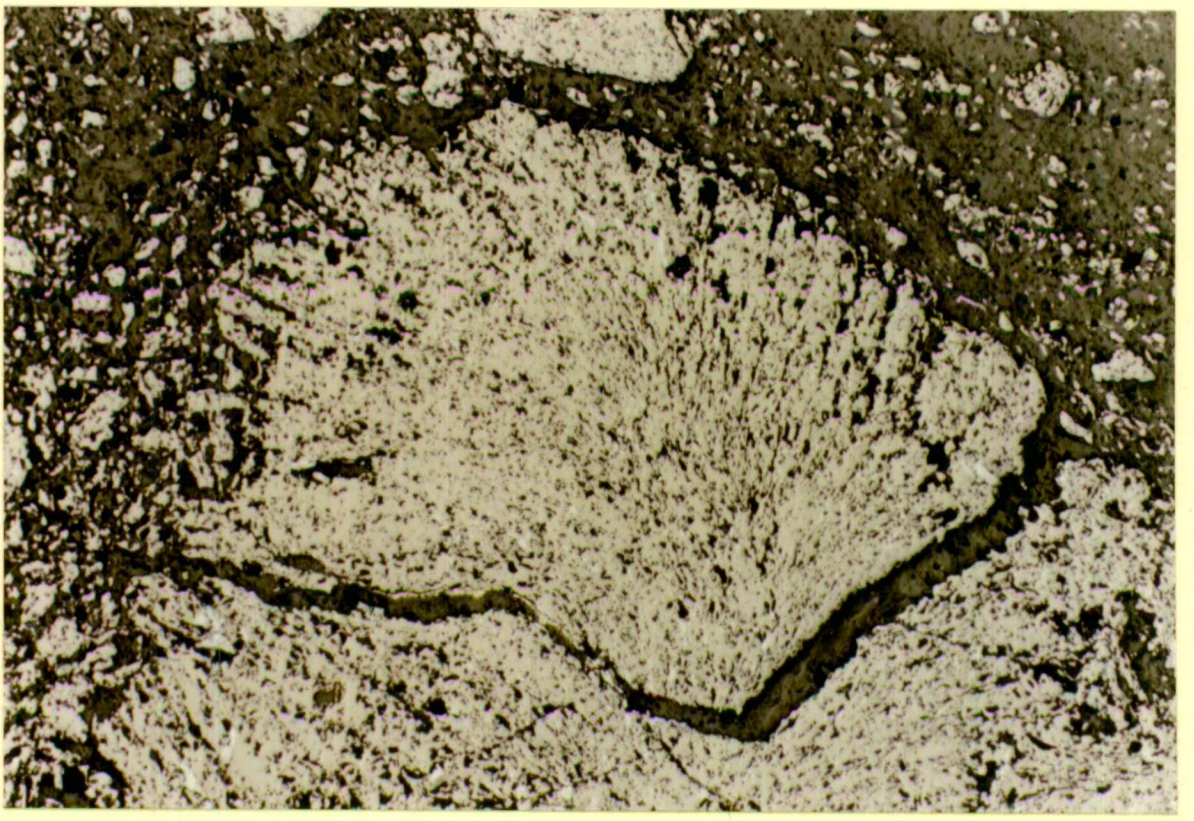

PLATE 8c

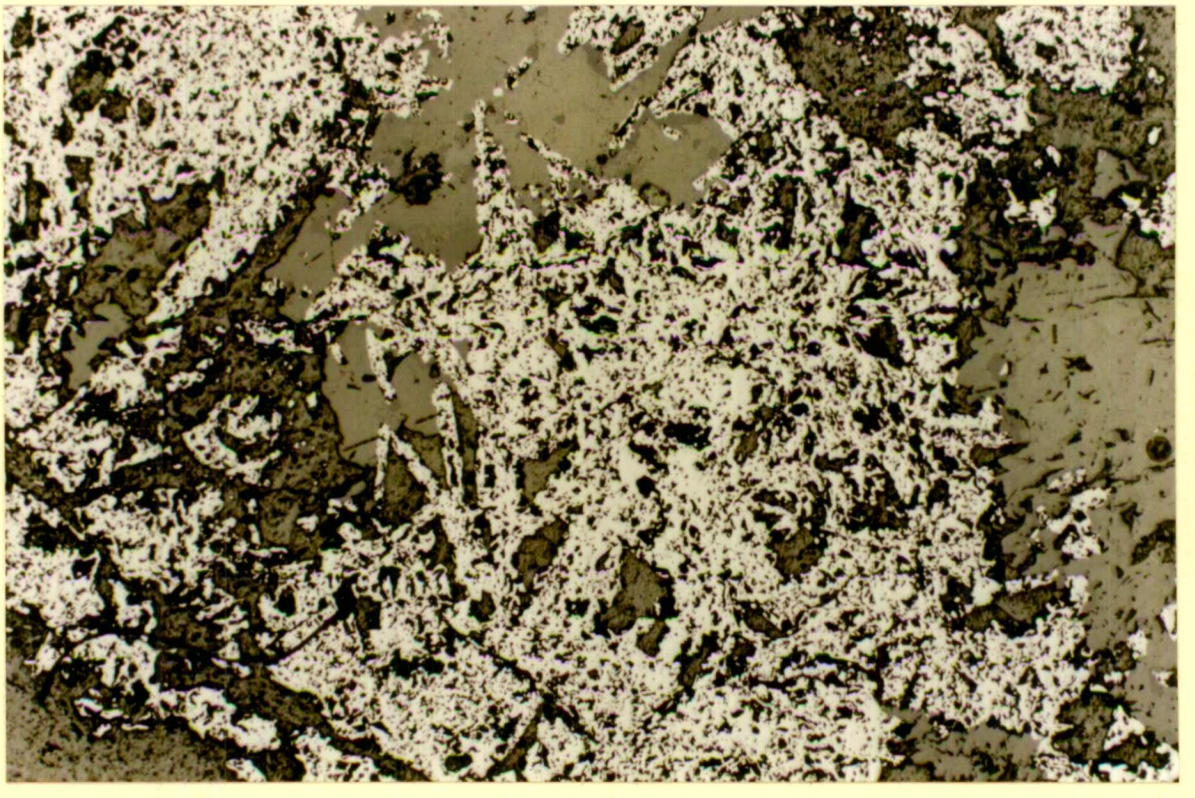

PLATE 8b

Spherulitic magnetite growth, replaced hematite, surrounded by chlorite (dark grey). The ironstone has undergone brittle fracturing, with magnetite clasts incorporated into the coarse grained, mineralising stage chlorite.
Thin section: M7541, WDUD 285, 54m, 5155E
FOV= 3.5mm

PLATE 8c

Skeletal/spongy texture of the Deeps ironstone. The replacement process has retained the primary hematite texture. Mid grey - quartz, dark grey - chlorite.
Thin section: M7539, WDUD 285, 39m, 5155E
FOV= 3.5mm

PLATE 9

Magnetite chlorite-altered sediment rock. Clasts of mildly chloritic sediments are surrounded by magnetite stringers in chlorite. The chlorite has pervasively replaced the sediments, giving rise to the rounding effect and breccia texture. Core: WDUD 490, 74m, 5275E

PLATE 9

space. Thus the ironstone had a primary porosity and permeability. Associated with the laths are clumps of clean, subhedral overgrowth magnetite. The laths have undergone some brittle deformation.

The magnetite-chlorite-altered sediment zone on the margin of the ironstone (5155E) appears to be a transition phase between the ironstone and stringer zone. The rock consists of fine grained mildly chloritised sediments surrounded by magnetite stringers and chlorite to give a pseudo breccia texture (Plate 9). Many of the magnetite stringers have been pulled apart and the gaps filled with coarse grained chlorite

4.2.2 Other Minerals in the Ironstone

Hematite

Hematite occurs in the ironstone as the result of martitisation, the alteration of magnetite to hematite. Martitisation is common throughout all the Tennant Creek deposits (Large 1975, Huston 1990b,1991, Huston et al 1992,)

The process of martitisation is regarded by Ramdohr (1980) as the aftermath of the ore forming process, caused by decreasing temperature and thus distinctly `ascendant' (hypogene). The hypogene nature of martitisation is indicated by the contemporaneous formation of independent, partly coarse grained hematite in the vicinity of the hematised magnetite.

At White Devil martitisation occurs with variable intensity throughout the deposit. Two zones of intense hematite alteration occur, on the 5135E section and within the Pinter ironstone. On 5135E (Figure 6) the intense hematite alteration occurs near the contact with the porphyry. Within the Pinter ironstone (5235E & 5265E Figure 6) the intense alteration occurs on both sides of the ironstone and in the upper portion.

Elsewhere in the ironstones the hematite alteration occurs along grain boundaries, around cavities and fractures and as replacement of complete grains.

Hematite crystals and laths occur along fractures and around cavities and often grow as a continuation of replacement of magnetite, such that the hematite lath is growing out of a replaced magnetite grain.

Plate 10a (TS M7561) from the Pinter ironstone (5235E), shows selective replacement, by hematite, of individual magnetite grains and rimming a cavity. Plate 10b (TS M7563) also from the Pinter ironstone shows martitisation along grain boundaries and Plate 10c (TS M7511) from 5205E shows almost complete alteration to hematite and the growth of hematite laths around chalcopyrite grains.

Hematite alteration is often strong along late stage quartz veins. The alteration is not continuous along the vein wall, but is selective of the grains it replaces.

Pyrite

The ironstones contain numerous pyrite grains which appear in equilibrium with the magnetite, quartz and chlorite (Plate 11).

The pyrite grains are irregular shaped and intergrown with the magnetite and quartz and generally fractured indicating the pyrite formed at the same time as the ironstone.

Quartz

The quartz grains intergrown with the magnetite have irregular grain boundaries, are generally equant, and have a moderate degree of undulose extinction. The controls on the shape of the quartz grains are unknown. Perhaps high pressures prohibited the quartz forming euhedral shapes.

Chlorite

As can be seen in Figure 6 the ironstones contain abundant chlorite.

The magnetite-quartz section of the Pinter ironstone contains what appears to be remnant chlorite within quartz (Plate 12). The chlorite occurs along and within the boundaries of three quartz grains, suggesting the quartz may have replaced the

PLATE 10a

Selective martitisation (light grey) of magnetite(mid grey). Replacement of single grains around cavities and edge of lath. Dark grey-quartz
Note the abundant cavities within the laths.
Thin section: M7561, WDUD 487, 6m, 5235E
FOV= .43mm

PLATE 10b

Martitisation along grain boundaries. The alteration highlights the irregular magnetite grains forming the lath.
Thin section: M7563, WDUD 487, 32m, 5235E
FOV= .43mm

PLATE 10c

Approaching complete martitisation (light grey) of magnetite (mid grey) and the growth of hematite laths within a cavity. Yellow - chalcopyrite.
Thin section: M7511, WDUD 468, 29m, 5205E
FOV= .87mm

PLATE 11

Pyrite (white) intergrown with magnetite (mid grey) and quartz (dark grey). The pyrite is irregular shaped and fractured indicating it formed early and in equilibrium with the magnetite and quartz.
Thin section: M7558, WDUD 487, 8m, 5235E
FOV= 3.5mm

PLATE 12

Remnant chlorite within magnetite-quartz of the Pinter ironstone. The chlorite occurs along the boundaries of several quartz grains and appears to have been replaced by the quartz. The chlorite was microprobed and will be discussed in chapter 6.

Thin section: M7561, WDUD 487, 6.5m, 5235E
FOV= 3.5mm

PLATE 13a

Coarse grained chlorite infilling the gaps between magnetite in magnetite chlorite rock.

Thin section: M7563, WDUD 487, 32m, 5235E
FOV= 3.5mm

PLATE 10a

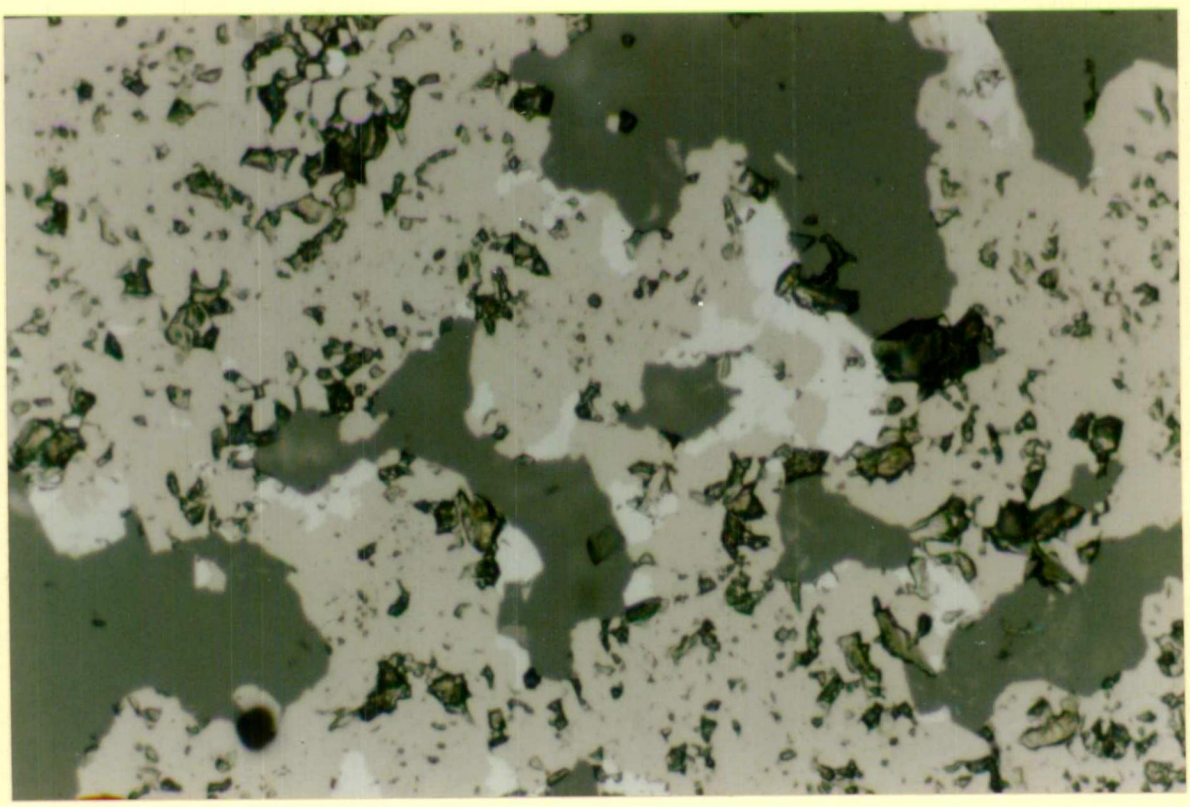

PLATE 10b

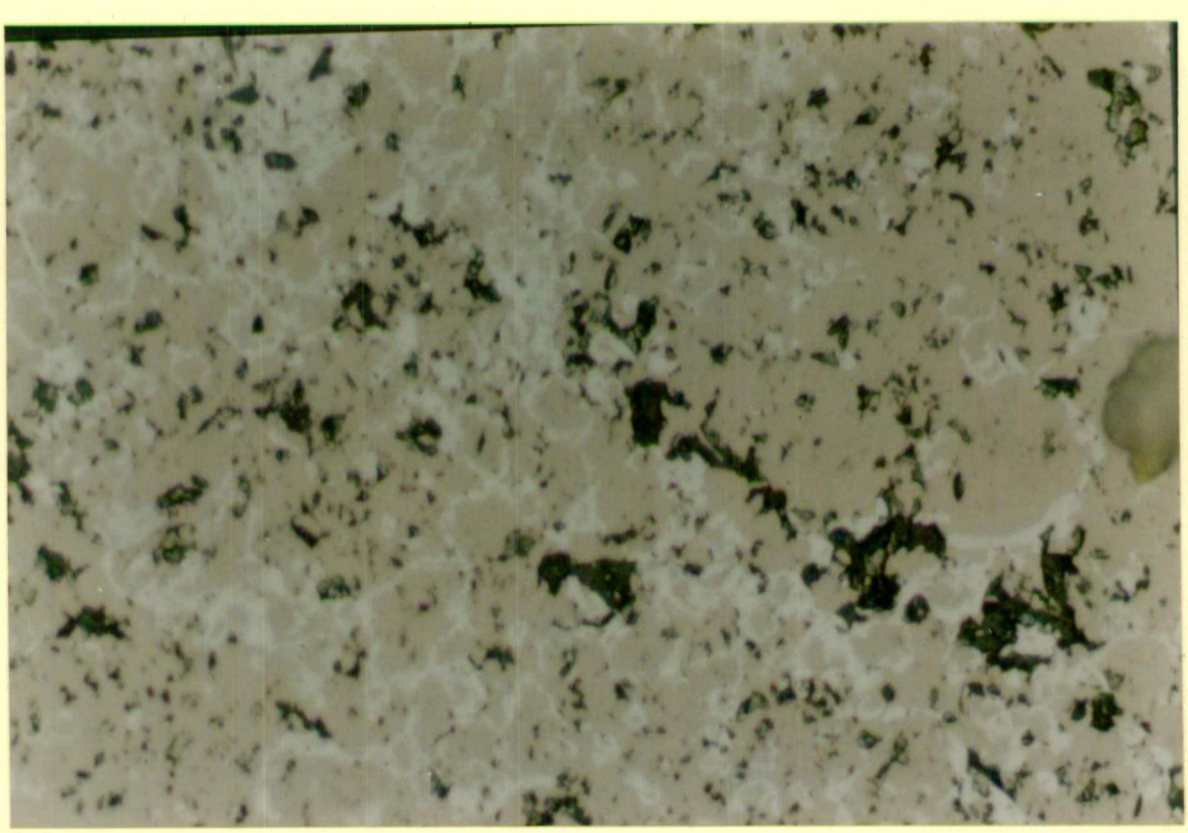

PLATE 10c

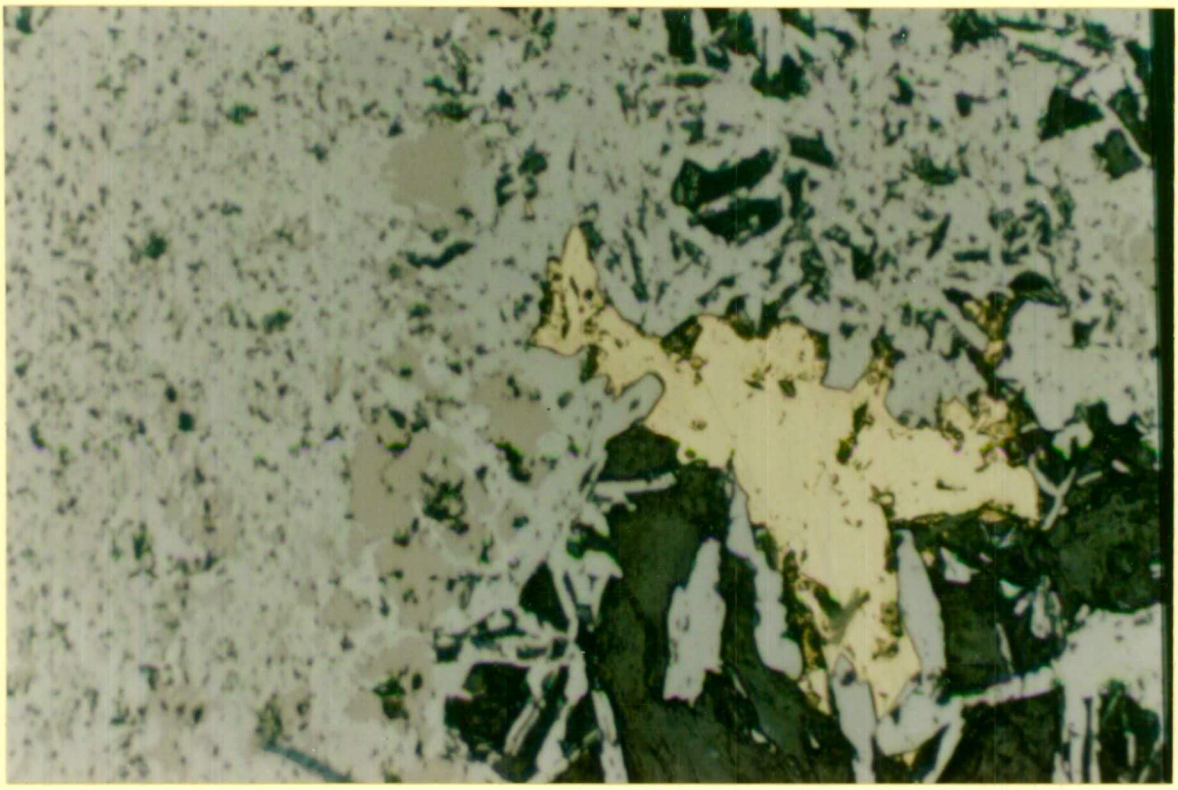

PLATE 11

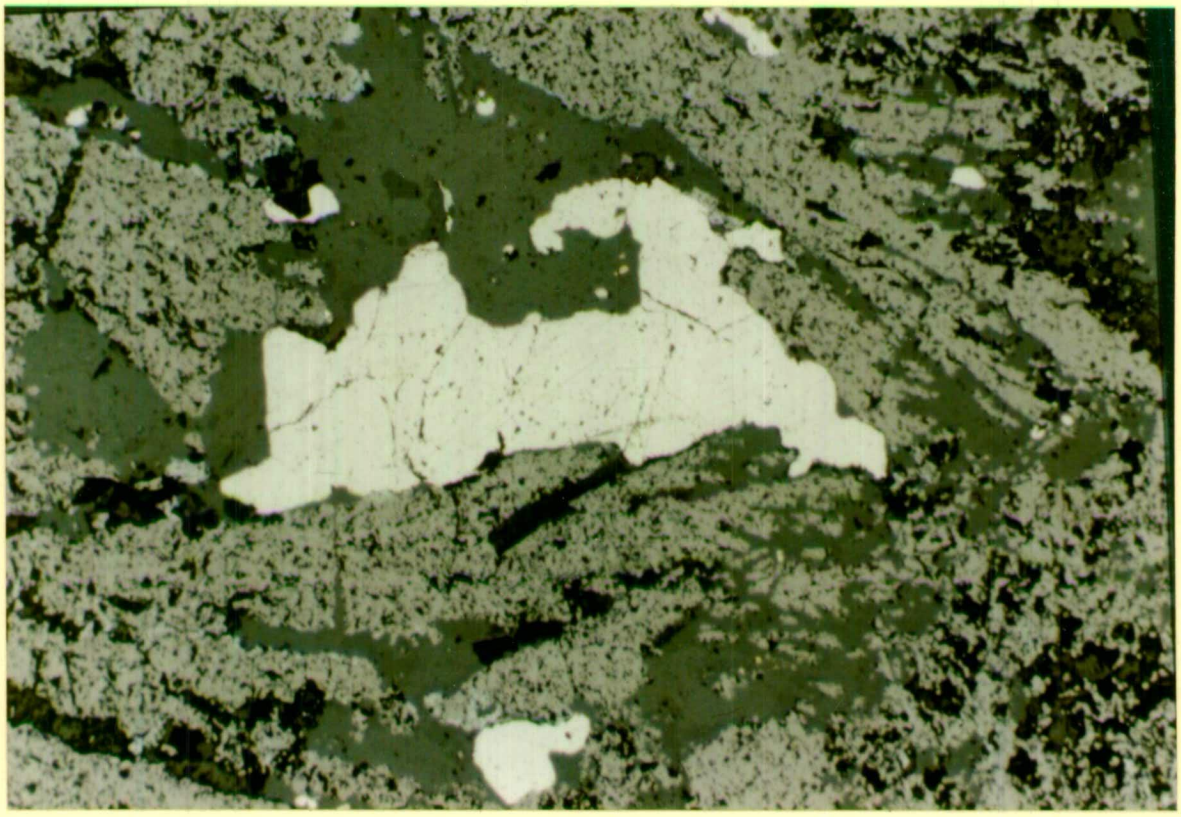

PLATE 12

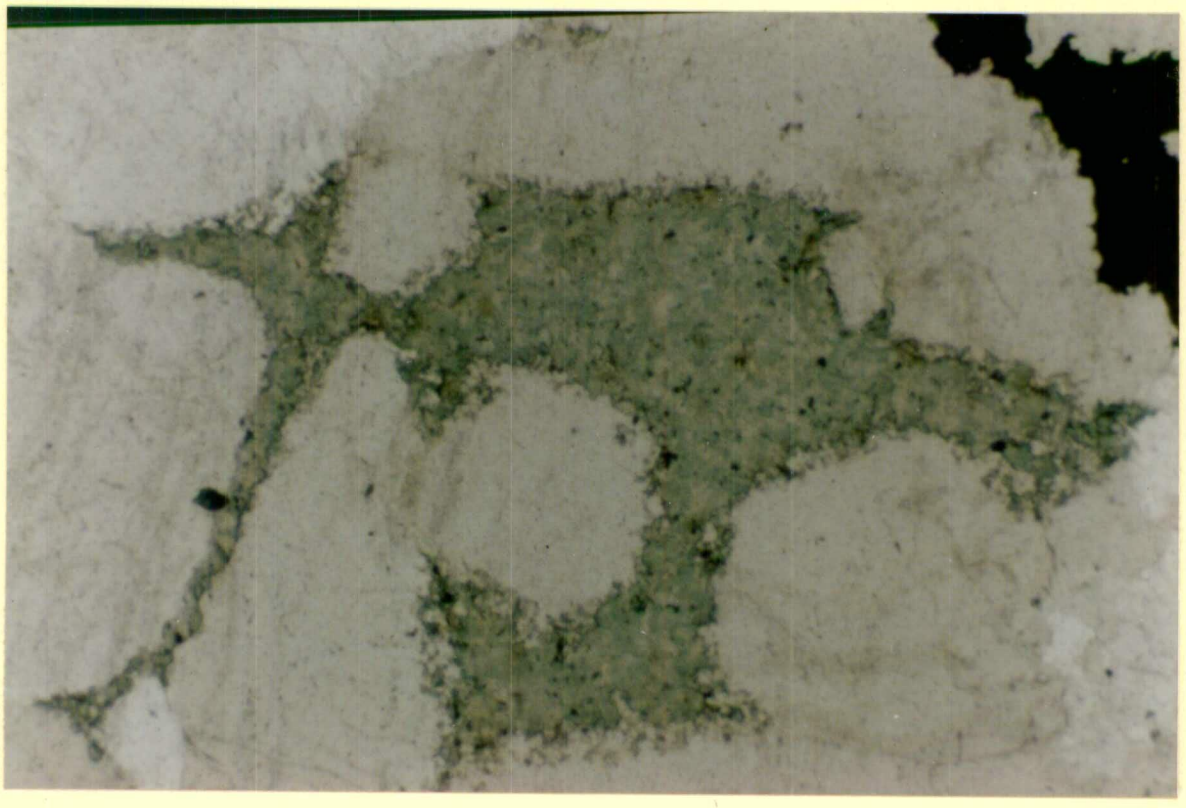

PLATE 13a

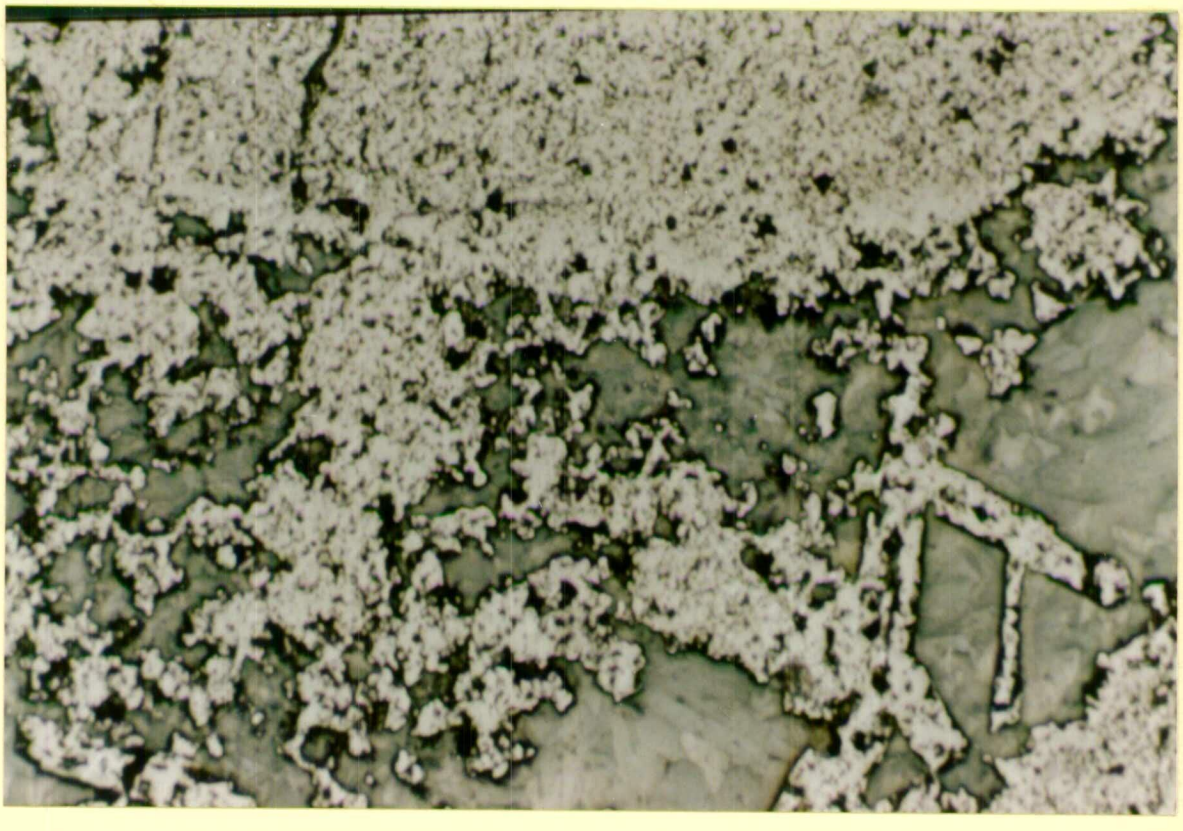

PLATE 13b

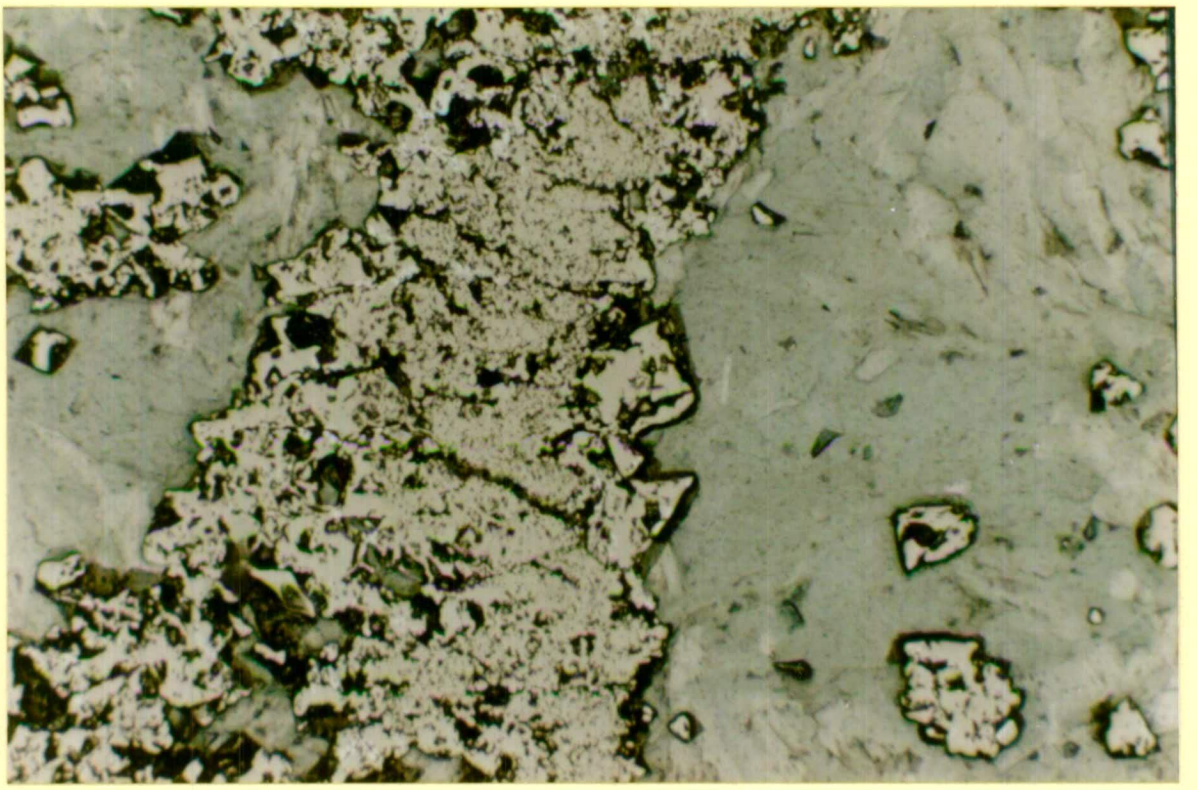

PLATE 14a

PLATE 13b

Magnetite lath within coarse grained chlorite. The chlorite also occurs within the lath. Subhedral grains of magnetite occur within the unfoliated chlorite. Note also the magnetite overgrowths on the lath.
Thin section: M7563, WDUD 487, 32m, 5235E
FOV= 1.7mm

PLATE 14a

Magnetite-talc-chlorite rock. Talc - light grey, chlorite - green, magnetite - black.
Core: WDUD 273, 49m, 5135E

PLATE 14b

Coarse grained chlorite being altered to talc, with the talc retaining the chlorite texture. Light green to white - talc, green - chlorite, orange - chalcopyrite, brown - magnetite.

Thin section: M7559, WDUD 487, 8m, 5235E
FOV = 1.7mm

PLATE 14c

Chlorite completely altered to talc. The talc still retains the coarse chlorite texture.

Thin section: M7558, WDUD 487, 8m, 5235E
FOV = .87mm

PLATE 14b

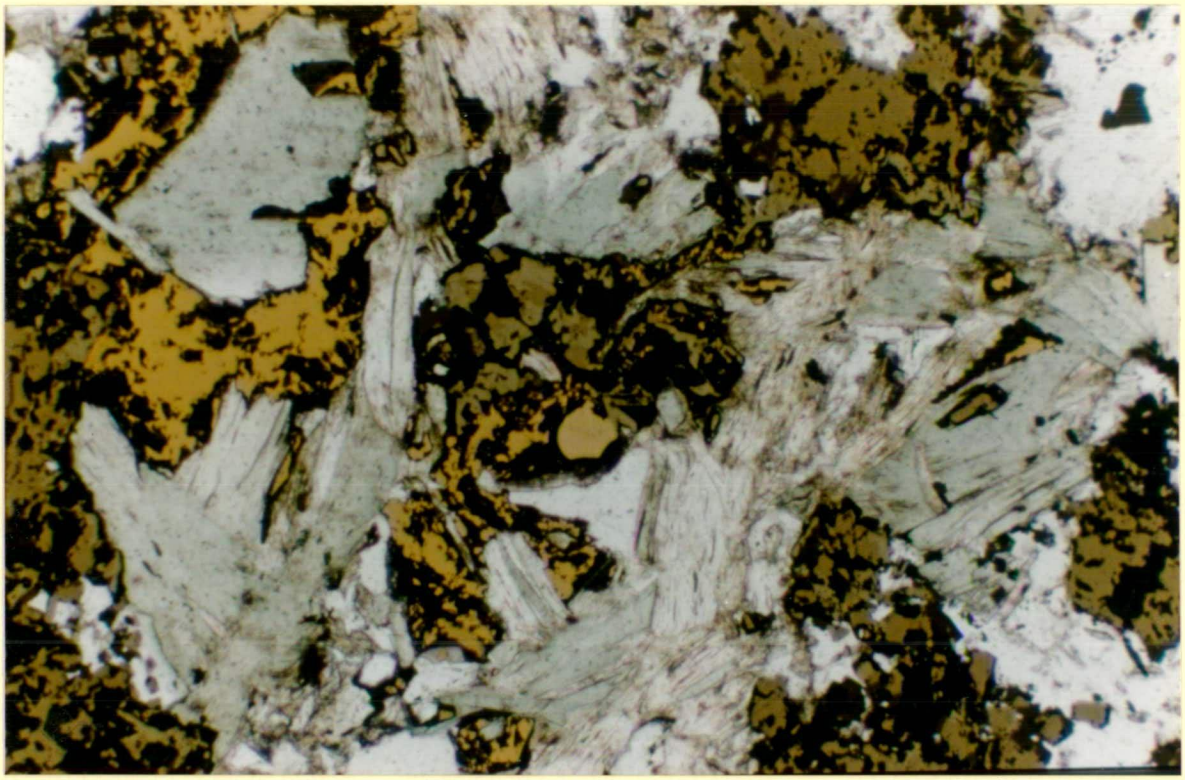

PLATE 14c

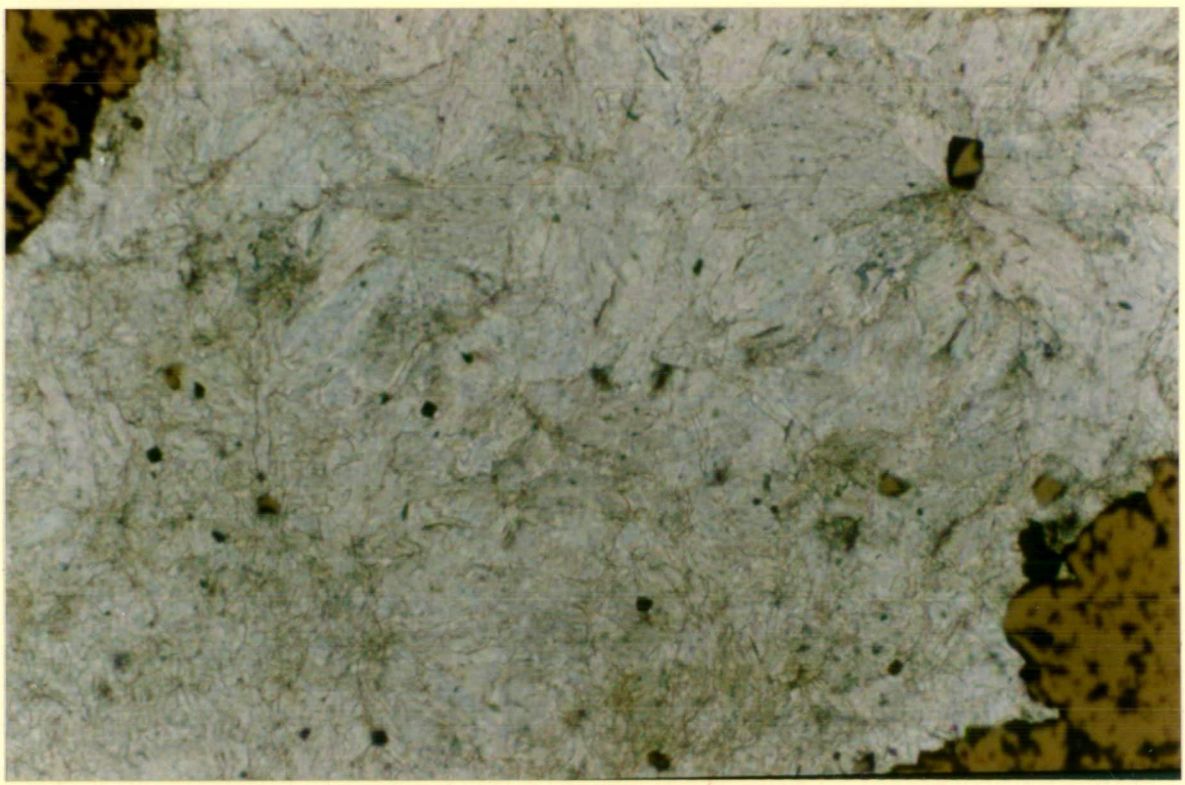

chlorite. The chlorite has been analysed using an electron microprobe and the results are discussed in chapter 6.

Elsewhere within the ironstone the chlorite occurs as large laths filling gaps between magnetite (Plates 13a,b)

Two visibly and compositionally different chlorites (Nguyen et al 1989, Edwards et al 1990, Huston et al in press) have been observed at White Devil, an early phase associated with ironstone formation and a later phase associated with the mineralising event. Both these chlorites can be seen in the ironstone depending on the proximity to mineralisation, but generally only the earlier phase is present.

Talc

Talc occurs as an alteration product of chlorite and as primary talc and is not confined to the ironstone.

Within the ironstone the alteration forms a magnetite-talc-chlorite rock, where the magnetite forms a skeletal structure filled with talc and chlorite (Plate 14a). Plates 14b and 14c shows talc partly and completely replacing chlorite, with the talc taking on the texture of the chlorite laths. Zones of fine grained talc also surround the replaced chlorite.

4.2.3 Southern, Tabular Ironstone

This ironstone consists of predominantly magnetite and minor chlorite. Thin section M7543 (5155E) of the Main Zone ironstone consists of a coalesced mass of small magnetite laths with the gaps filled with chlorite.

Within the ironstone are small fracture or breccia zones and the contact with the altered sediments is fractured with small fragments of magnetite incorporated into the altered sediment.

The tabular ironstone is essentially a small version of the large ironstone.

4.2.4 Stringer Zone

The magnetite-altered sediment stringer zone consists of what are essentially "mini" ironstones in a highly chloritically altered and sheared sediment host. The magnetite stringers have similar shape and texture to the larger ironstones.

The lensoidal stringers are aligned sub parallel to the shear and have undergone extension fracturing as shown in Plate 15. This photo shows a fractured stringer within fine grained altered sediments. The fracture has been filled with coarse grained unfoliated chlorite. Nguyen et al (1989) noted the presence of north-south extension cracks in stringers and the shear zone, indicating that brittle deformation occurred during the latter part of the ductile shearing event.

In thin sections M7540 & 42 (5155E) and M7508 (5245E) overgrowths of magnetite were observed in the fractures in the stringers, indicating the deformation occurred whist magnetite was replacing the hematite laths and overgrowth magnetite was being formed. Overgrowths of magnetite also occur on the edges of laths, in vugs and fractures. These stringers are fractured parallel to the shear indicating the stringers acted as rigid bodies within the shear and were subsequently fractured. The stringers display some open space filling (Plate 16) and the coarse grained unfoliated chlorite indicates the fracture acted as a low pressure zone and was not subject to further shearing (Plate 17). The chlorite within the fracture has the same colour as in the chloritic sediment.

The stringers have the same spongy texture as the larger ironstone, indicating they formed in a similar manner. Also within the altered sediments are numerous single subhedral magnetite grains which appear to have grown within the altered sediment. In thin section M7538 (5155E) individual laths can be observed within the fine grained chloritic groundmass and in thin section M7555 individual subhedral magnetite grains occur within coarse grained chlorite.

4.3 SUMMARY

The ironstones and stringers consist of a skeletal or spongy mass of intergrown magnetite laths pseudomorphed after hematite.

Primary magnetite occurs as subhedral to euhedral overgrowths on the laths and as single grains and small masses in coarse grained chlorite in the Stringer zone and contact zone of the Tabular Ironstone.

Fractured pyrite occurs intergrown with the magnetite laths and chlorite, quartz and talc occur between the laths.

The ironstone has undergone partial hematisation due to martitisation, particularly the Deeps Ironstone-porphyry contact and the edges of the Pinter Ironstone.

The Tabular Ironstone, Stringers and southern margin of the Deeps and Pinter Ironstone show brittle deformation.

PLATE 15

Fractured magnetite stringer within fine grained chloritic sediment. Stringer is extended in direction of shear.
Thin section: M7541, WDUD 285, 54m, 5155E
FOV= 3.5mm

PLATE 16

Open space quartz and chlorite growth within fractured magnetite stringer in magnetite chlorite-altered sediment rock within the Deeps ore zone.
Thin section: M7538, WDUD 285, 36m,5155E
FOV=3.5mm

PLATE 15

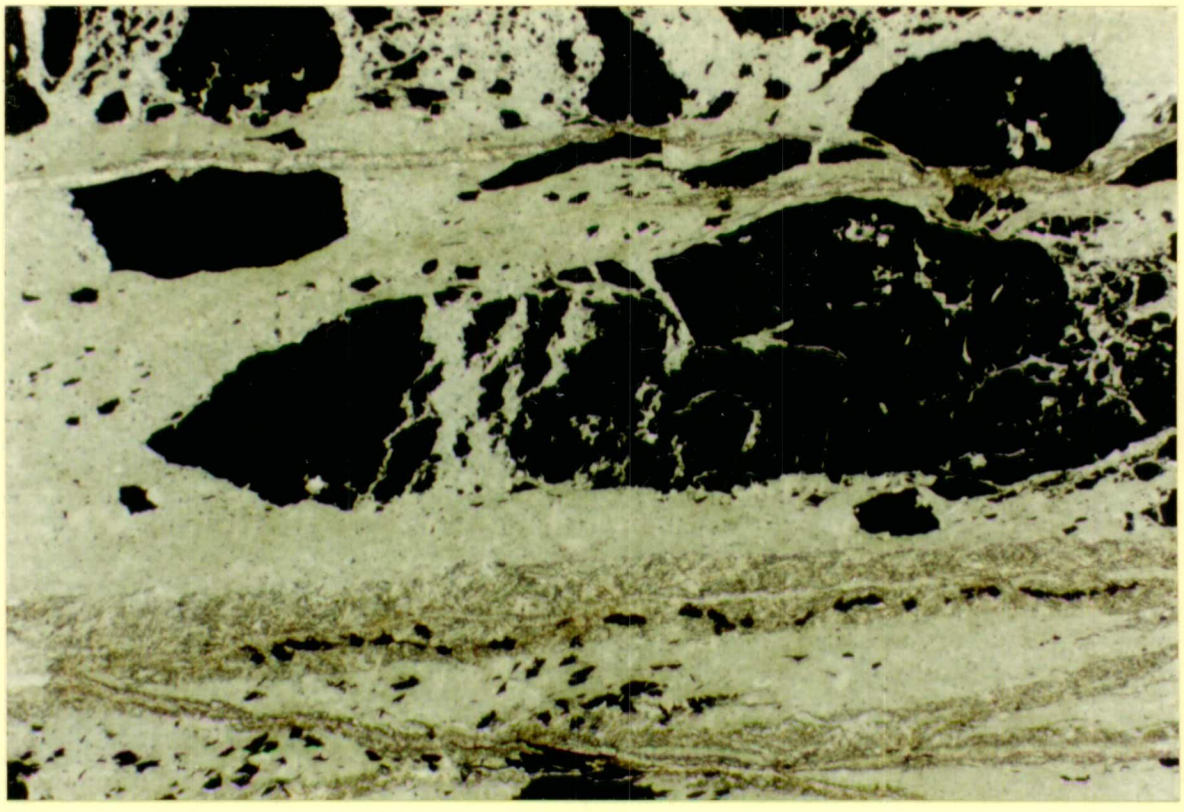

PLATE 16

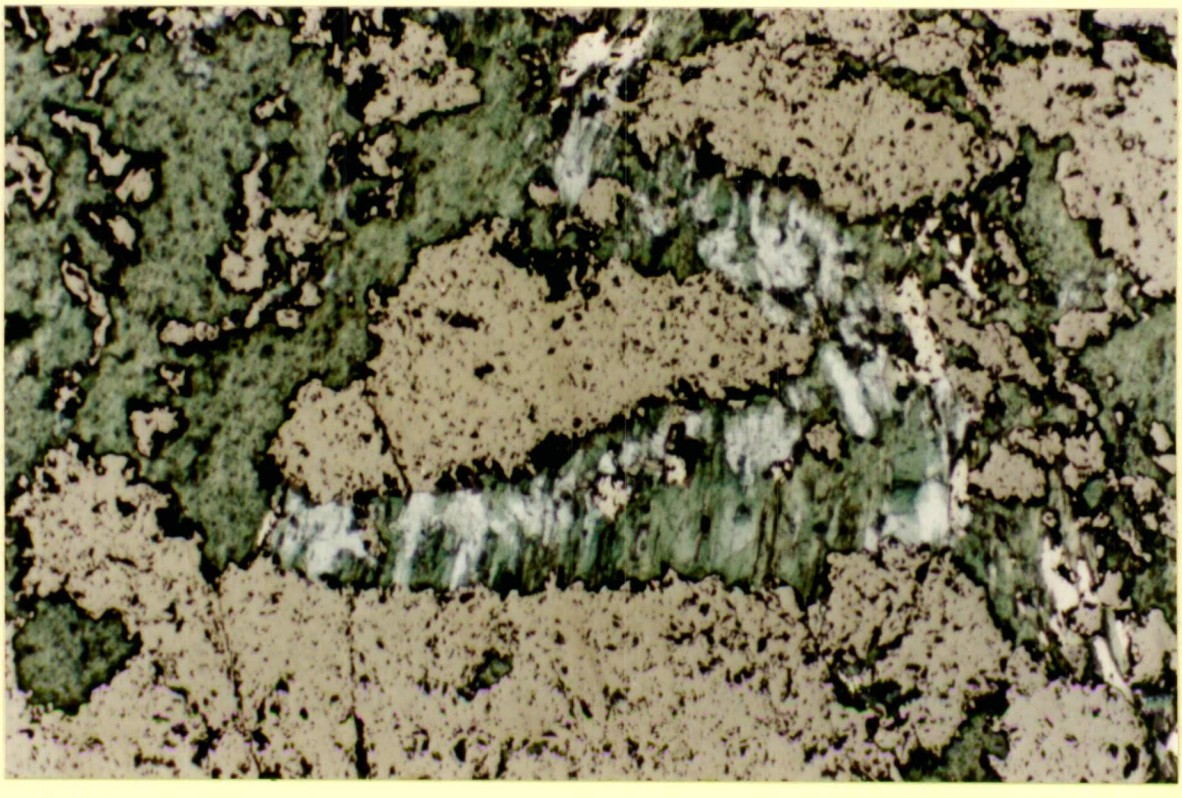

PLATE 17

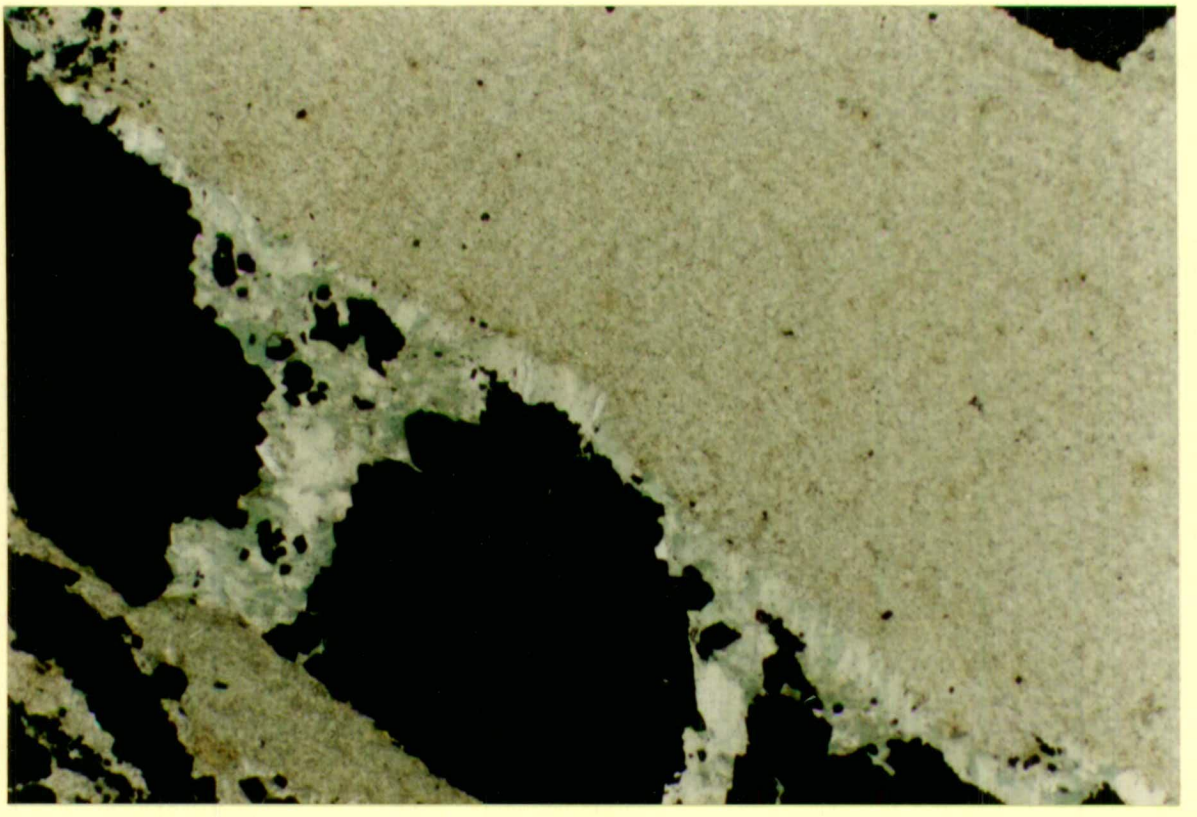

PLATE 17

Fractured magnetite stringer within fine grained chloritic altered sediment. The fractures have been filled with coarse grained unfoliated chlorite. The chlorite in the altered sediment is foliated in the shear direction.

Thin section: M7514, WDUD 359, 24.5m, 5095E
FOV= 3.5mm

5 OREBODIES

At White Devil two styles of gold, bismuth, copper mineralisation occur:

*i. **Main Zone style***: hosted within highly chloritic sediments and magnetite stringers on the contact of the Tabular Ironstone. Examples of this style are the Main Zone, West Lodes and several of the Pinter Lodes.

*ii. **Deeps style***: is more akin to the characteristic Tennant Creek Model developed by Large (1975), where the mineralisation is hosted by magnetite chlorite towards the base of a large ironstone.

The Main Zone and Deeps orebodies are discussed in detail in the next sections.

The term `bismuth sulphosalts' is used as a general term for the bismuth minerals present.

5.1 MAIN ZONE

The Main Zone orebodies occur between 5075E and 5180E, from 930RL to below 700RL. These orebodies are narrow, 1-2m wide, located between the footwall Tabular Ironstone and a strong hangingwall shear, on the northern side. Generally the shear marks a decrease in the magnetite content of the altered sediments.

The ore is hosted within magnetite stringers and chlorite within the altered sediments. The magnetite content is variable, between approximately 30% and 90%. Minor mineralisation occurs within the contact zone of the ironstone, in magnetite chlorite or magnetite-altered sediments.

Gold

The gold is scattered irregularly throughout the orebody. The gold mineralisation contains abundant associated pyrite, minor bismuth sulphosalts occurring as high grade patches and minor copper generally towards the hanging wall. The detailed metal distribution is discussed in section 5.5.

In thin section M7514 (5095E), from the Lower Main Zone, the gold occurs within magnetite laths (Plate 18a), intergrown with bismuth sulphosalts, within coarse grained chlorite (Plate 18b) and associated with chlorite and quartz. In M7514 a large gold grain (90um) intergrown with bismuth sulphosalts and chalcopyrite occurs between magnetite laths within coarse grained chlorite.

Bismuth and Chalcopyrite

Both bismuth sulphosalts and chalcopyrite occur in a similar manner to gold, within vugs in the magnetite laths and within coarse grained chlorite. The occurrences of the coarse grained chlorite have been discussed in Chapter 4 and will be further discussed in the Chapter 6.

5.2 DEEPS OREBODY

The Deeps orebody consists of two subparallel lenses which coalesce to form a single body of 25 m thickness on the 5165E section (Figures 4 & 5). Although similar in gold grade the host rocks vary slightly. The southern lens is hosted by the magnetite chlorite-altered sediment breccia and altered sediment with magnetite stringers, within the ductile to brittle deformation transition zone. The northern lens is hosted by magnetite chlorite-altered sediment and within the magnetite chlorite zone of the large ironstone.

The orebody is predominantly gold with associated bismuth sulphosalts. On the 5135E and 5145E sections a large pod of bismuth sulphosalts mineralisation is hosted within sigmoidal tension gashes within the ironstone.

CYMOIDAL?

Gold

The gold occurs as individual grains within magnetite and coarse grained chlorite (Plate 19a) and as minute veins in magnetite (Plate 19b). The occurrence of gold well within the magnetite lath indicates that the magnetite maintained a porosity

which allowed introduction of the mineralising fluids. It may be argued that the vug filling gold entered the lath along a fracture not visible on the thin section, i.e. in the 3rd dimension. This is unlikely as numerous grains of gold were observed within laths from different thin sections and only one, (Plate 19b), was observed associated with a fracture.

The gold also occurs intergrown with bismuth sulphosalts and chalcopyrite within magnetite laths and between laths associated with coarse grained chlorite. Plate 20a shows a gold grain and several bismuthinite grains within skeletal magnetite and coarse grained chlorite. Both the gold and bismuth sulphosalts completely fill the spaces and have sharp contacts with the magnetite but not with the chlorite indicating the gold and bismuth sulphosalts co-precipitated with the chlorite. Plate 20b shows an intergrowth of gold and bismuth sulphosalts within magnetite and coarse grained chlorite, magnetite chlorite rock. A grain of gold can be seen within a vug in the magnetite. In thin section M7546A (5160E) gold fills a fracture within early pyrite. The same pyrite grain contains two remnant arsenopyrite grains.

Plate 20c shows an intergrowth of gold, bismuthinite and chalcopyrite within magnetite and chlorite. The texture of the magnetite in the plate is different to the majority of the ironstone as it is subhedral and forms individual grains. This magnetite is primary as opposed to replacement and grew within chlorite in an almost open space during or immediately post replacement process. The magnetite grains have undergone selective hematite alteration.

The gold is distributed randomly throughout the magnetite chlorite. In the magnetite chlorite-altered sediments the gold occurs in the chlorite-magnetite stringers surrounding the altered sediments.

Apart from being associated with gold, bismuth sulphosalts and chalcopyrite occur as intergrowths within the ironstone (Plate 21a), in sigmoidal tension fractures intergrown with chlorite (Plate 21b) and within chlorite and quartz.

PLATE 18a

Gold grain within magnetite lath in Lower Main Zone Orebody.
Thin section: M7514, WDUD 359, 24.5m, 5095E
FOV = 3.5mm

PLATE 18b

Gold grain and bismuth (light grey) within coarse grained chlorite in Main Zone Orebody.
Thin section: M7543, WDUD 285, 56.4m, 5155E
FOV = 0.87mm

PLATE 18a

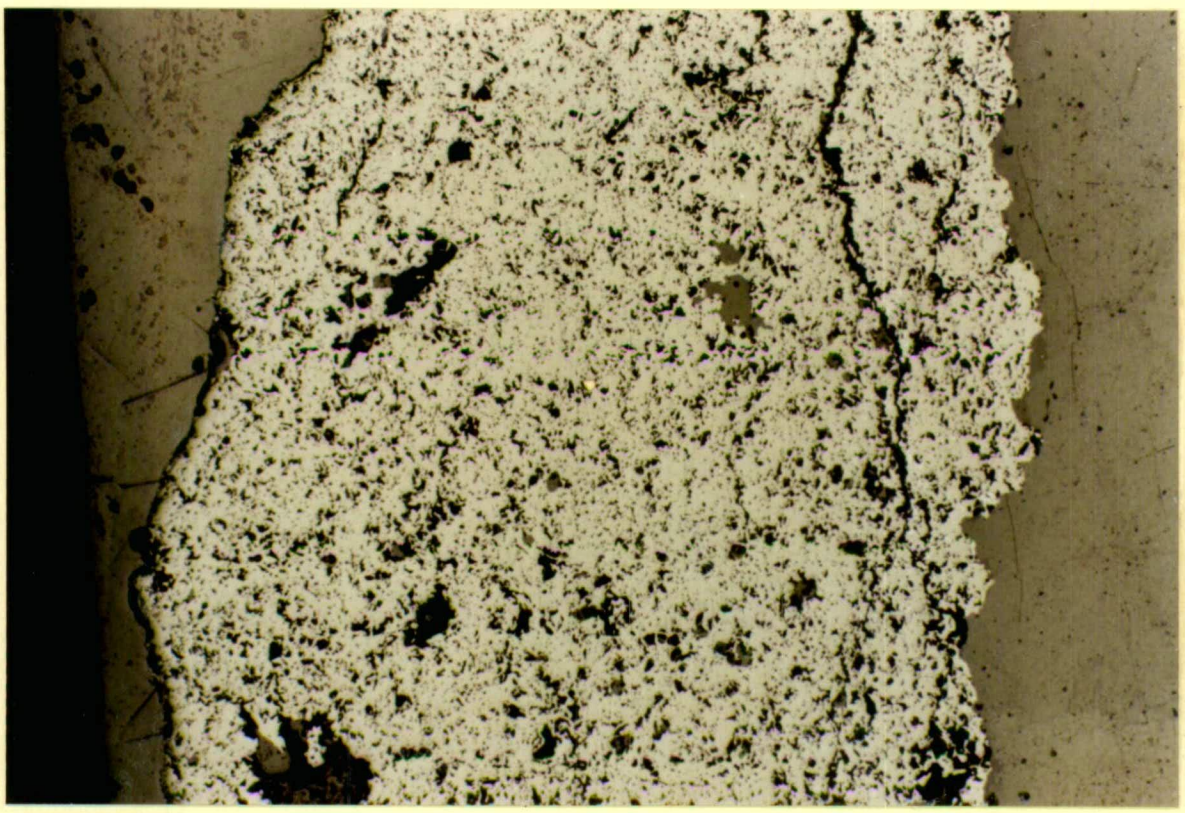

PLATE 18b

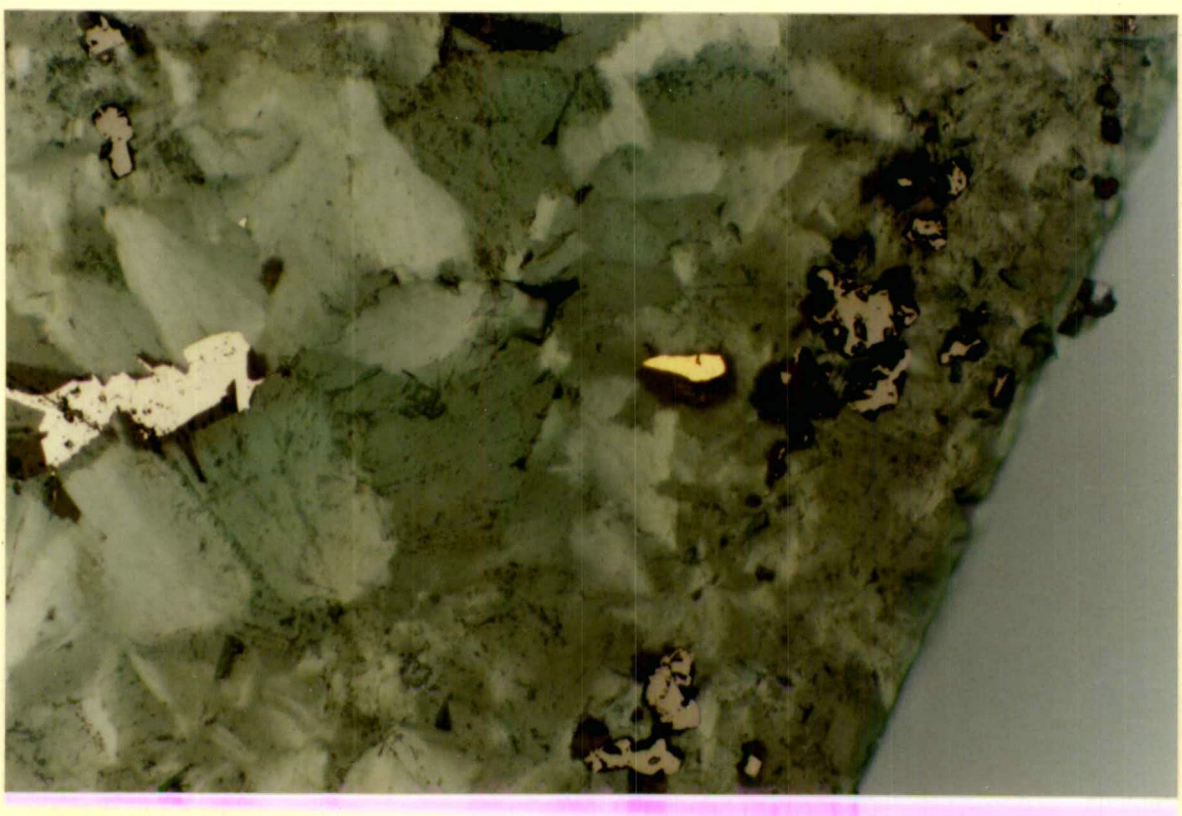

PLATE 19a

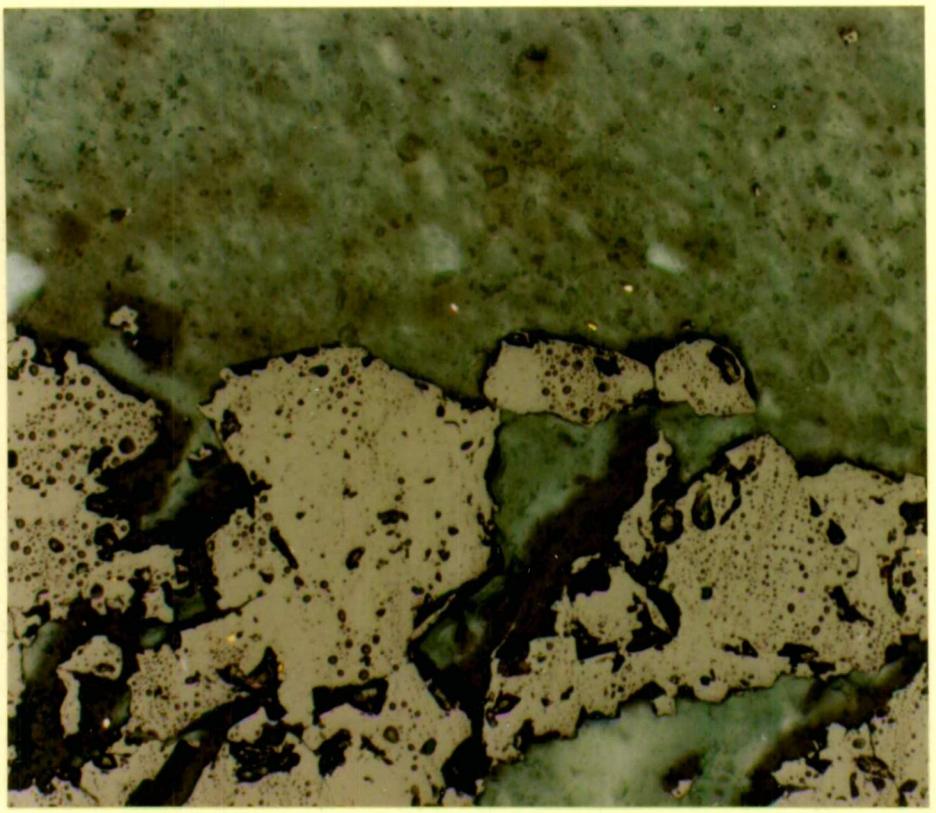

PLATE 19b

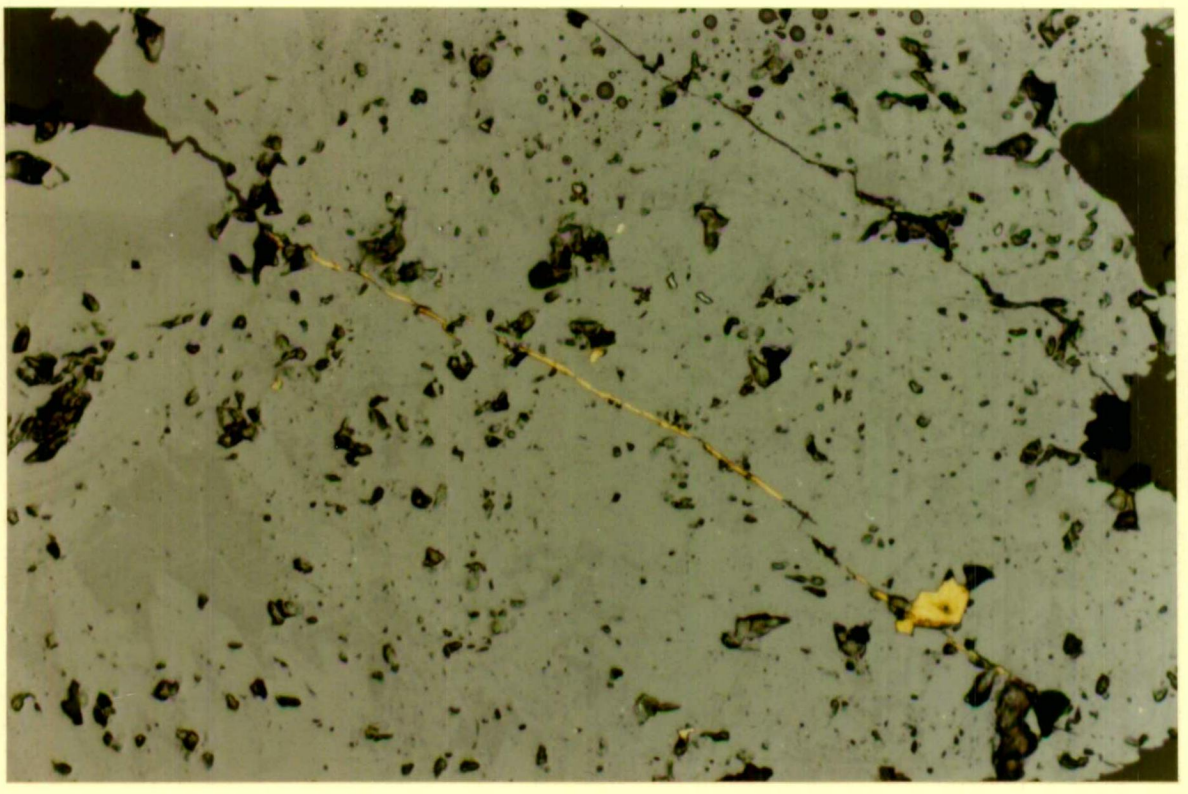

PLATE 19a

Gold grain in magnetite and coarse grained chlorite in Deeps Orebody (north lens).
Thin section: M7539, WDUD 285, 39.7m, 5155E
FOV = 0.87mm

PLATE 19b

Gold occurring as bleb in vug and as minute vein along fracture in south lens of Deeps Orebody.
Thin section: M7542, WDUD 285, 48.6m, 5155E
FOV = 0.43mm

PLATE 20a

Gold and bismuthinite within skeletal magnetite (mid grey) in the north lens of the Deeps Orebody. Gold and bismuthinite (light grey) infill gaps between magnetite and is intergrown with the chlorite (dark grey).
Thin section: M7538, WDUD 285, 36.1m, 5155E
FOV= 0.87mm

PLATE 20b

Intergrowth of gold and bismuth (light grey) magnetite (mid grey) and chlorite (dark grey) in magnetite chlorite of the north lens of the Deeps Orebody.
Thin section: M7538, WDUD 285, 36.1m 5155E
FOV=0.87mm

PLATE 20a

PLATE 20b

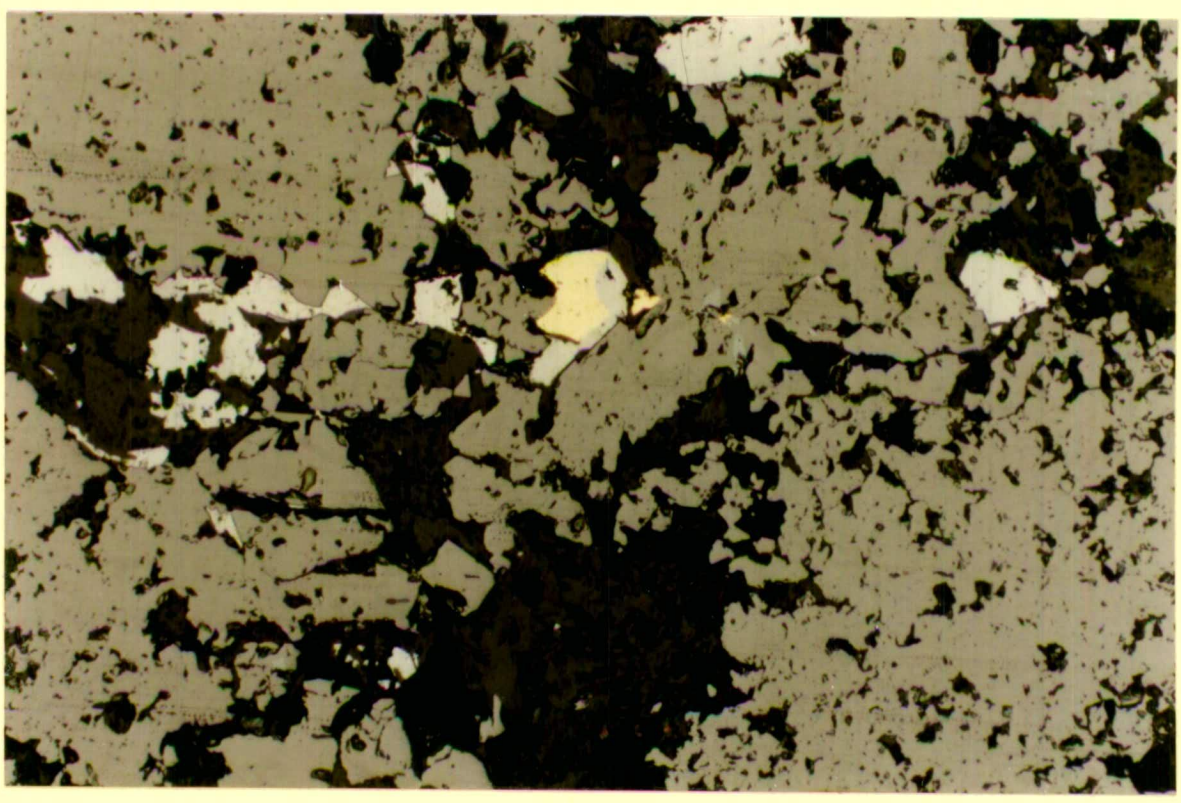

PLATE 20c

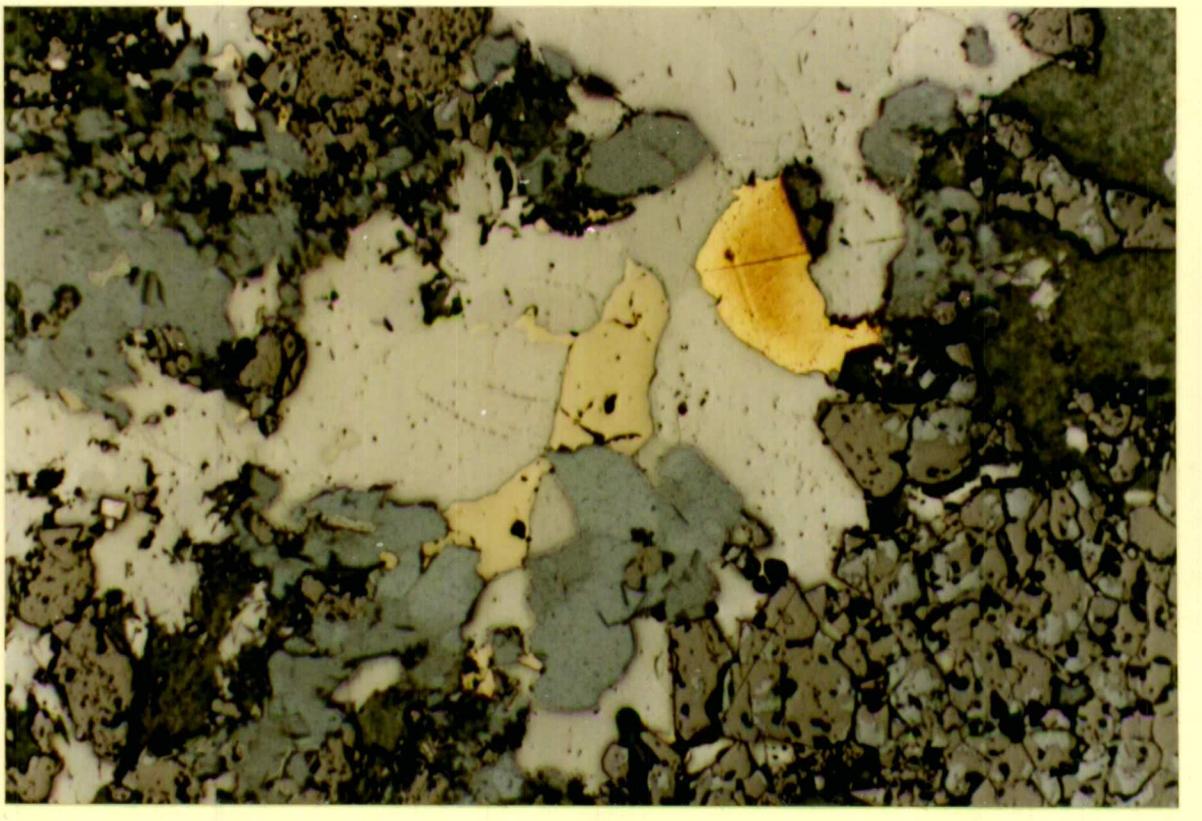

PLATE 21a

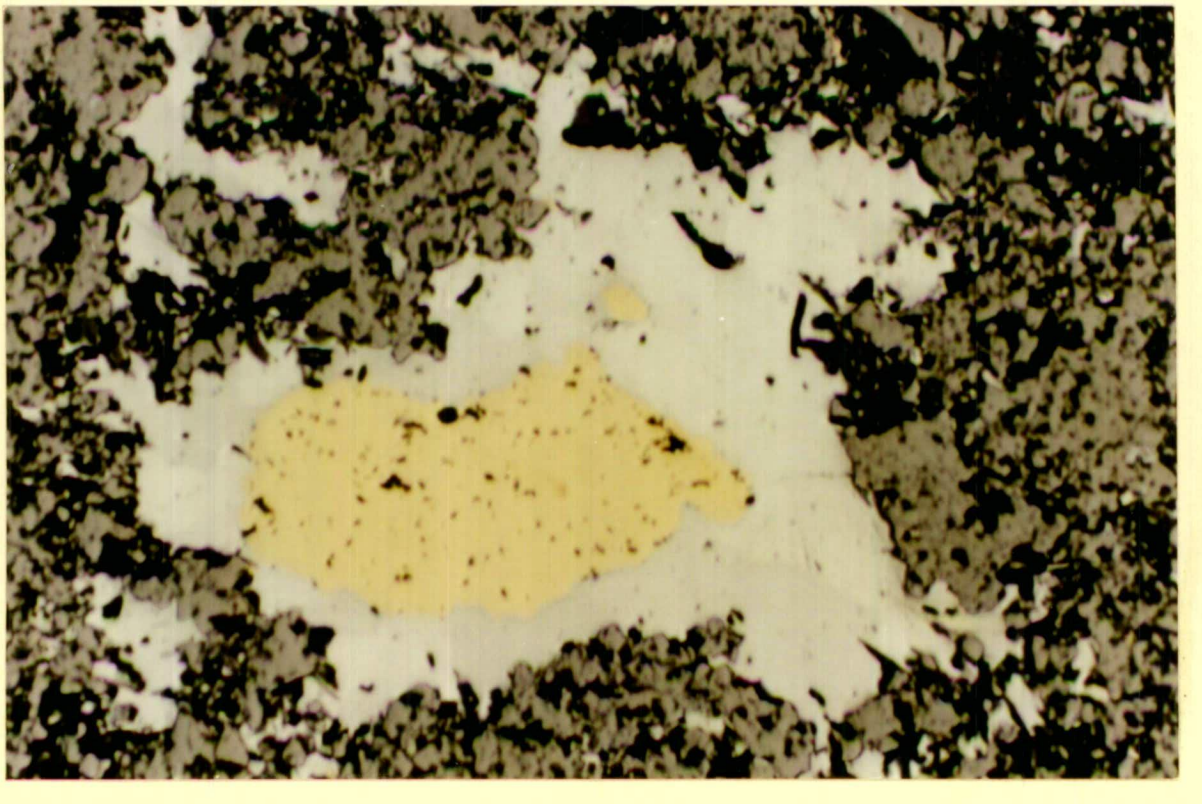

PLATE 20c

Intergrowth of gold (dark yellow), bismuthinite (high relief grain, left edge), chalcopyrite (blue green) and pyrite (pale yellow), surrounded by quartz (light grey) and magnetite in the Deeps Orebody. The unusual colours are due to uneven polishing.

Thin section: M7546a, WDUD 312, 6.4m, 5160E
FOV=3.5mm

PLATE 21a

Intergrowth of chalcopyrite and bismuthinite in magnetite adjacent to the Deeps Orebody.

Thin section: M7537, WDUD 285, 27.7m, 5155E
FOV= 3.5mm

PLATE 21b

Bismuth and chlorite within sigmoidal tension gashes in magnetite ironstone of the Deeps ironstone. This texture is described as `ribbon texture' by Edwards et al (1990).
Core: 5145E

PLATE 21c

Myrmekitic intergrowth of bismuthinite (light grey) and emplectite (grey-brown) in magnetite, adjacent to the Deeps Zone.
Thin section: M7541, WDUD 285, 54.4m, 5155E
FOV = 0.43mm

PLATE 21b

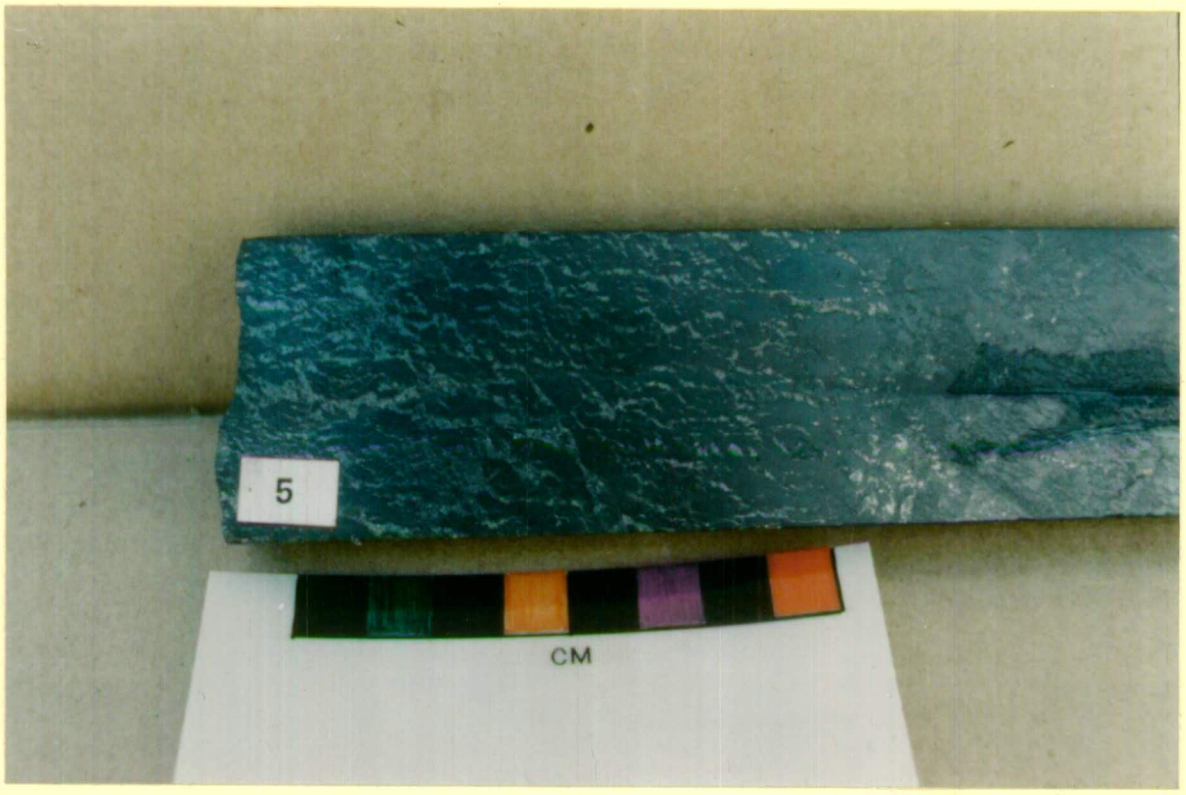

PLATE 21c

PLATE 22

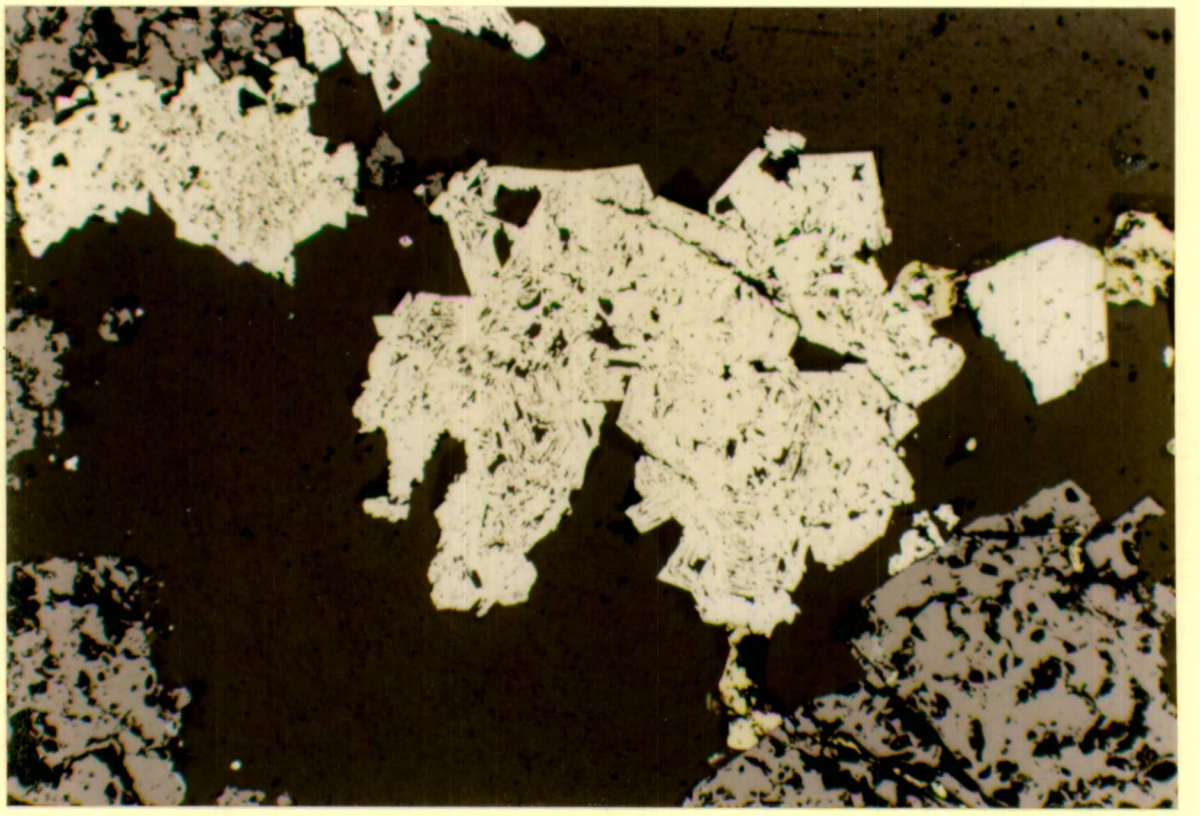

PLATE 23

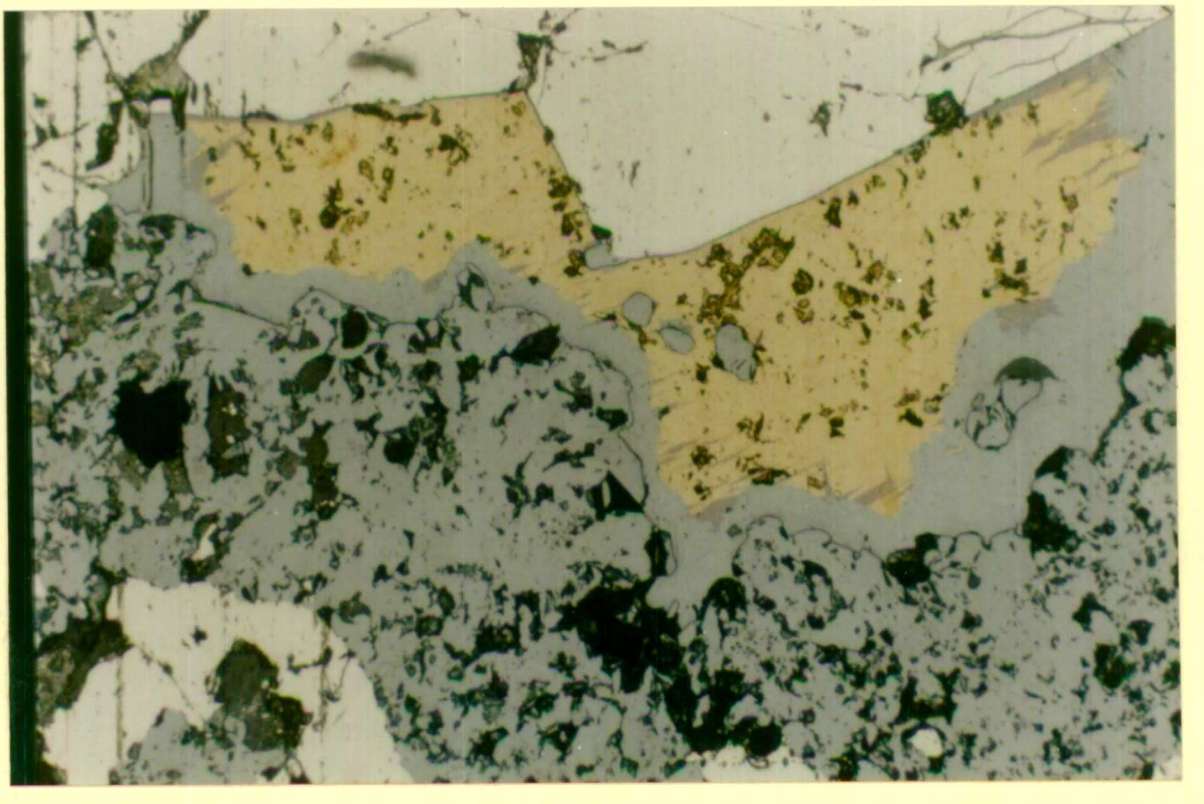

PLATE 22

Skeletal pyrite intergrown with chalcopyrite and quartz and overgrown on magnetite, adjacent to the Deeps Ironstone. The skeletal texture of the pyrite suggests rapid growth.

Thin section: M7540, WDUD 285, 45m, 5155E
FOV= 1.7mm

PLATE 23

Chalcopyrite with rim of chalcocite and bornite alteration in contact with hematised magnetite (martitised) and early pyrite within the large ironstone on 5205E.

Thin section: M7510, WDUD 468, 26.8m, 5205E
FOV= 0.87m

Bismuth Sulphosalts

The two common bismuth sulphosalt minerals are bismuthinite and emplectite. In thin section M7544 (5155E) bismuthinite occurs as large angular blobs and needle-like clusters intergrown with quartz within gaps between the magnetite laths. The bismuthinite also contains euhedral pyrite grains and chlorite laths. In thin section M7542 (5155E) bismuthinite occurs as an overgrowth on early pyrite and intergrown with later pyrite in chalcopyrite. In thin section M7538 (5155E) bismuthinite occurs with chlorite in pull apart fractures in magnetite laths. The bismuthinite grains are orientated in the same direction as the chlorite laths, indicating the two minerals deposited together and the chlorite controlled the orientation of the bismuthinite grains. Plate 21c, M7541 (5155E) shows a myrmekitic intergrowth of bismuthinite and emplectite within magnetite.

Chalcopyrite

Chalcopyrite occurs in the magnetite chlorite in much the same manner as the bismuth sulphosalts, as vug fillings within magnetite, intergrown with chlorite and quartz. In thin section M7536 (5155E) chalcopyrite occurs between hematite needles growing into a quartz vein, indicating that martitisation was occurring during chalcopyrite precipitation or that the chalcopyrite precipitation continued into the martitisation phase. The second option is consistent with the model proposed by Huston et al (in press). Also in this thin section, within the quartz vein, a bismuth sulphosalts grain contains a small chalcopyrite grain and is rimmed by numerous small hematite crystals, indicating that this bismuth sulphosalts grain had finished precipitating prior to martitisation.

5.3 OTHER MINERALISATION

This section covers ore and accessory minerals not of economic interest and includes bornite, chalcocite, pyrite, marcasite, sphalerite, galena, monazite, rutile, carbonates and hematite. The occurrence of chalcopyrite and bismuth sulphosalts outside the ore zone is also discussed.

Pyrite

Within both the Deeps and Main Zone orebodies pyrite was deposited with gold mineralisation. Plate 22 shows rapidly grown subhedral to euhedral skeletal pyrite within quartz and as an overgrowth on magnetite and intergrown with chalcopyrite. The subhedral to euhedral boundaries indicated that precipitation slowed down and that the pyrite was growing in an "open space".

In the Main Zone pyrite occurs as subhedral overgrowths on magnetite and is intergrown with quartz and chlorite. This pyrite is not fractured, indicating it formed post deformation and post magnetite deposition.

Within the magnetite-talc on 5095E (TS M7513) a large pyrite grain contains overgrowths and inclusions of later stage marcasite.

Hematite

Minor hematite alteration along fractures within the magnetite laths was observed in the Main Zone. The paragenetic model proposed by Huston et al (in press) infers that the alteration of magnetite to hematite drove the chemical reactions that precipitated the ore minerals. If this is the case then this alteration is not part of the martitisation process.

Chalcopyrite

Outside the orebodies chalcopyrite generally occurs within fracture veins with chlorite and quartz in the ironstone or scattered throughout the stringer zone and altered sediment.

On section 5205E (TS M7510) chalcopyrite has been altered to bornite and chalcocite during martitisation (Plate 23). The chalcopyrite is attached to an early pyrite grain within hematised magnetite. The chalcocite alteration forms a rim around the chalcopyrite and the bornite occurs as slivers or grain boundary alteration within the chalcopyrite and chalcocite.

Within the large ironstone on 5135E chalcopyrite, intergrown with quartz, occurs within a fracture in an early pyrite grain. The chalcopyrite has a rim of chalcocite, digenite-covellite and late stage carbonates fill the remaining spaces.

Sphalerite and Galena

On 5255E (TS M7501) in the dolomite at the base of the Pinter ironstone, sphalerite, galena and chalcopyrite are intergrown with dolomite and magnetite. The chalcopyrite has undergone minor alteration to covellite and a grain of sphalerite with chalcopyrite disease was observed. Recent work by Bortnikov et al (1991) on Russian deposits containing chalcopyrite diseased sphalerite concluded that it could be formed by either replacement of Fe rich sphalerite by chalcopyrite or by co-precipitation.

Galena and sphalerite have also been reported in a deep drillhole beneath the Main Zone, and in thin sections studied by Huston (pers comm).

Monazite

In M7501 (5255E) and M7505 (5265E) several cubic and irregular grains with very high birefringence colours, within altered sediment, were observed. In M7501 the grain was intergrown with magnetite and in M7505 it was intergrown with sulphide stage pyrite. Microprobe analysis revealed the grains to be monazite -

(Ce,La,Nd,Sm,Gd)PO4. Several grains of rutile, as single grains and overgrowths on pyrite, were also observed within altered sediments.

Bismuth

The magnetite-quartz ironstone on 5135E (TS M7550) contains bismuthinite and emplectite and possibly other bismuth sulphosalts minerals. Emplectite occurs rimming a small cavity filled with quartz and in a vein intergrown with bismuthinite, chalcopyrite and hematite. This occurrence is near the large bismuth pod between 5140 and 5150E but is 20m from any gold mineralisation and highlights how far the mineralising fluids could penetrate the ironstone along fractures or through pore spaces.

5.4 SUMMARY

The various intergrowths of gold, bismuth and chalcopyrite indicate co-precipitation during the mineralising phase. This feature has been well documented by Nguyen et al (1989), Edwards et al (1990) and Huston et al (in press). The occurrence of chalcopyrite and hematite intergrown indicates that chalcopyrite, but not with gold or bismuth sulphosalts, indicates that chalcopyrite continued to precipitate during the martitisation process. This is in agreement with the model proposed by Huston et al (in press) (Figure 7).

The occurrence of single gold, bismuth sulphosalts and chalcopyrite grains indicates that the conditions commonly permitted only precipitation of single elements.

The occurrence of gold, bismuth sulphosalts and chalcopyrite within unfractured magnetite laths indicates the laths retained a porosity which enabled the mineralising fluids to percolate the laths.

Gold, bismuth and chalcopyrite occurs intergrown with coarse grained chlorite, indicating the chlorite formed during the mineralising process. This chlorite is not restricted to the orebodies but also occurs along fractures in non mineralised zones.

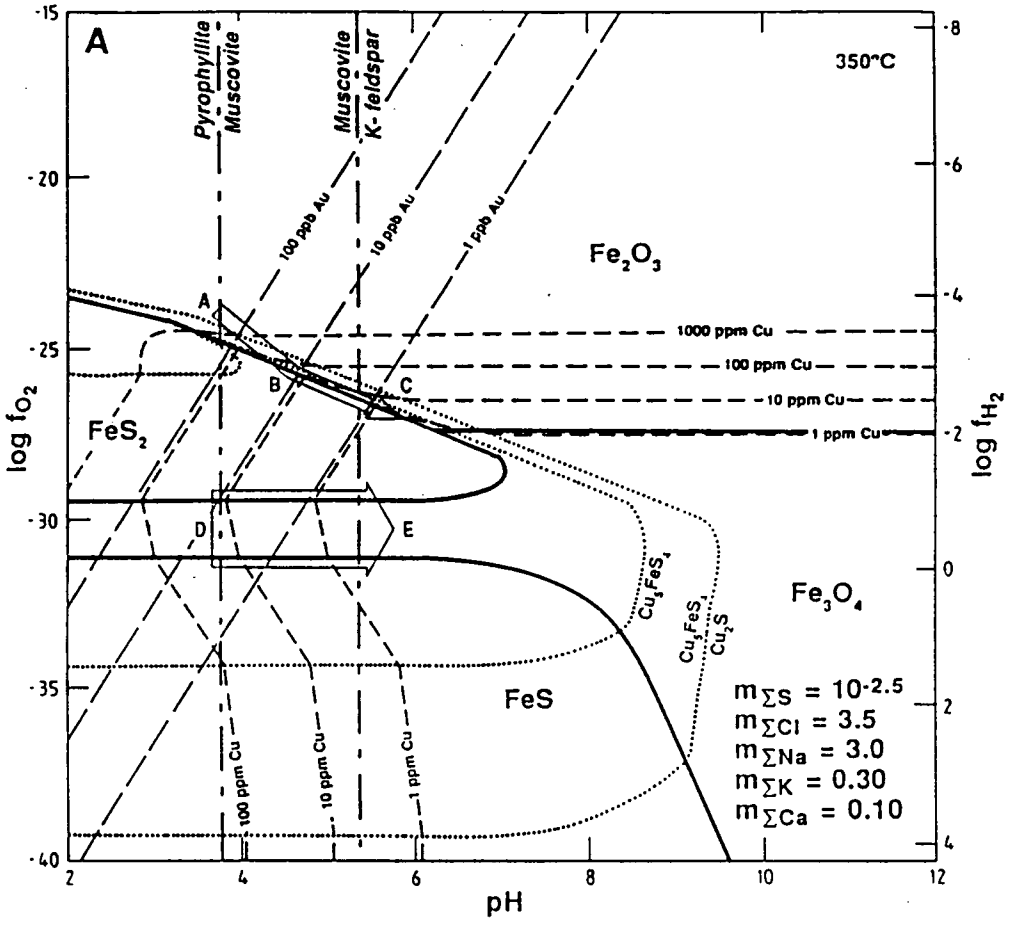

Figure 7 - Log fo_2-pH diagram at 350° c.
Showing formation path for White Devil
(after Huston et al in press)

5.5 CONTROLS ON MINERALISATION

A general model for the formation of Tennant Creek style deposits is presented by Large (1991). Genetic models for White Devil have been proposed by Hy (1988), Nguyen et al (1989), Edwards et al (1990) and Huston et al (in press). These models suggest structural control on the location of the mineralisation within the ironstone and stringer zone.

Nguyen et al (1989) says that the magnetite commonly has a breccia texture and the mineralisation fills the fractures. Hy (1988) showed that there is a direct correlation between deformation and gold mineralisation for the upper Main Zone and West Lode orebodies. The high grade mineralisation occurred where the deformation was greatest,within the highly sheared stringer zone on the hangingwall of the brittly deformed ironstone.

Within the Deeps ironstone Nguyen et al (1989) observed gold, bismuth and chalcopyrite filling regular tension cracks such as those shown in Plate 21b.

During this study of the Deeps and Main Zone orebodies it became evident that there was another control on the location of the mineralisation.

In hand specimen the magnetite chlorite hosting the Deeps mineralisation has a breccia-like texture, but this appearance results from the skeletal texture of the magnetite and the infilling chlorite. The rock does contain fractures, but these are planar rather than breccia.

In thin section the mineralisation observed was within unfractured magnetite laths or within chlorite infilling the spaces between the laths. The only exception to this is shown in Plate 19b. These observations suggest that the mineralising fluids percolated along primary porous zones in the ironstone.

Plate 20b demonstrates this concept. Within the ironstone gold, bismuth sulphosalts and chlorite have been deposited between undeformed and unfractured magnetite laths and grains.

In the magnetite chlorite-altered sediment rock, hosting the southern lens of the Deeps orebody the mineralisation occurs within the stringer magnetite and chlorite surrounding the altered sediment clasts.

The fracturing of the altered sediments created a structurally controlled channelway for the mineralising fluids but within the stringer material the mineralisation occurs as it does in the magnetite chlorite, within the magnetite laths and in the infilling chlorite (Plate 19a).

In the Main Zone orebodies the ore minerals are hosted within the magnetite stringers and laths and surrounding coarse grained chlorite, between the highly sheared and chloritic altered sediments. The deformation prepared the rock for magnetite and chlorite deposition which retained a porosity allowing the mineralising fluids to pass through the rocks.

Away from the ore zones the porosity of the ironstone decreases due to a high proportion of magnetite laths and thus smaller spaces and the presence of quartz infilling the gaps.

The location of the ore zones adjacent the two major ironstones indicates that the fluid paths followed the ironstone contacts rather than flowing throughout the whole shear or that ironstone was required for precipitation of mineralisation.

The proposed model for emplacement of the ore minerals encompasses both structural and primary porosity controls. Within the magnetite chlorite of the Deeps and Main Zone orebodies the mineralisation is controlled by the porosity between the magnetite laths.

The magnetite chlorite-altered sediments and stringer zone were structurally prepared and the porosity increased by shearing and brittle fracturing prior to and after ironstone formation. The later mineralising fluids used the same pathway and deposited the ore minerals within the magnetite and chlorite.

Within the ironstone the brittle fractures are generally filled with quartz,chlorite and minor sulphide mineralisation. The bismuth mineralisation between 5140 and 5150E is structurally controlled, occurring in sigmoidal tension fractures.

5.6 METAL ZONATION

The general metal zonation for Tennant Creek deposits was developed by Large (1975) for the Juno Mine. The deposit had a vertical zonation from a gold rich zone near the base of the large ironstone, which in turn was surrounded by overlapping shells of bismuth and then copper mineralisation.

The general zonation of White Devil will be discussed first followed by a detailed description of the metal distribution in the Main Zone orebody.

The White Devil deposit has a gross lateral zonation from west to east with the Wynn Lens, West Lodes and western parts of the Main Zone orebodies containing more copper than the remainder of the deposit. The copper content also decreases with depth. Only the eastern ends of the West Lodes, Main Zone, Deeps and Pinter Lodes contain significant bismuth sulphosalts (Figure 8). Within the orebodies the distribution of the metals is erratic and the bismuth sulphosalts and copper values are generally low, making it difficult to recognise zonation.

Figure 8 shows the gold orebodies (>5g/t), copper and bismuth mineralisation (>0.5%) as recorded on drill sections.

On 4995E the Lower and Upper West Lodes and Wynn Lens contain minor copper and only a small patch of bismuth sulphosalts. However on other sections the West Lodes contain significant copper mineralisation, particularly on the hangingwall side of the orebody. Much of the copper on 4995E is not associated with gold.

The western end of Main Zone orebodies (section 5095E) contains significant copper associated with the gold orebodies. Minor bismuth sulphosalts occurs in the Lower Main Zone orebody. Within the Lower Main Zone at 730RL there is a coarse zonation from gold to bismuth to copper in the hangingwall.

Section 5135E contains both the Main Zone and western end of the Deeps orebodies. Between 760 and 800RL the Main Zone contains associated gold and copper but the other copper mineralisation occurs between the gold bodies. The

bismuth sulphosalts at 800RL, 5100N occurs within tension gashes in the ironstone. The Deeps orebody on this section does not contain associated bismuth sulphosalts or copper. This zonation has similarities to that at Juno.

On section 5155E the Deeps orebody contains significant bismuth sulphosalts but, only minor copper mineralisation. The majority of the copper occurs within the stringer zone between the gold orebodies.

In general the presence of bismuth sulphosalts in the gold orebody greatly increases the gold grade. For example, in hole WDUD 285 within the magnetite chlorite-altered sediment-bismuth zone the gold grades are consistently higher than outside the bismuth zone but still in the same rock type.

Within the Pinter Lodes (5235E) the gold bodies are well separated from the copper and bismuth sulphosalts. The majority of the bismuth sulphosalts occurs between 800 and 850RL, and the copper occurring around 900RL, suggests a coarse vertical zonation.

On 5265E all the mineralisation is clustered between 750 and 850RL, partly due to the limited number of drillholes. The upper lodes contain associated copper and bismuth sulphosalts, whereas the other lodes are gold only. Significant copper occurs between 750 and 780RL, near the start of the drill holes, and bismuth sulphosalts occurs around 850RL.

The metal distribution and zonation is constrained by the availability of suitable host rocks. Unlike the Juno deposit,which had a relatively uniform lithological zoning, the White Devil lithologies change rapidly, especially laterally. The rock units are generally elongate, narrow packages (Figure 4) which do not lend themselves to developing clear mineral zonation.

In summary the available assay data shows that there does not appear to be a close association between gold, bismuth sulphosalts and copper mineralisation, except for the two instances described on sections 5095 and 5235E.

SECTION 4995E

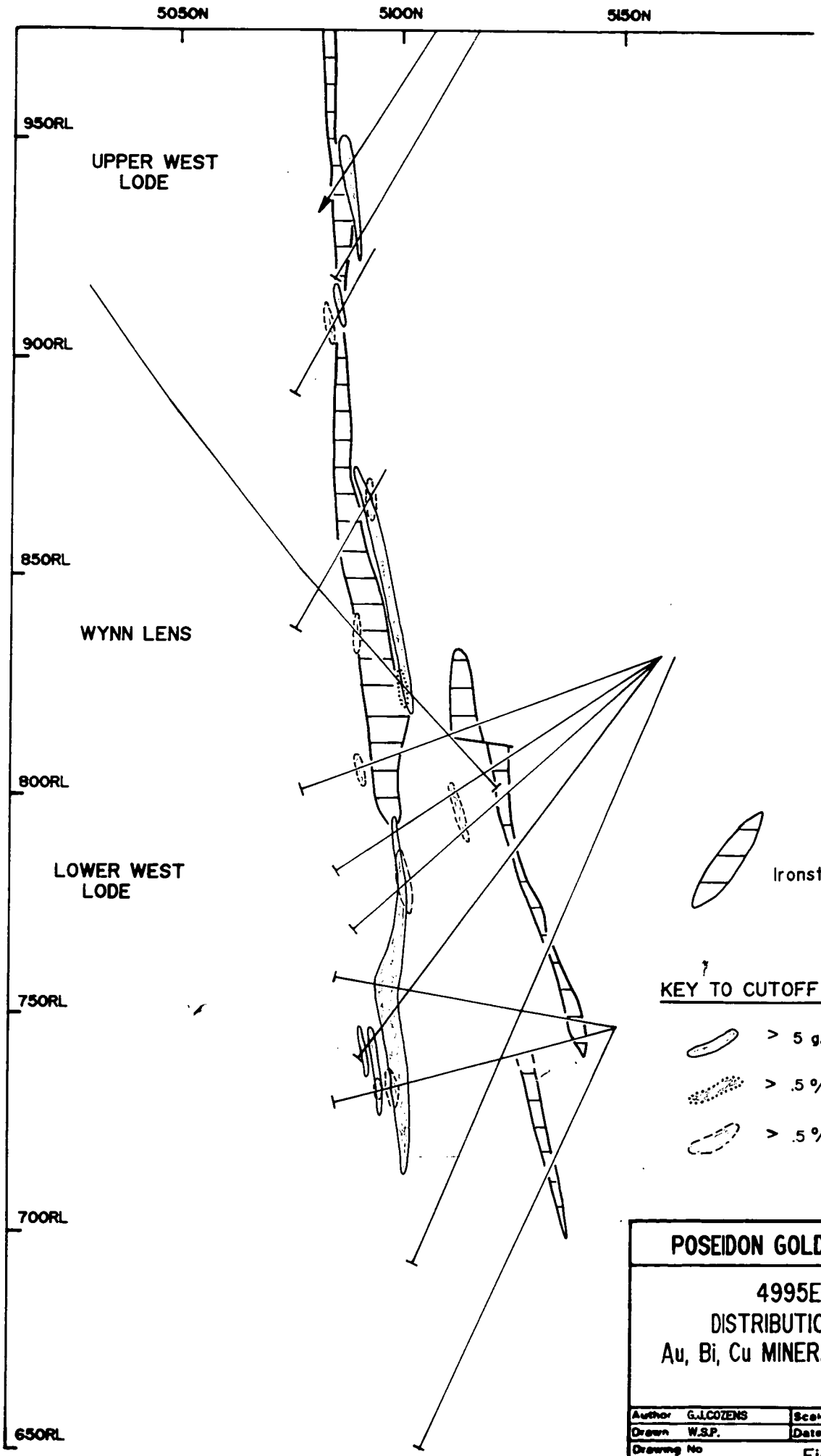

POSEIDON GOLD LIMITED

4995E
DISTRIBUTION OF
Au, Bi, Cu MINERALISATION

Author	G.J.COZENS	Scale	1 : 1250
Drawn	W.S.P.	Date	APRIL, 1992
Drawing No		Figure	8 (i)

SECTION 5095E

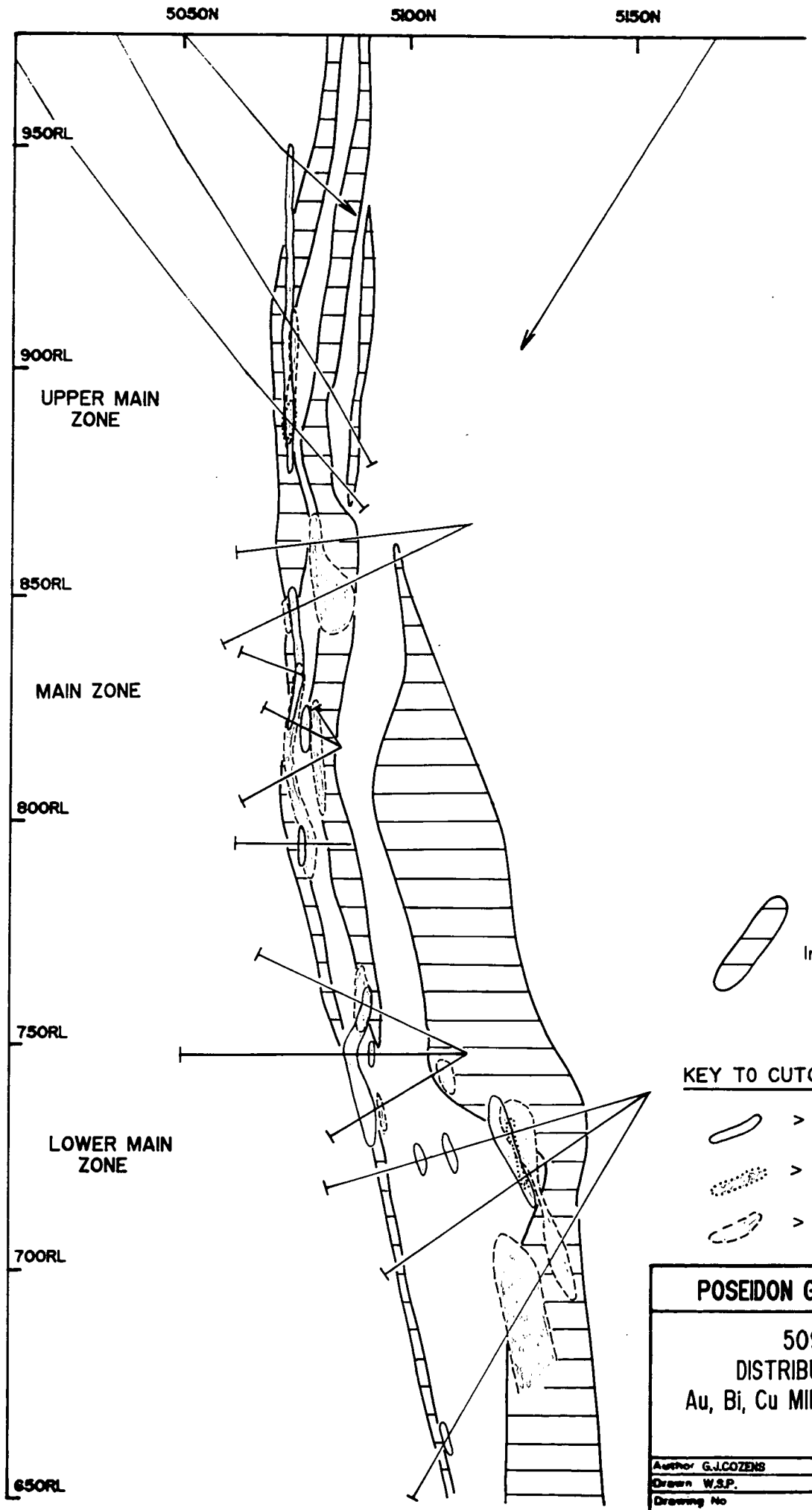

POSEIDON GOLD LIMITED

5095E
DISTRIBUTION OF
Au, Bi, Cu MINERALISATION

Author G.J.COZENS	Scale 1 : 1250
Drawn W.S.P.	Date APRIL 1992
Drawing No	Figure 8 (ii)

SECTION 5135E

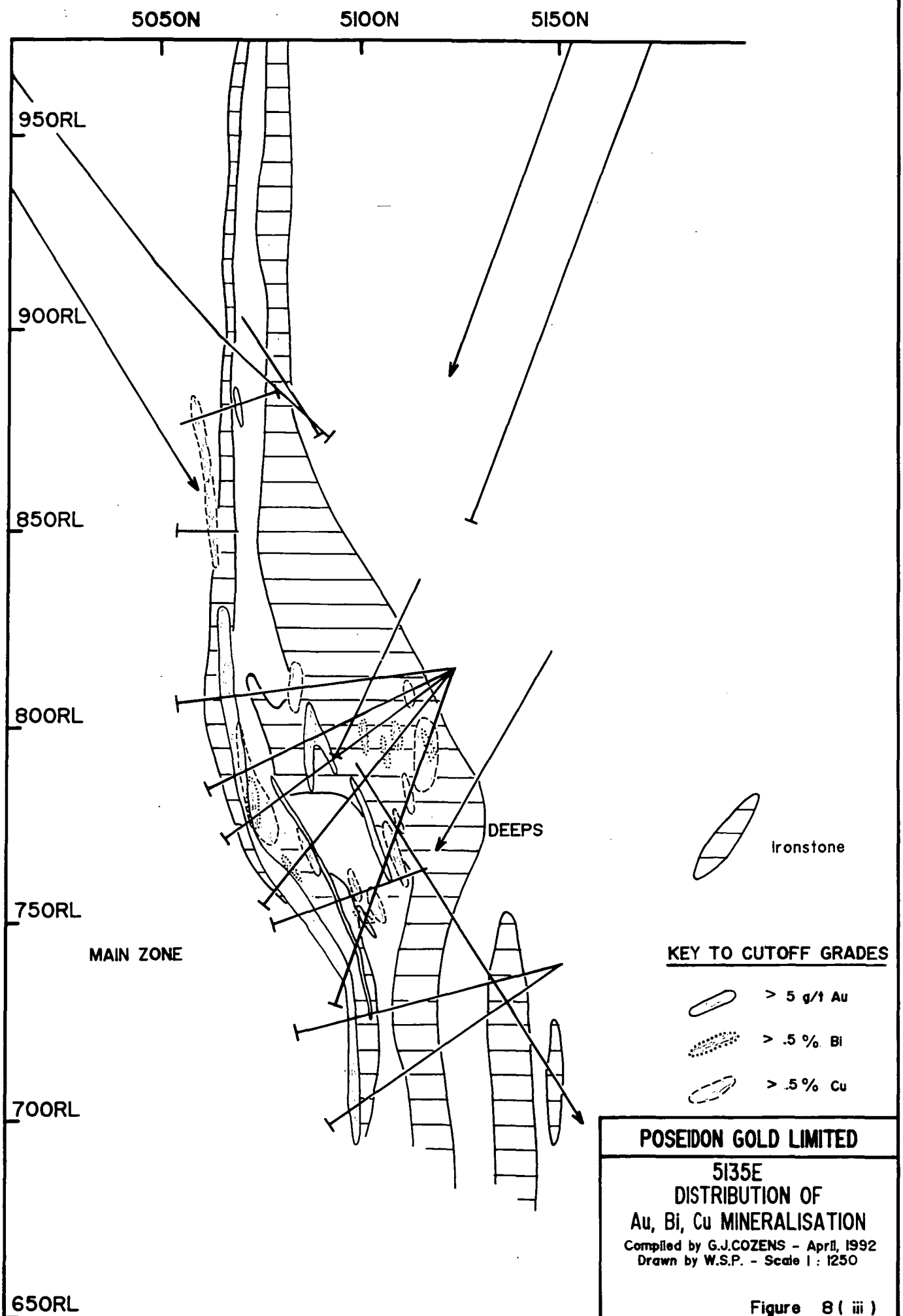

POSEIDON GOLD LIMITED

5135E
DISTRIBUTION OF
Au, Bi, Cu MINERALISATION

Compiled by G.J.COZENS - April, 1992
Drawn by W.S.P. - Scale 1 : 1250

Figure 8 (iii)

SECTION 5155E

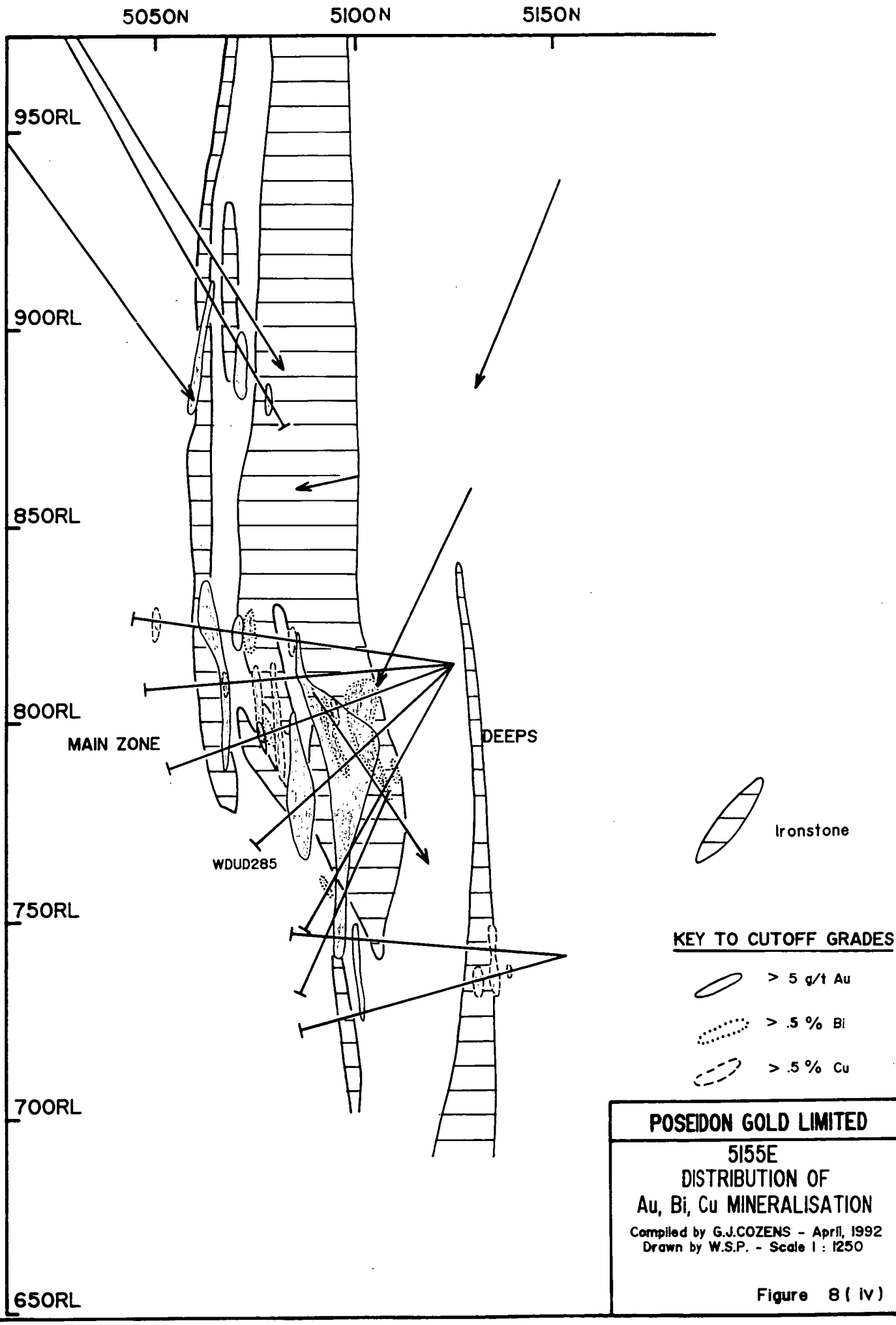

POSEIDON GOLD LIMITED

5155E
DISTRIBUTION OF
Au, Bi, Cu MINERALISATION

Compiled by G.J.COZENS - April, 1992
Drawn by W.S.P. - Scale 1 : 1250

Figure 8 (iv)

SECTION 5235E

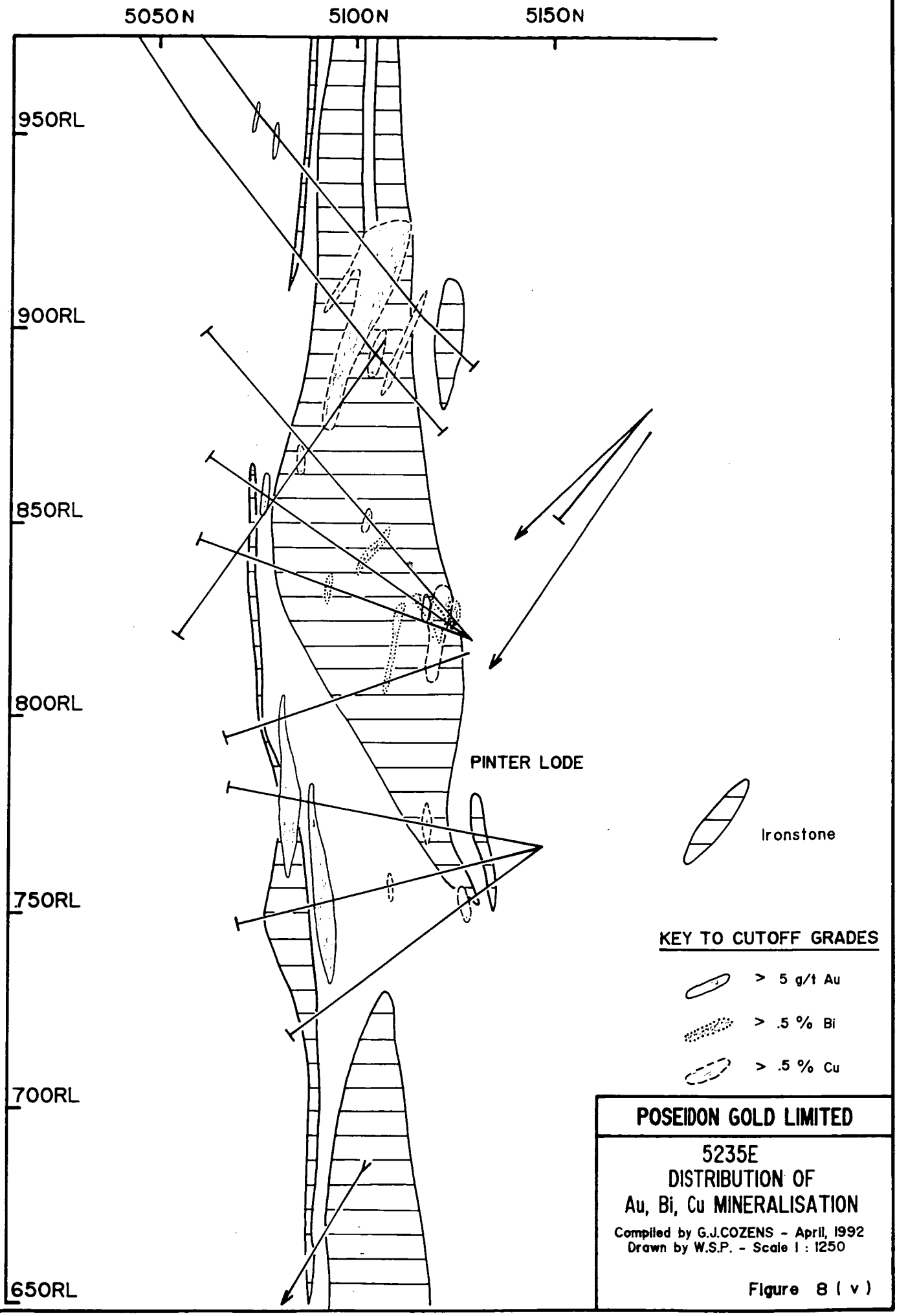

POSEIDON GOLD LIMITED

5235E
DISTRIBUTION OF
Au, Bi, Cu MINERALISATION

Compiled by G.J.COZENS - April, 1992
Drawn by W.S.P. - Scale 1 : 1250

Figure 8 (v)

SECTION 5265E

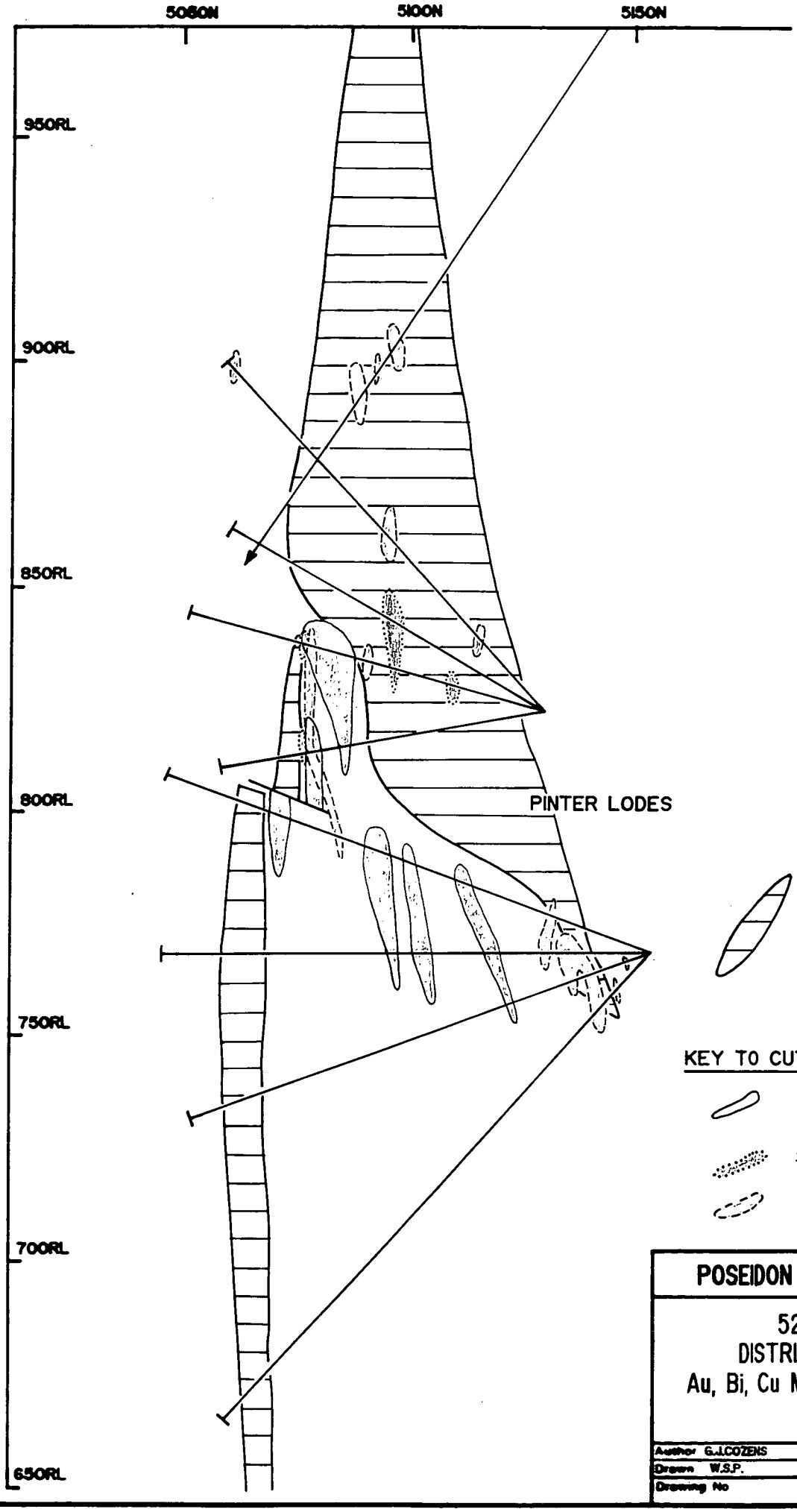

POSEIDON GOLD LIMITED

5265E
DISTRIBUTION OF
Au, Bi, Cu MINERALISATION

Author G.J.COZENS	Scale 1 : 1250
Drawn W.S.P.	Date APRIL, 1992
Drawing No	Figure 8 (vi)

5.6.1 Main Zone Metal Distribution

In this section the gold, bismuth and copper distribution within the Main Zone Orebody will be examined. The orebody decreases in strike length and width with depth and plunges steeply west. The orebody has been displaced by faults in two places on the 830 and 815 levels. Within the mined orebody the metal distribution and grades are very irregular, as can be seen in figure 9.

Gold

On each level the orebody consists of several very high grade zones surrounded by low or subgrade (<5g/t) zones. The gold (>5g/t) occurs in a semi-continuous lode in the western part of the orebody, but then occurs as pods towards the eastern end of the body. The high grade gold zones in the middle of the orebody and eastern end form a continuous west plunging high grade core to the orebody

Bismuth

Only minor high grade (>1%) bismuth pods occur on 830 and 815 levels, with the majority of the values less than 0.1%. The 795 level contains a higher proportion of values above 0.5% and a larger pod of high grade bismuth. The highest bismuth value is 6.2% from a 0.5m wide channel sample.

Copper

The 830 level contains a large zone of elevated copper near the hangingwall and several small patches of 0.5 to 1% values. The remainder of the level is less than 0.1%. The 815 level contains two zones of elevated copper, both near the fault zones, separated by low to barren values. The 795 level contains a large zone of elevated copper values near the start of the orebody and low values associated with the high grade gold values. The highest copper value of 8.2% occurs on the 795 level and is associated with several values between 1 and 4%.

Comparison of gold, bismuth and copper

A comparison of the distribution of the three metals shows that the high grade bismuth values are intimately associated with the highest gold values. The copper occurs adjacent to or overlaps the high gold values, generally towards the hangingwall, but occurs on both sides of the orebody. On the 795 level the high copper is well separated from the high gold and bismuth.

The lower grade (5-20g/t) gold zones contain significant elevated copper values (>0.5%). The high copper and bismuth, apart from overlapping in small patches on 830 and 795, occur separately. There is significant overlap in the lower grades. Within the orebody there are several barren zones common to gold, bismuth and copper.

In summary the high grade gold zones contain only minor high grade copper but are associated with the high grade bismuth zones. The high grade copper and bismuth zones generally occur as small pods rather than continuous zones.

There does not appear to be a distinct zoning within the orebody, mainly due to the poddy and erratic nature of the metal values and distribution. However a few generalisations can be made. The high copper and bismuth zones do not overlap, the high copper flanks the high gold zones. In the lower grade zones copper and gold commonly occur together, but bismuth and copper occur separately.

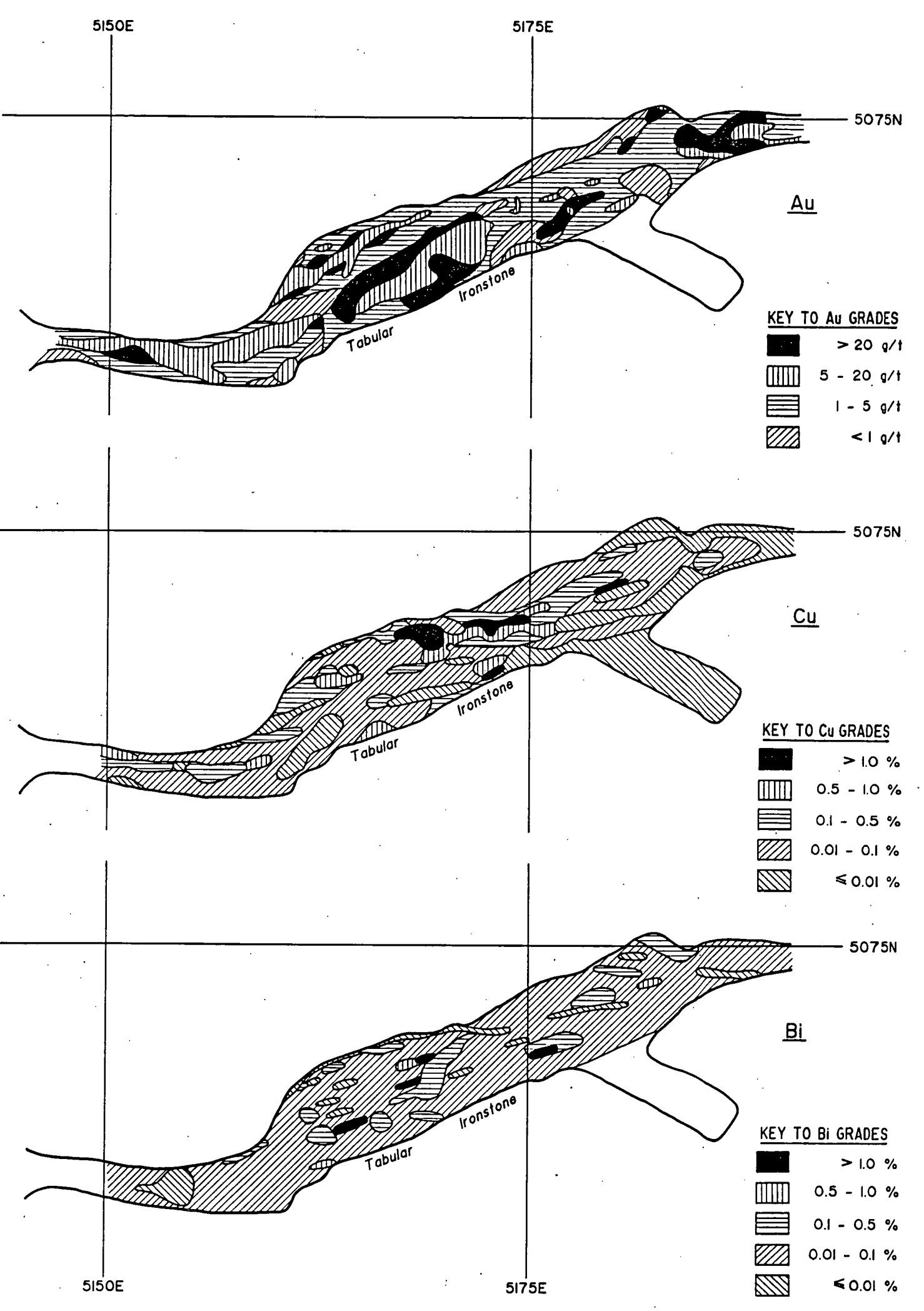

METAL 'ZONING' WITHIN MAIN 'ZONE' OREBODY

830 LEVEL

Figure 9

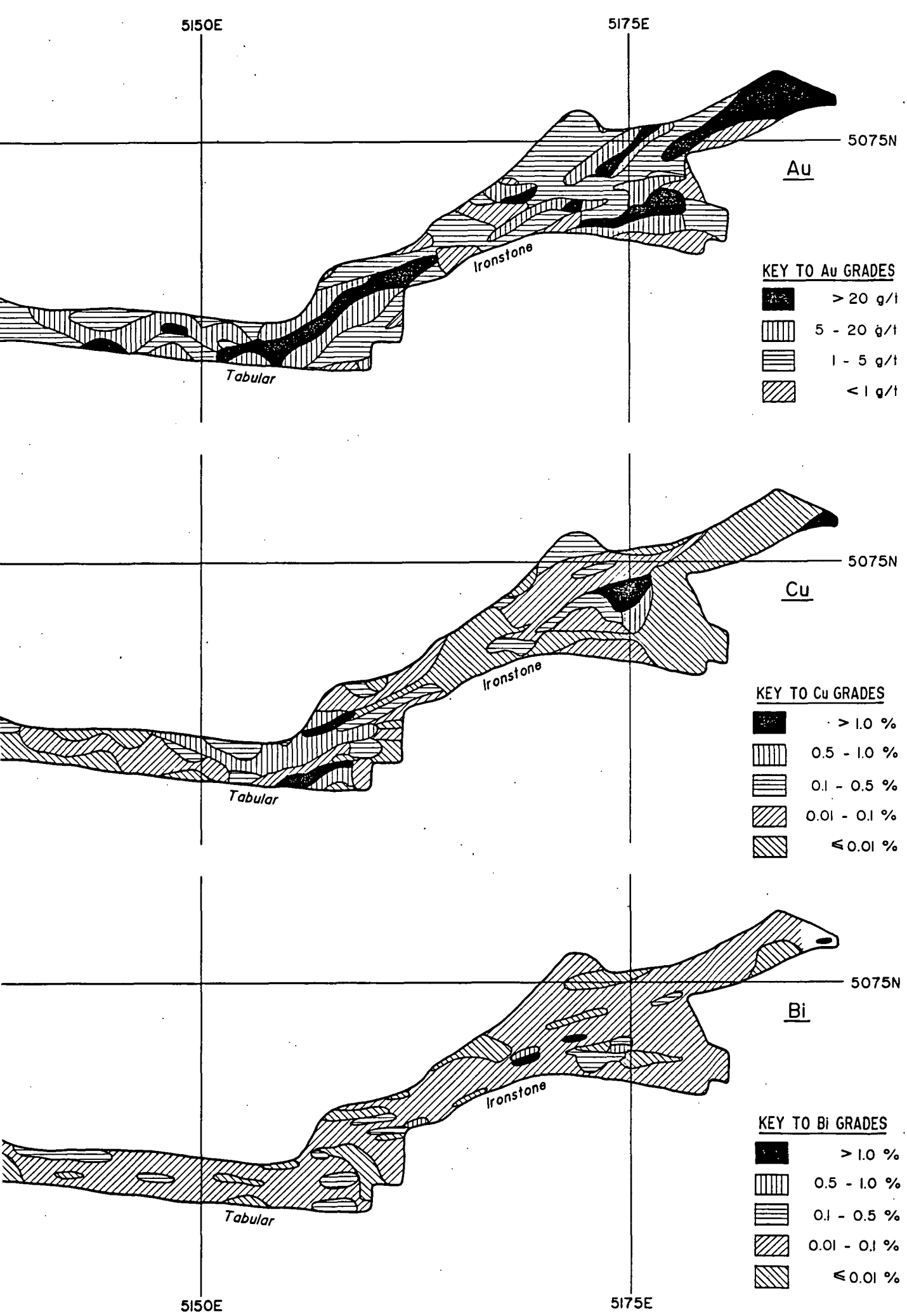

METAL 'ZONING' WITHIN MAIN 'ZONE' OREBODY

815 LEVEL

Figure 9

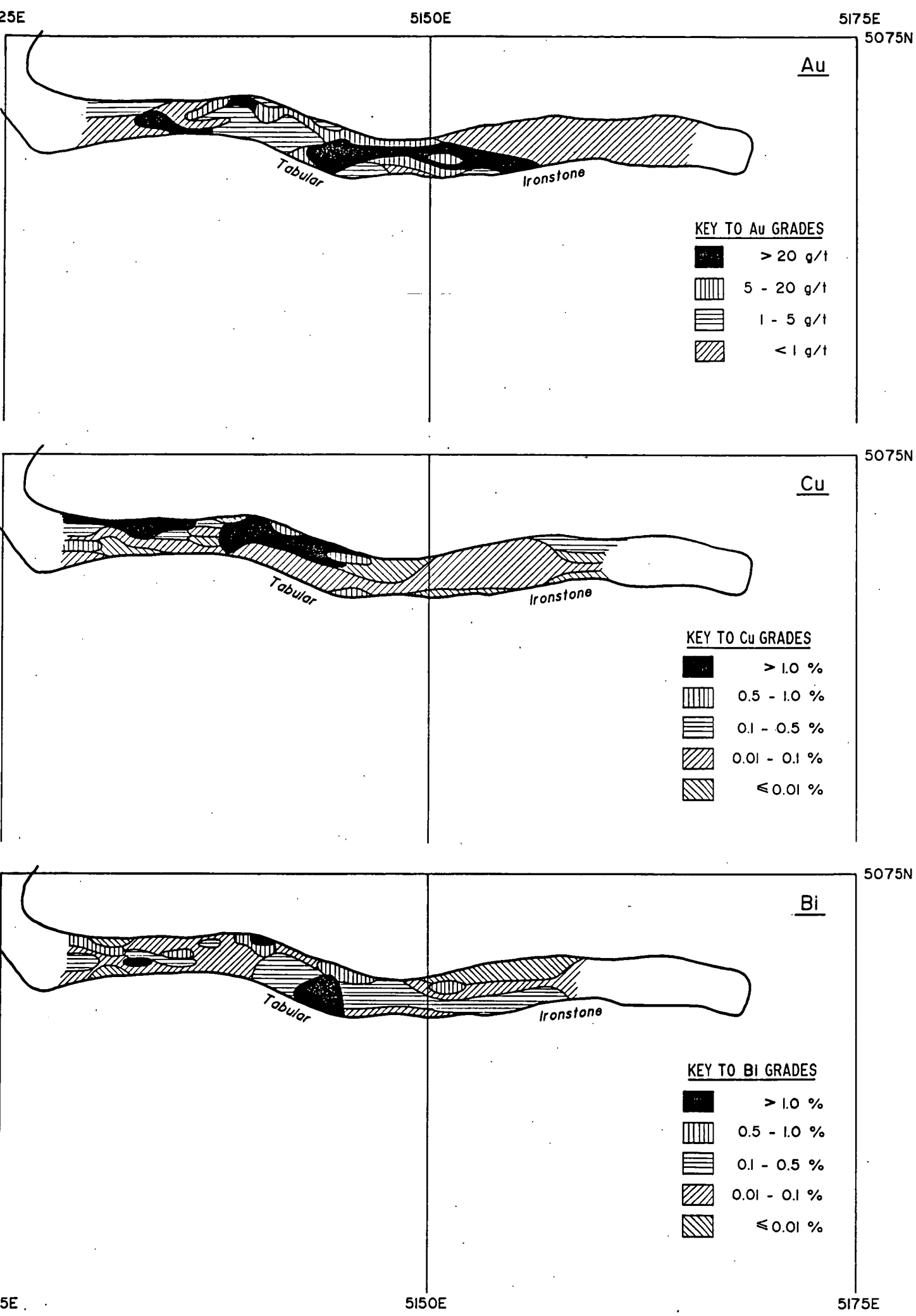

METAL 'ZONING' WITHIN MAIN 'ZONE' OREBODY

795 LEVEL

Figure 9

6 CHLORITE

6.1 INTRODUCTION

Several previous workers (Large 1975, Edwards 1987, Nguyen et al 1989, Wedekind et al 1989) have analysed the chlorites associated with the deposits. Large (1975) showed that the Juno deposit was zoned with respect to Mg-Fe content of the chlorites. The chlorites in the stringer zone at the base of the ore zone were Fe rich and those at the uppermost part of the magnetite-chlorite body,adjacent to the talc alteration were Mg rich. The ore mineralisation contained Mg chlorite. Also the Al content decreased and Si increased vertically and the chlorite composition ranged from pycnochlorite to ripidolite. The distinguishing feature between the two chlorites is the number of Si cations, pycnochlorite has between 5.6 and 6.2 and ripidolite between 5 and 5.6. Ripidolite can also contain a wide range of Fe content, from 2 to 8 cations (Fig 81, Deer et al 1989).

Wedekind et al (1989) noted a similar relationship between Fe and Mg rich chlorite at the Warrego deposit, with the chlorite in the gold rich pods being Mg rich.

Nguyen et al (1989) analysed chlorite intergrown with bismuthinite and gold from the Deeps and Main Zone orebodies at White Devil, which had a compositional range between ripidolite and pycnochlorite. Nguyen et al (1989) noted that chlorite formed throughout the mineralisation process and that the early chlorite was not confined to the ore zone but formed an alteration envelope around the shear zone. Later chlorite occurred in tension cracks in magnetite and displayed growth fibres and underwent partial replacement by sulphide mineralisation and gold. Further chlorite formed contemporaneously with the mineralisation.

Edwards et al (1990) noted that the chlorite associated with mineralisation at White Devil was Mg rich compared to the relative Fe rich chlorite in the surrounding altered sediments.

Petrographic studies by Huston (1990a,b) of Gecko, White Devil and barren ironstones showed that coarse grained unfoliated chlorite with anomalous "Berlin Blue"

birefringence was associated with Au-Bi-Cu mineralisation and the chlorite associated with barren ironstones was foliated and showed normal interference colours.

To follow-up this earlier work a petrographic and microprobe study was undertaken on chlorites throughout the White Devil deposit.

6.2 PETROGRAPHY

The aim of this portion of the study is to investigate the distribution of the different chlorites recognized by Huston (1990a,b) and their relationship to mineralisation and the ironstones.

The two major interference colours of the chlorites observed are green and purple (Berlin Blue, Huston 1990a,b). Under normal light the chlorites are visibly different, being apple green and darker green respectively. Plate 24 shows the two chlorites under normal light.

Chlorite in Weakly Mineralised Ironstones

Within the magnetite-quartz Pinter ironstone (M7559,M7561) small patches of coarse grained green chlorite occur in quartz and with minor chalcopyrite, well away from gold mineralisation. The chlorite in Plate 12 from thin section M7561 appears to have been partially replaced by quartz and the chlorite in Plate 25 has been partially altered to talc.

Magnetite-chlorite Pinter ironstone (M7563) shows "lacework" textured magnetite laths filled with coarse grained light green chlorite. Within later fractures in the ironstone purple chlorite occurs.

Within the hematite-magnetite portion of the Pinter ironstone on 5205E (M7511), two phases of chlorite were observed in fractures. The green chlorite occurs in a small horizontal fracture and later purple chlorite intergrown with hematite occurs in a vertical vein. The hematite probably formed during the martitisation process late in the mineralising stage.

In the hematite-quartz-minor pyrite portion of the Deeps ironstone on 5135E (M7549) green chlorite occurs around a fractured early formed pyrite grain within quartz. A small hematite crystal is embedded in the chlorite and grows into the quartz. This section shows that the chlorite grew later than the fracturing of the pyrite and was affected by the hematisation process. The quartz has possibly replaced much of the chlorite.

Within fractures in the tabular ironstone on 5135E (M7556) purple chlorite occurs. No sulphide minerals occur in the section. Within the fracture the chlorite is intergrown with hematite and quartz, indicating the chlorite formed late in the mineralising process and the chlorite is not intimately associated with mineralisation.

Sections M7555 and M7543 show the contact zone between the tabular ironstone and altered sediment-magnetite stringer Main Zone ore. Vugs and cavities in and between the magnetite laths are filled with coarse grained purple chlorite and the spaces between the magnetite blebs are filled with fine grained foliated purple chlorite, similar to that in the altered sediments.

The ironstones contain green chlorite as remnant grains well away from mineralisation and in early fractures. Purple chlorite occurs in later fractures and among magnetite laths in the vicinity of mineralisation or towards the centre of the shear zone.

Chlorite in Gold Orebodies

The magnetite chlorite-altered sediment ore from the Pinter Lodes contains both green and purple chlorite. The coarse grained green chlorite occurs around magnetite grains and in fractures whereas the fine grained purple chlorite is foliated and may represent relict altered sediment. In some thin sections the foliated chlorite is a mixture of green and purple indicating overprinting by one of the chlorites.

In the Pinter stringer ore on 5265E the altered sediment clasts contain fine grained foliated green chlorite and coarser green chlorite amongst the magnetite grains.

The Main Zone stringer ore contains fine grained foliated purple chlorite in the altered sediment clasts and coarse grained purple around the magnetite. Gold, bismuth and copper mineralisation occurs within both the fine and coarse grained chlorite, but generally within the coarse grained chlorite. In fractures in the magnetite stringers, where chlorite has an open space growth texture, bismuth has grown parallel to chlorite laths. The coarse grained chlorite near the ironstone contact contains fractured magnetite fragments which appear to have been broken off the ironstone, suggesting brittle deformation of the ironstone contact.

The Deeps ore (M7537,M7538,M7546a) contains both fine and coarse grained purple chlorite around magnetite and in altered sediment clasts in the magnetite chlorite-altered sediment ore.

Chlorite in the Stringer Zone

Within the altered sediment-magnetite stringer zone the altered sediments contain foliated purple chlorite and the magnetite stringers are surrounded by coarse grained purple chlorite.

The occurrence of the coarse grained, unfoliated randomly orientated chlorite around the magnetite stringers suggests special conditions of formation. The stringers acted as a rigid body within the sheared sediments and thus chlorite within them grew in a strain free zone. The effect of the can be seen in Plate 26.

Many of the stringers have been fractured in the direction of shearing, as defined by the chlorite foliation. Within these fractures chlorite occurs as random platelets or with open space filling textures, such as interlocking laths growing perpendicular to the fracture wall, and is often intergrown with quartz.

Plate 26 shows the contact between an altered sediment clast and magnetite chlorite stringers. Both the chlorites have purple interference colours.

In the Main Zone area, near the contact with the tabular ironstone the altered sediment contains numerous grains of magnetite, either as primary crystals or

PLATE 24

Two colours of chlorite in normal light. Small horizontal vein contains apple green chlorite which has green interference colours and the vertical vein with hematite intergrown contains darker chlorite with purple (Berlin Blue-Huston 1990a,b) interference colours.
Thin section: M7511, WDUD 468, 28.9m, 5205E
FOV= 3.5mm

PLATE 25

Chlorite partially altered to talc, Pinter Ironstone.
Thin Section: M7561, WDUD 487, 6.6m, 5235E
FOV= 6.9mm

PLATE 24

PLATE 25

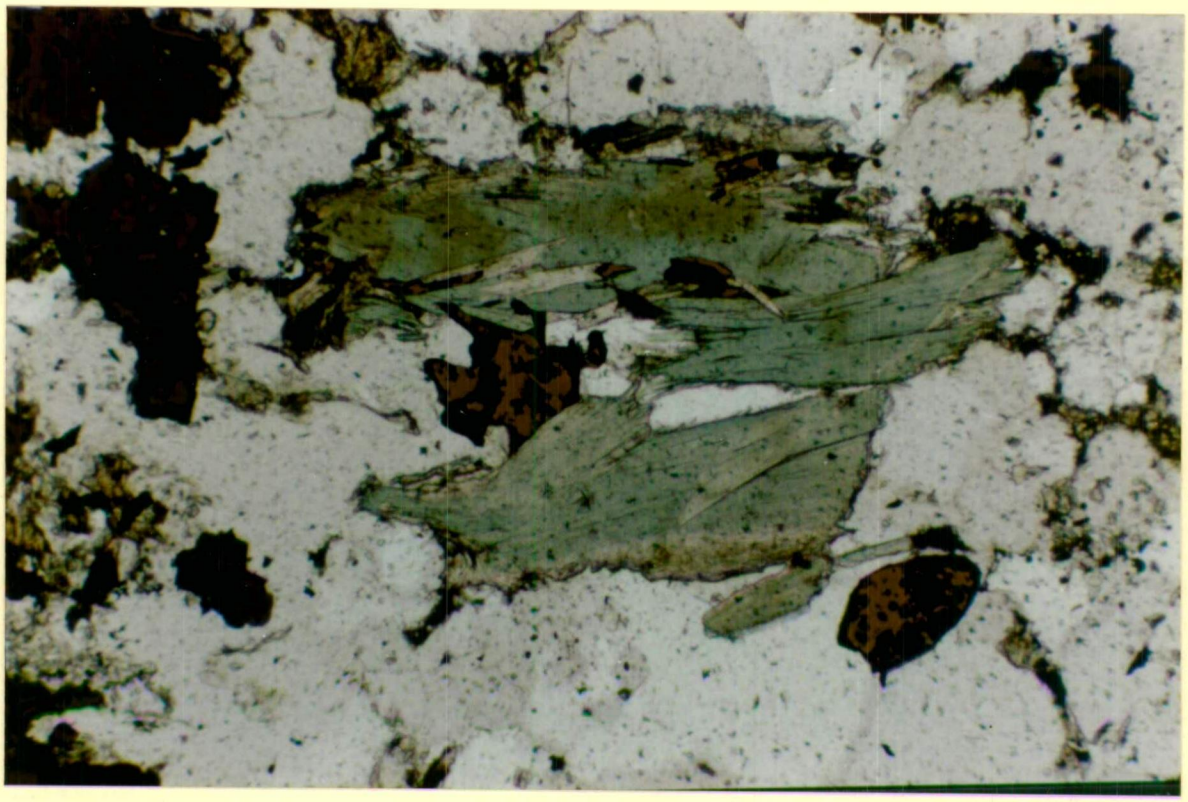

PLATE 26

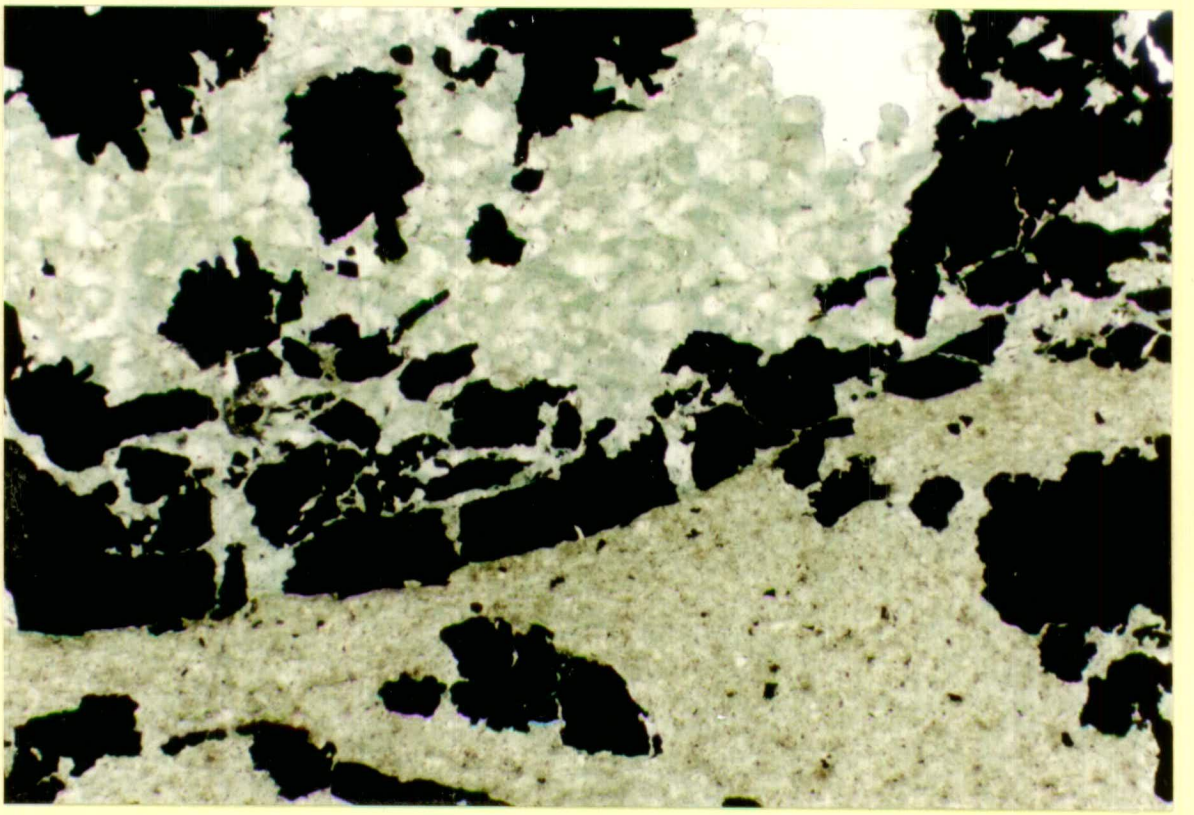

PLATE 27

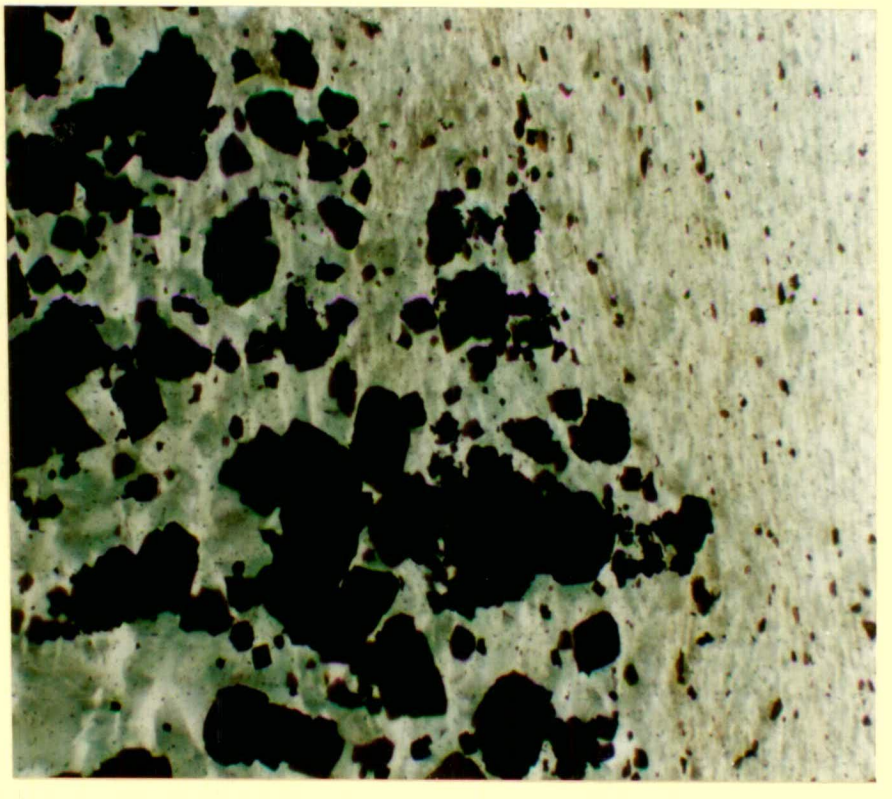

PLATE 26

Contact between altered sediment (fine grained chlorite) and coarse chlorite amongst magnetite. The coarse chlorite is non foliated and appears to have formed in a "strain free" zone, being shielded by the magnetite.
Thin section: M7539, WDUD 285, 39.7m, 5155E
FOV= 3.5mm

PLATE 27

Magnetite grains and coarse chlorite grading into finer chlorite within stringer material. Some of the magnetite is euhdral grains and other is fragments from the nearby tabular inronstone.
Thin section: M7555, WDUD 273, 61m, 5135E
FOV= 1.7mm

PLATE 28

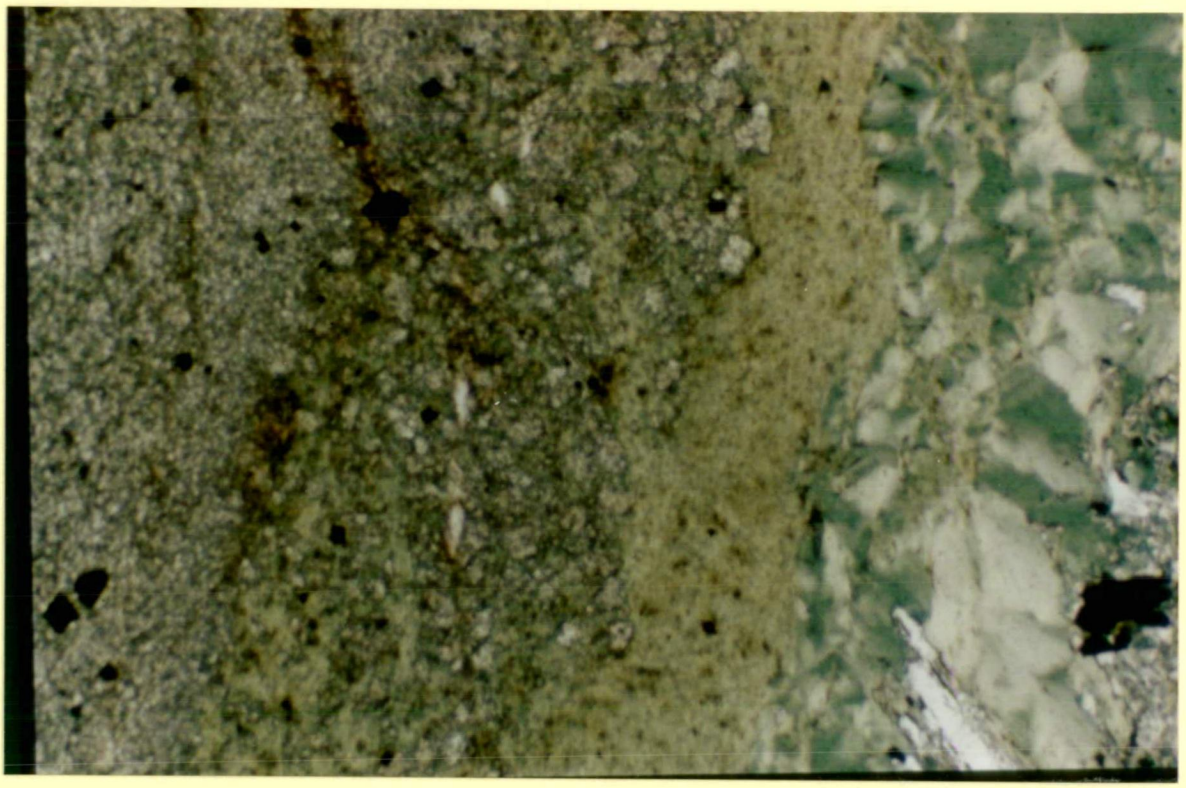

fragments from the larger ironstone. The coarse grained chlorite filling around the grains grades into fine grained foliated chlorite of altered sediments, (Plate 27).

The main feature of the stringer zone chlorites is that within the highly sheared altered sediments the chlorite around the magnetite stringers is unfoliated.

Chlorite in Altered Sediment

In the altered sediments within the shear zone the groundmass chlorite is fine grained foliated purple chlorite. The chloritic sediments outside the ore zone have been partially altered to purple chlorite. Where later quartz-chlorite veins occur, the vein chlorite is coarse purple and the vein contact areas have been pervasively altered to purple chlorite.

In M7553, altered sediment contains fine grained purple adjacent to coarse grained green chlorite. The green chlorite has been partially altered to talc, whereas the purple is unaltered. Plate 28 shows chloritic sediment and a coarse grained chlorite vein. The vein and groundmass contains purple chlorite and the vein contact has been pervasively altered to coarser purple chlorite. In chloritic sediments associated with the South Lower Main Zone orebody on 5075E, a quartz vein contains blue chlorite.

Talc

In the Pinter ironstone green chlorite has been altered to talc, Plate 25. In the Main Zone, green chlorite in the ironstone has been altered to talc, whereas the purple chlorite has not.

The talc generally has the same coarse texture as the original chlorite grains. However in the Main Zone area, fine grained talc occurs, which may represent replacement of altered sediment.

Talc occurring within the altered sediments was not studied.

Conclusions

Both green and purple chlorite occur throughout the deposit and adjacent to each other in places. There are no obvious petrographic differences between the purple and green chlorite. Purple chlorite is not restricted to the orebodies. Only green chlorite has been observed as being altered to talc. Unfoliated coarse grained chlorite occurs in vugs and around magnetite in the ironstone, around the magnetite stringers and in quartz veins in the altered sediments.

Altered sediments contain fine grained foliated chlorite. However, chlorite in altered sediments within magnetite-chlorite-altered sediments adjacent to the large ironstone was not foliated. Blue chlorite occurs in a quartz vein in altered sediments associated with the South Lower Main Zone orebody on 5075E and pervasive alteration of vein contact area has occurred. Gold, bismuth and copper occur intergrown in coarse grained chlorite around magnetite stringers.

Huston (1990a,b) proposed the presence of Berlin Blue coloured chlorite as an indicator of mineralisation. The only blue chlorite observed in this study occurred in a quartz vein in altered sediments associated with the South Lower Main Zone orebody on 5075E. However abundant purple chlorite was observed associated with the mineralisation and throughout the shear. Discussions with D. Huston have revealed that he grouped Berlin Blue and purple chlorite together. The occurrence of coarse grained chlorite associated with mineralisation may be a useful indicator of the presence of mineralisation.

6.3 MICROPROBE STUDY

A total of 86 microprobe analyses of chlorite, talc and biotite were made using the University of Tasmania's Cameca microprobe. Tables 1 and 2 show representative analyses of the chlorites, talc and biotite sampled. Appendix 1 gives the complete analyses and sample descriptions. The numbers in parentheses beside sample numbers in the text correspond to analyses in Tables 1 and 2 and Figure 11.

The scatterplots in Figure 10 show that there is a strong positive relationship between Si-Mg, Al-Fe and a strong negative relationship between Si-Fe, Si-Al and Fe-Mg for all the chlorites analysed. The Al vs Mg plot shows some scattering and a slight negative relationship.

Figure 10b shows the majority of the chlorites are of ripidolite composition and a small population falls in the pycnochlorite field. Three analyses fall outside the named chlorite fields and one analysis within the diabantite field. This diagram shows that these analyses are in agreement with previous studies.

Ironstone

Two samples of remnant green chlorite within magnetite-quartz ironstone were analysed and shown in Table 1, analyses 1 & 2. The Fe/Fe+Mg ratio shows that these chlorites are Mg rich. Chlorite from sample M7561(1) contains higher Si,Al and Mg but lower Fe than M7564. On Figure 11, M7561 plots at the Mg rich end of the graph and M7564 plots towards the middle. M7561 came from the northern edge of the Pinter ironstone whereas M7564(2) came from near the contact of the ironstone with the stringer zone. Despite similar appearances and setting within the ironstone, it appears that sample M7564 may have undergone minor alteration to increase its Fe content. Both samples were located well away from mineralisation. However fluids passing through the shear zone may have penetrated the ironstone sufficiently to alter M7564.

In sample M7563(3), coarse grained green chlorite in magnetite chlorite ironstone adjacent to M7564, has a similar composition to M7564, indicating the chlorites formed from the same fluid, whereas the chlorite in M7561 formed from a different fluid.

Magnetite chlorite ironstone near the contact of the tabular ironstone with altered sediments containing 3.8g/t Au, in the Lower West Lode area, sample M7533(4), contains purple Fe chlorite with a Fe/Fe+Mg ratio of 55.8.

TABLE 1 WHITE DEVIL CHLORITE ANALYSES
Representative chlorite analyses
Complete analyses are tabled in Appendix 1

	1	2	3	4	5	6	7	8
SAMPNO	M7561	M7464	M7563	M7533	M7557	M7557	M7504	M7504
EASTING	5235	5235	5235	4995	5265	5265	5265	5265
COLOUR	GREEN	GREEN	GREEN	PURPLE	GREEN	PURPLE	GREEN	GREEN
CRS/FINE	COARSE	COARSE	COARSE	COARSE	COARSE	FINE	COARSE	FINE
Si	5.78	5.36	5.36	5.44	5.37	5.43	5.74	5.7
Ti	0.01	0	0	0	0.01	0.01	0.01	0.01
Al	4.44	5.12	5.1	4.85	5.15	4.99	4.35	4.48
Cr	0	0	0	0.01	0.01	0.01	0	0
Mg	6.5	5.32	5.32	4.35	5.47	5.49	6.87	6.72
Ca	0	0.01	0.01	0	0	0.01	0	0.01
Mn	0.02	0.02	0.02	0.02	0.01	0.01	0.01	0.01
Fe	3.21	4.23	4.27	5.47	4.01	4.09	3.1	3.16
TOTAL	19.96	20.06	20.08	20.13	20.03	20.04	20.08	20.09
Fe/Fe+Mg	33.2	44.36	44.64	55.83	42.35	42.76	31.13	32.09
Al(iv)	2.22	2.64	2.64	2.56	2.63	2.57	2.26	2.3
T(C)	253.32	297.84	297.84	289.36	296.78	290.42	257.56	261.8

	9	10	11	12	13	14	15	16	17
SAMPNO	M7503	M7503	M7521	M7521	M7538	M7509	M7509	M7506	M7506
EASTING	5255	5255	5015	5015	5155	5225	5225	5265	5265
COLOUR	PURPLE	PURPLE	PURPLE	PURPLE	PURPLE	PURPLE	GREEN	PURPLE	GREEN
CRS/FINE	FINE	COARSE	FINE	COARSE	FINE	FINE	COARSE	COARSE	COARSE
Si	5.17	5.18	5.24	5.1	5.54	5.24	5.16	5.49	5.48
Ti	0.01	0.01	0.01	0.01	0.01	0.01	0.01	0.01	0.01
Al	5.46	5.44	5.36	5.55	4.73	5.27	5.54	4.97	4.91
Cr	0	0	0	0	0	0	0	0	0.01
Mg	3.91	4.04	3.71	3.6	5.4	4.8	4.62	5.78	5.92
Ca	0.01	0	0.01	0.01	0	0.01	0.01	0	0
Mn	0.02	0.01	0.01	0.02	0.02	0.02	0.02	0.01	0.01
Fe	5.53	5.42	5.72	5.84	4.38	4.79	4.72	3.74	3.71
TOTAL	20.11	20.12	20.06	20.13	20.08	20.14	20.06	20.00	20.04
Fe/Fe+Mg	58.65	57.39	60.66	61.89	44.92	50.06	50.59	39.31	38.59
Al(iv)	2.83	2.82	2.76	2.9	2.46	2.76	2.84	2.51	2.52
T(C)	317.98	316.92	310.56	325.4	278.76	310.56	319.04	284.06	285.12

Analyses: 1-2 Remnant chlorite in magnetite-quartz ironstone

3-4 Chlorite in magnetite-chlorite ironstone

5-13 Chlorite in either fine grained altered sediment or as coarse grained around magnetite in orebodies
Coarse chlorite contains Au-Bi-Cu mineralisation.

14-17 Stringer Zone chlorite, fine grained in altered sediments and coarse grained around magnetite

TABLE 1 WHITE DEVIL CHLORITE ANALYSES
Representative chlorite analyses
Complete analyses are tabled in Appendix 1

	18	19	20	21	22	23	24	25
SAMPNO	M7522	M7522	M7534	M7534	M7517	M7517	M7517	M7518
EASTING	5015	5015	4995	4995	5075	5075	5075	5075
COLOUR	PURPLE	PURPLE	PURPLE	GREEN	BLUE	BLUE	BLUE	BLUE
CRS/FINE	FINE	COARSE	FINE	COARSE	COARSE	VEIN	FINE	VEIN
Si	5.25	5.28	5.57	5.55	5.16	5.14	6.32	5.12
Ti	0.01	0.01	0.02	0.01	0.02	0.01	0.01	0
Al	5.34	5.24	4.77	4.84	5.5	5.58	4.92	5.57
Cr	0.01	0	0	0	0	0	0	0
Mg	3.77	3.79	4.93	5.08	2.73	2.73	2.32	4.21
Ca	0	0	0.01	0.01	0	0	0	0
Mn	0.03	0.01	0.01	0.01	0.02	0.02	0.02	0.01
Fe	5.65	5.75	4.73	4.52	6.64	6.56	5.62	5.17
TOTAL	20.07	20.09	20.03	20.02	20.07	20.04	19.21	20.09
Fe/Fe+Mg	60.11	60.33	49.04	47.17	70.91	70.62	70.86	55.18
Al(iv)	2.75	2.72	2.43	2.45	2.84	2.86	1.68	2.88
T(C)	309.5	306.32	275.58	277.7	319.04	321.16	196.08	323.28

	26	27	28	29	30	31	32	33
SAMPNO	M7519	M7519	M7544	M7544	M7545	M7545	M7553	M7553
EASTING	5075	5075	5155	5155	5155	5155	5135	5135
COLOUR	PURPLE	PURPLE	PURPLE	PURPLE	PURPLE	PURPLE	PURPLE	GREEN
CRS/FINE	FINE	COARSE	COARSE	FINE	FINE	COARSE	FINE	COARSE
Si	5.35	5.24	5.21	5.6	6.95	5.21	5.6	5.52
Ti	0.01	0	0.01	0.01	0.02	0.01	0.01	0.01
Al	5.28	5.33	5.32	5.21	6.18	5.36	4.56	4.73
Cr	0	0	0	0	0.01	0.01	0	0
Mg	4.46	4.38	3.65	3.3	1.85	3.53	5.88	5.94
Ca	0.01	0	0	0	0	0	0.01	0
Mn	0.01	0.01	0.02	0.02	0.01	0.02	0.01	0
Fe	4.87	5.11	5.93	5.58	2.93	5.97	4.04	3.88
TOTAL	19.99	20.07	20.13	19.72	17.93	20.1	20.11	20.88
Fe/Fe+Mg	52.29	53.92	61.96	62.94	61.47	62.93	40.88	39.54
Al(iv)	2.65	2.76	2.79	2.4	1.05	2.79	2.4	2.48
T(C)	298.9	310.56	313.74	272.4	129.3	313.74	272.4	280.88

Analyses 18-21 Magnetite-altered sediments, magnetite rich altered sediments

22-25 Blue chlorite in quartz vein in altered sediments

26-33 Altered sediments with minor pyrite and quartz

TABLE 2 WHITE DEVIL TALC AND BIOTITE ANALYSES
Representative talc and biotite analyses
Complete analyses are tabled in Appendix 1

TALC

	34	35	36	37	38	39
SAMPNO	M7513	M7513	M7559	M7559	M7558	M7558
EASTING	5095	5095	5235	5235	5235	5235
COLOUR	GREEN	TALC	TALC	GREEN	TALC	GREEN
CRS/FINE	COARSE					
Si	5.66	10.15	10.16	5.58	10.06	5.6
Ti	0.01	0	0	0	0	0
Al	4.53	0.04	0.04	4.44	0.04	4.6
Cr	0	0	0	0.01	0.01	0
Mg	6.18	6.58	6.65	6.71	6.69	6.61
Ca	0.01	0.01	0	0	0.01	0
Mn	0.03	0	0	0.01	0	0.02
Fe	3.66	1.06	0.97	3.24	1.03	3.57
TOTAL	20.07	17.83	17.82	19.99	17.84	20.1
Fe/Fe+Mg	37.31	13.88	12.71	32.68	13.37	36.22

	40	41	42	43	44
SAMPNO	M7552	M7552	M7552	M7524	M7524
EASTING	5135	5135	5135	4995	4995
COLOUR	PURPLE	GREEN	TALC		TALC
CRS/FINE	COARSE			COARSE	
Si	5.61	6.07	10.14	5.71	10.18
Ti	0	0	0	0	0
Al	4.66	4.12	0.05	4.59	0.09
Cr	0	0	0	0	0
Mg	5.25	5.39	6.14	6.89	6.63
Ca	0.01	0.01	0	0	0
Mn	0.01	0	0	0.03	0
Fe	4.51	4.22	1.49	2.75	0.87
TOTAL	20.05	19.81	17.77	19.97	17.77
Fe/Fe+Mg	46.27	43.89	19.43	28.79	11.66

Analyses 34-35 Remnant green chlorite in talc ,intergrown with magnetite and chalcopyrite

36-39 Chlorite and talc in Pinter ironstone

40-42 Chlorite and talc from magnetite-talc zone of Deeps ironstone

43-44 Chlorite and talc from Lower West Lode area

TABLE 2 cont WHITE DEVIL TALC AND BIOTITE ANALYSES
Representative talc and biotite analyses
Complete analyses are tables in Appendix 1

BIOTITE

	M7518	M7524 R1a	M7524 R1c	M7545 R1	M7545 R2
SiO2	35.35	40.18	40.48	35.46	31.74
TiO2	0.22	0.48	0.44	0.14	0.10
Al2O3	28.82	13.77	14.02	26.68	22.06
CR2O3	0.01	0.00	0.00		
MgO	6.56	19.75	18.83	6.43	9.46
CaO	0.01	0.07	0.00	0.03	0.04
MnO	0.05	0.03	0.10	0.18	0.11
FeO	15.42	13.81	14.00	17.88	27.06
Na2O				0.12	0.05
K2O				4.98	1.21
H2O	12.40	12.55	12.53	3.86	3.77
F				0.28	0.11
Cl				0.00	0.03
TOTAL	98.84	100.64	100.41	96.05	95.74
O=F				-0.12	-0.04
O=Cl				0.00	-0.01
TOTAL	98.84	100.64	100.41	95.93	95.68

Figure 10.
Plots of Si vs Al, Fe vs Mg, Si vs Mg, Si vs Fe, Al vs Fe and Al vs Mg of the chlorite and talc analyses.

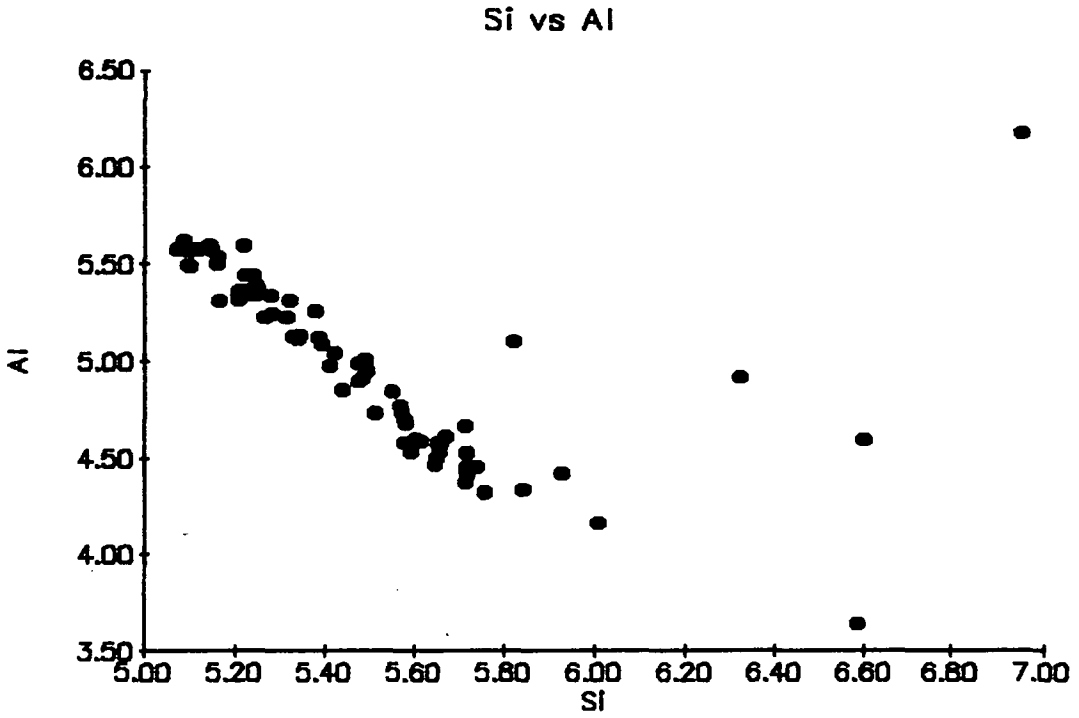

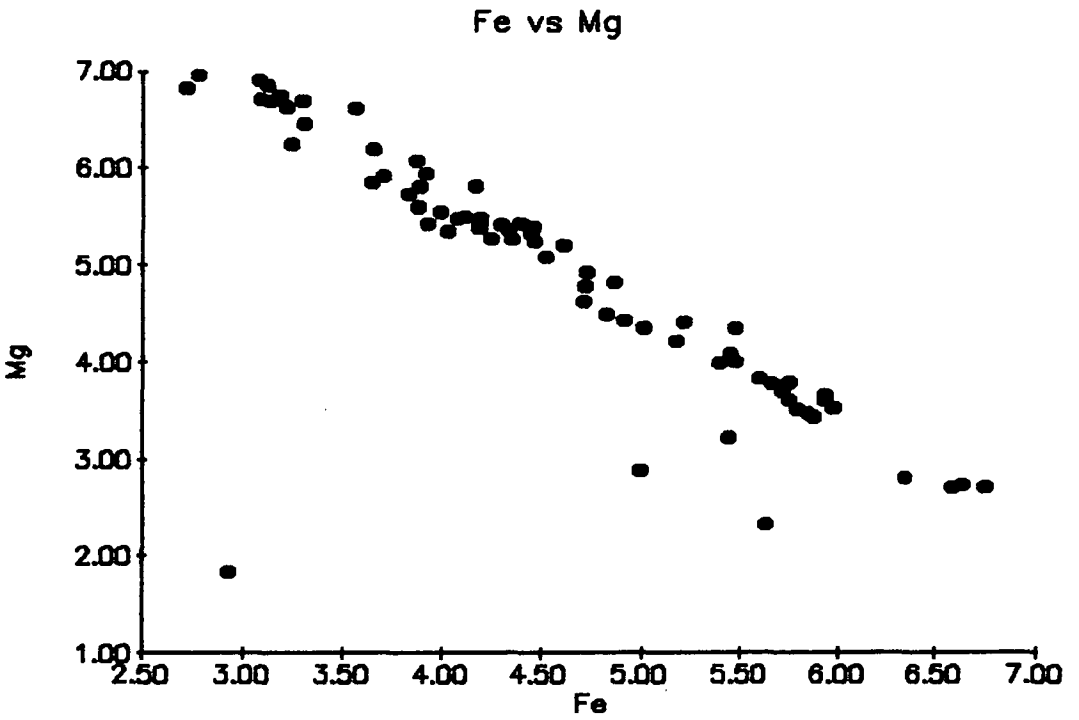

Figure 10 (cont.)

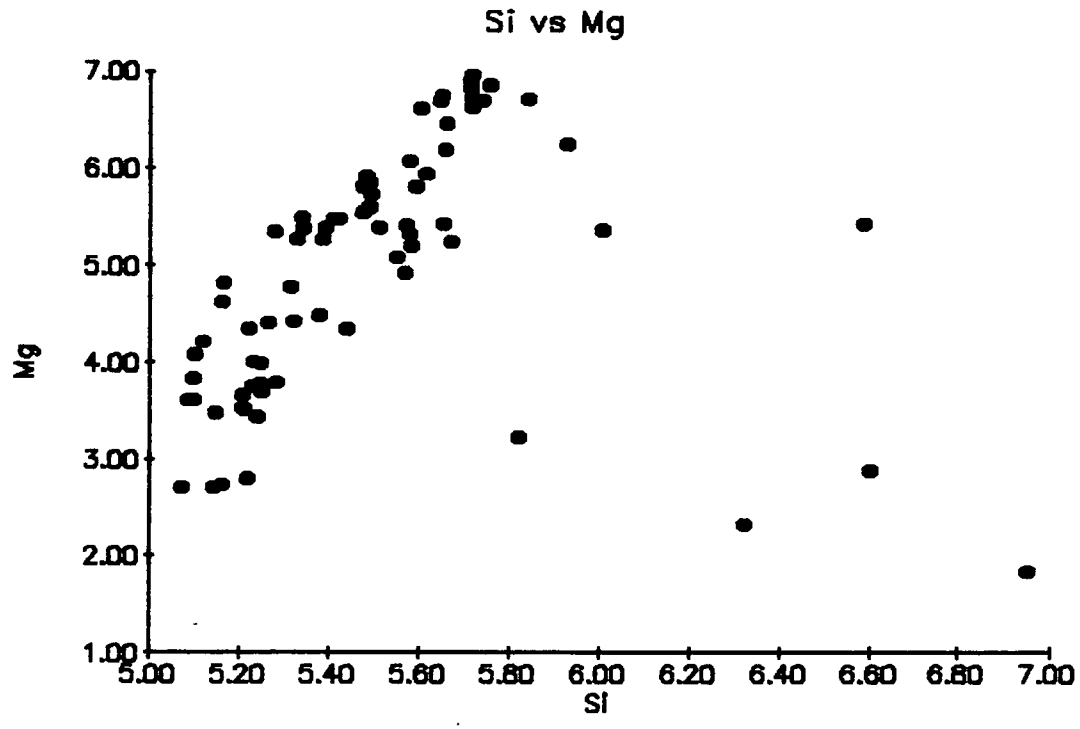

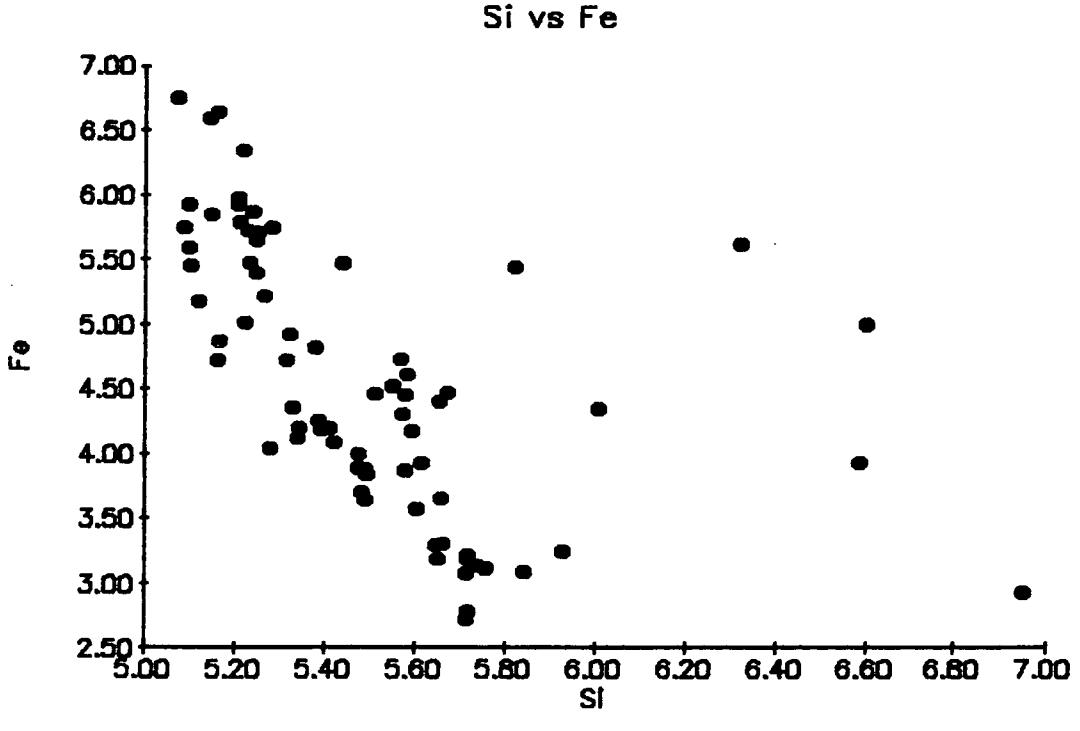

Figure 10 (cont)

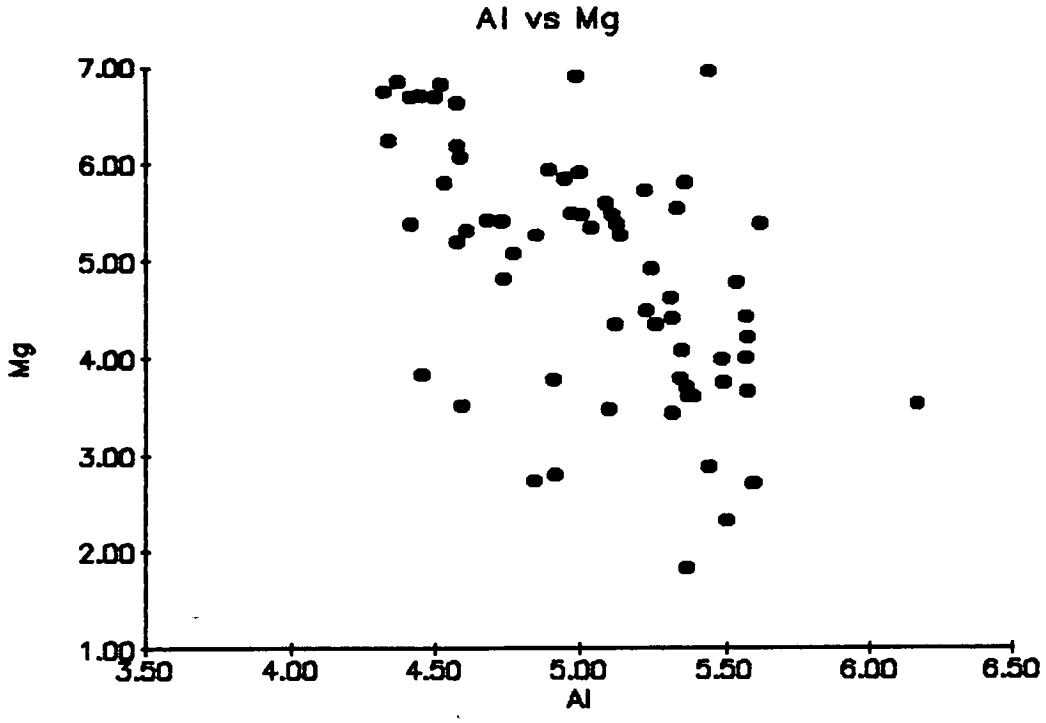

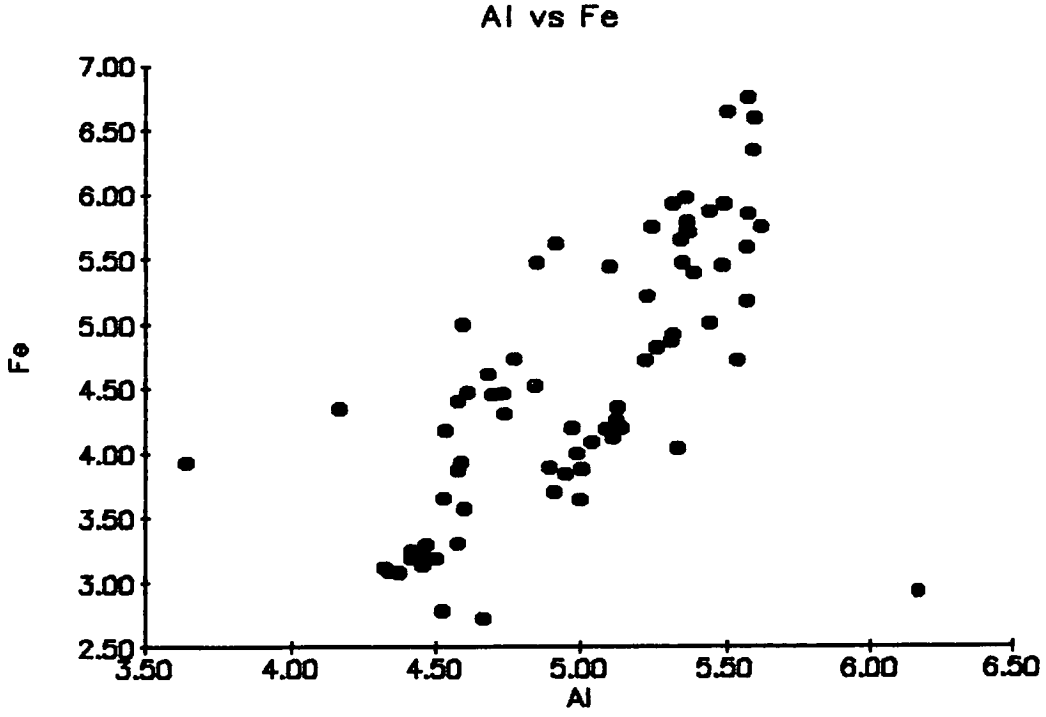

Figure 10b
Mod from Fig 81, Deer et al 1989

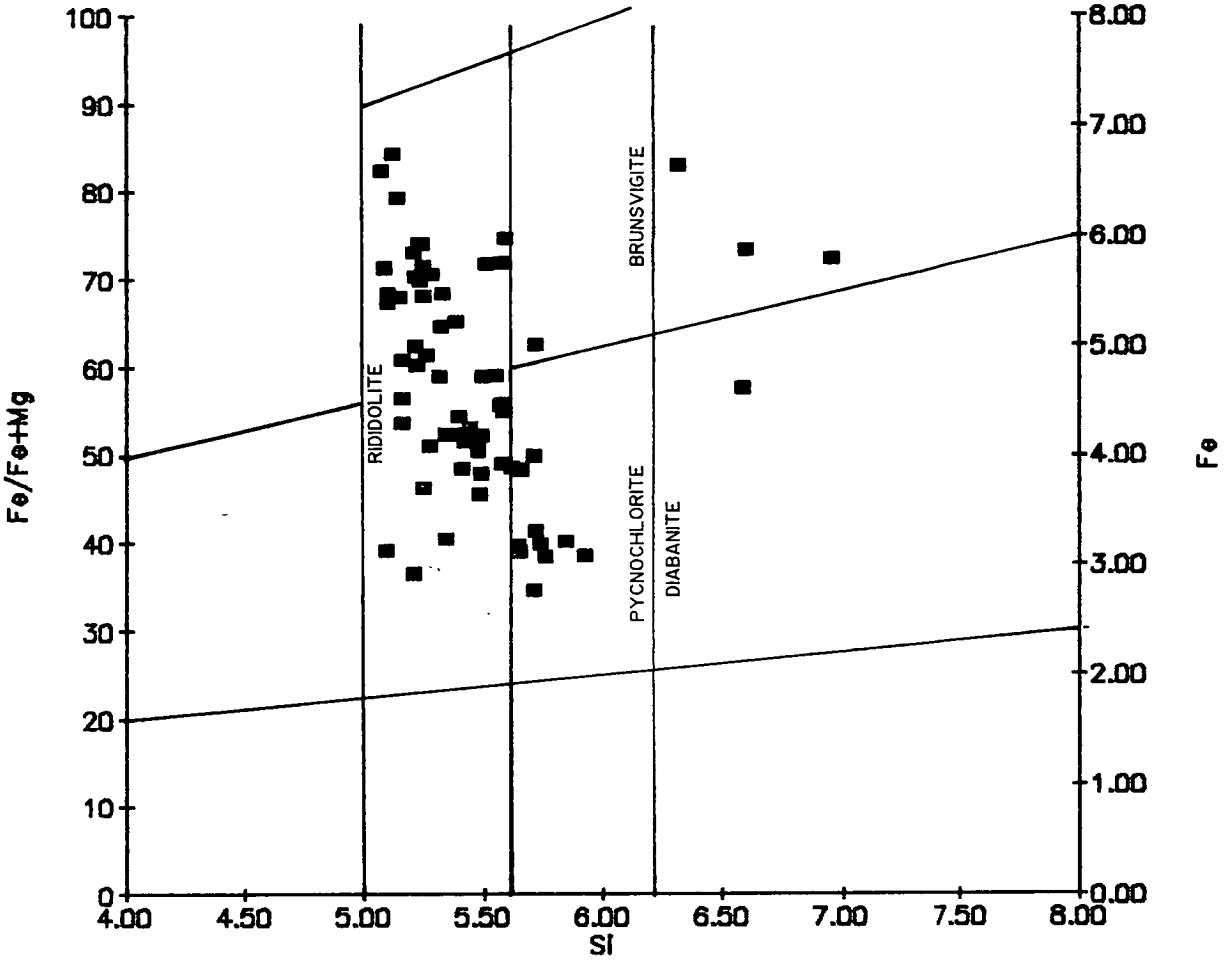

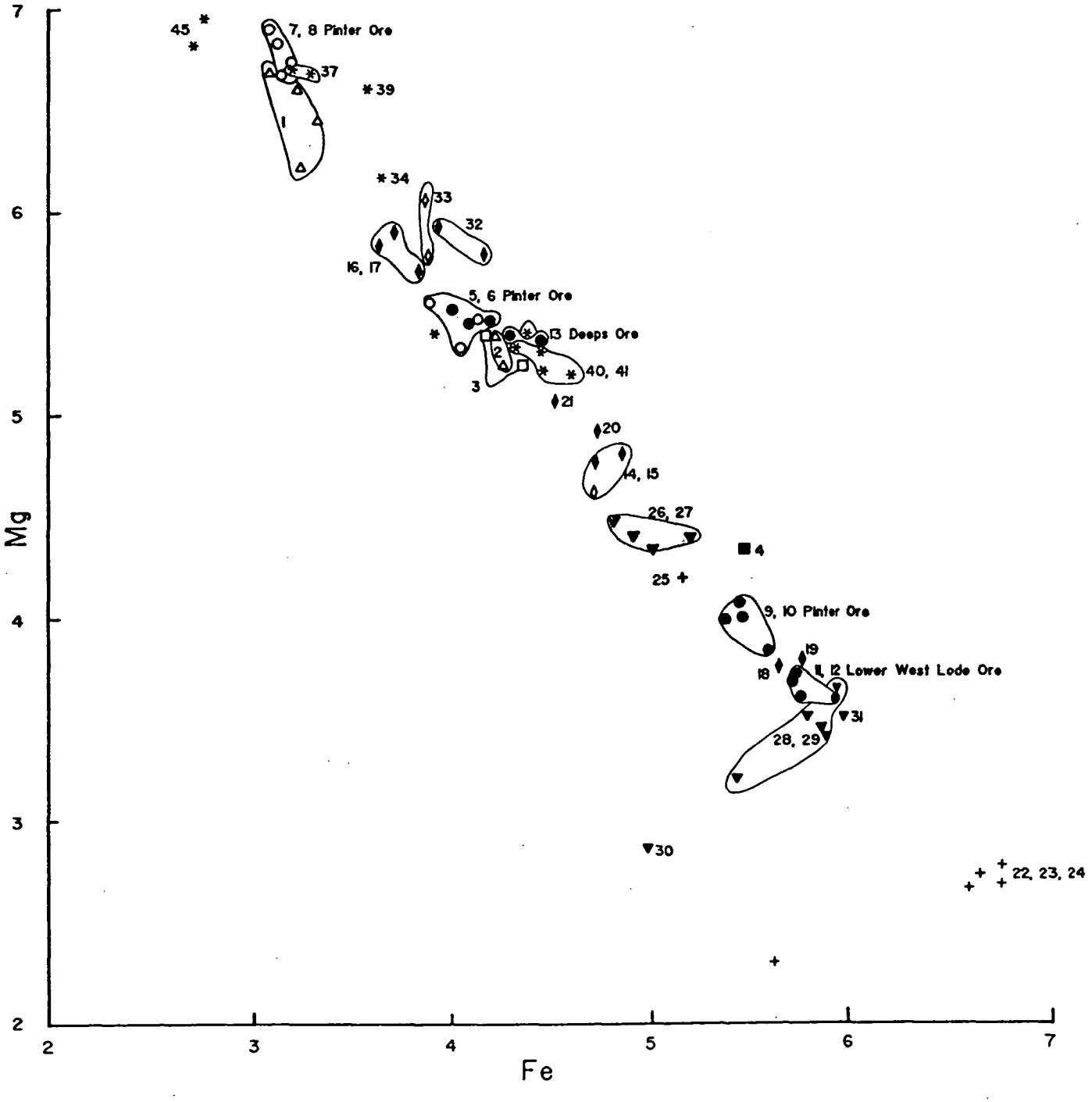

KEY

Chlorite Purple	Chlorite Green	
●	○	Ore
▲	△	MQ + chlorite
♦	◊	AS/m, MAS
■	□	M/C
✳	✳	Chlorite associated with talc
▼	▽	AS
	+	Blue chlorite

POSEIDON EXPLORATION LIMITED

Fe vs. Mg scatterplot showing different chlorite colours and associations. Numbers refer to analyses in tables 1 and 2

Compiled	Date	Scale	Plan No.
G.J.Cozens	June, 1992	N.T.S.	Fig. 11

These analyses have shown that green Mg-chlorite occurs in the ironstone well away from mineralisation and Fe-chlorite occurs near mineralisation.

Ore

The chlorite analyses from the Pinter, Deeps and Lower West Lode ore zones show a wide range of Fe and Mg values, from Fe-rich to Mg-rich. The Pinter Lodes show the widest variation.

Sample M7557(5,6) of altered sediment-magnetite stringer Pinter ore contained both coarse-grained green and fine grained purple chlorite. The green chlorite occurred around the magnetite and the purple in the altered sediments. The chlorites have slightly different compositions, with the purple containing lower Al, higher Si and Fe. The samples both have Fe/Fe+Mg ratios about 42 and are thus Mg chlorites. This sample shows that there is very little compositional difference between green and purple chlorite.

Sample M7504(7,8) from the same cross section, is of stringer ore containing both coarse grained green chlorite around the magnetite and fine grained green chlorite in the altered sediment. The samples have very similar compositions and the low Fe/Fe+Mg ratio indicates that they are very Mg rich. The Mg and Fe values in this sample are similar to those in M7561, from the northern edge of the Pinter Ironstone.

Sample M7503(9,10) is vastly different to the previous Pinter ore samples, being Fe rich, with a Fe/Fe+Mg ratio of 57 to 58. The sample is of stringer ore and contains coarse and fine purple chlorite. The coarse has higher Mg and lower Fe values than the fine.

Sample M7521(11,12) of Lower West Lode ore consists of coarse purple chlorite among magnetite, quartz and bismuth and fine purple chlorite in altered sediments. The chlorite are very Fe rich with Fe/Fe+Mg ratios between 60 and 62. The coarse chlorite has slightly lower Si and Mg and higher Al and Fe than the fine. The coarse chlorite is intergrown with bismuth, indicating contemporaneous formation.

This sample has similarities to M7503 from the Pinter Lode, despite being at opposite ends of the deposit.

A sample of Deeps magnetite-chlorite altered sediment ore, M7538(13), containing fine grained purple chlorite in the altered sediment has a Fe/Fe+Mg ratio of 45, indicating that it is Mg chlorite.

Thus within the ore zones the chlorites have a very wide range of Fe-Mg content and the purple chlorites appear to be Fe rich relative to the green which are Mg rich.

Stringer Zone

Samples from the stringer zone comprise altered sediments with magnetite stringers and the more magnetite rich magnetite-altered sediment rock. These samples show a wide range of Fe and Mg values.

Sample M7509(5225E)(14,15) contains fine purple chlorite in the sediment and coarse green chlorite among the magnetite. The green chlorite contains lower Si, Mg and Fe and higher Al than the purple. The sample has a Fe/Fe+Mg ratio of 50 to 51, indicating that it is Fe rich.

Sample M7506(5265E)(16,17) consists of a coarse purple chlorite vein containing magnetite within coarse green chlorite adjacent to a Pinter Lode gold pod. The chlorites are Mg rich, Fe/Fe+Mg ratio of 39, and the green contains slightly more Mg than the purple. This chlorite is not as Mg rich as the chlorite within the gold pod, sample M7504.

Sample M7522(18,19) of magnetite-altered sediment from 5015E contains fine and coarse purple Fe chlorite, with a Fe/Fe+Mg ratio of 60. This sample is adjacent to the ore sample M7521, which is also Fe rich. The coarse chlorite has lower Al and higher Fe content than the fine.

Sample M7534(20,21) of magnetite-altered sediments adjacent to the tabular ironstone on 4995E contains fine purple Mg-chorite in the altered sediments and coarse

green among the magnetite. The green chlorite has slightly lower Si and Fe and higher Al and Mg content than the purple.

The stringer zone chlorites show a wide range of Fe and Mg values, ranging from Fe rich to Mg rich. The stringer chlorites have similar compositions to nearby ore zones indicating the same fluids flowed throughout the shear zone. Where purple and green chlorite coexist, they have essentially the same composition.

Altered Sediments

Both samples M7517(22,23,24) and M7518(25) contain blue chlorite in quartz veins in altered sediment. Sample M7517 is from the South Lower Main Zone orebody on 5075E and consists of altered sediments with minor magnetite stringers. The blue chlorite occurs in a quartz vein and in the enclosing sediment and is extremely Fe rich, with a Fe/Fe+Mg ratio of 71. The Fe/Fe+Mg ratio and colour of the chlorite is similar to the Berlin Blue chlorite of Kranidiotis and Maclean (1987) observed at the Phelps Dodge massive sulphide deposit. The purple chlorite at White Devil corresponds to their violet chlorite. The chlorite in the sediment contains slightly lower Mg, Fe Al and higher Si than the vein chlorite. The chlorite contains a normal amount of water and according to Deer, Howie and Zussman(1989) is not oxidised chlorite. The blue chlorite in sample M7518 is not as Fe rich as M7517 despite occurring at the same location.

Sample M7519(26,27), also from 5075E, is of coarse grained purple chlorite within fine grained purple altered sediments. This sample is Fe rich with a Fe/Fe+Mg ratio of 53 and has a similar composition to M7518. The coarse chlorite contains higher Fe, Al and lower Si and Mg than the fine.

Sample M7544(28,29) of altered sediment and quartz-chlorite vein from the south side of the tabular ironstone, on the edge of the shear, on 5155E contains Fe rich fine purple chlorite in the altered sediment and coarse purple in the vein. A traverse across the sediments and vein was sampled to test for variations in composition and the effects of pervasive alteration. The analyses are shown in Figure 12. The graph

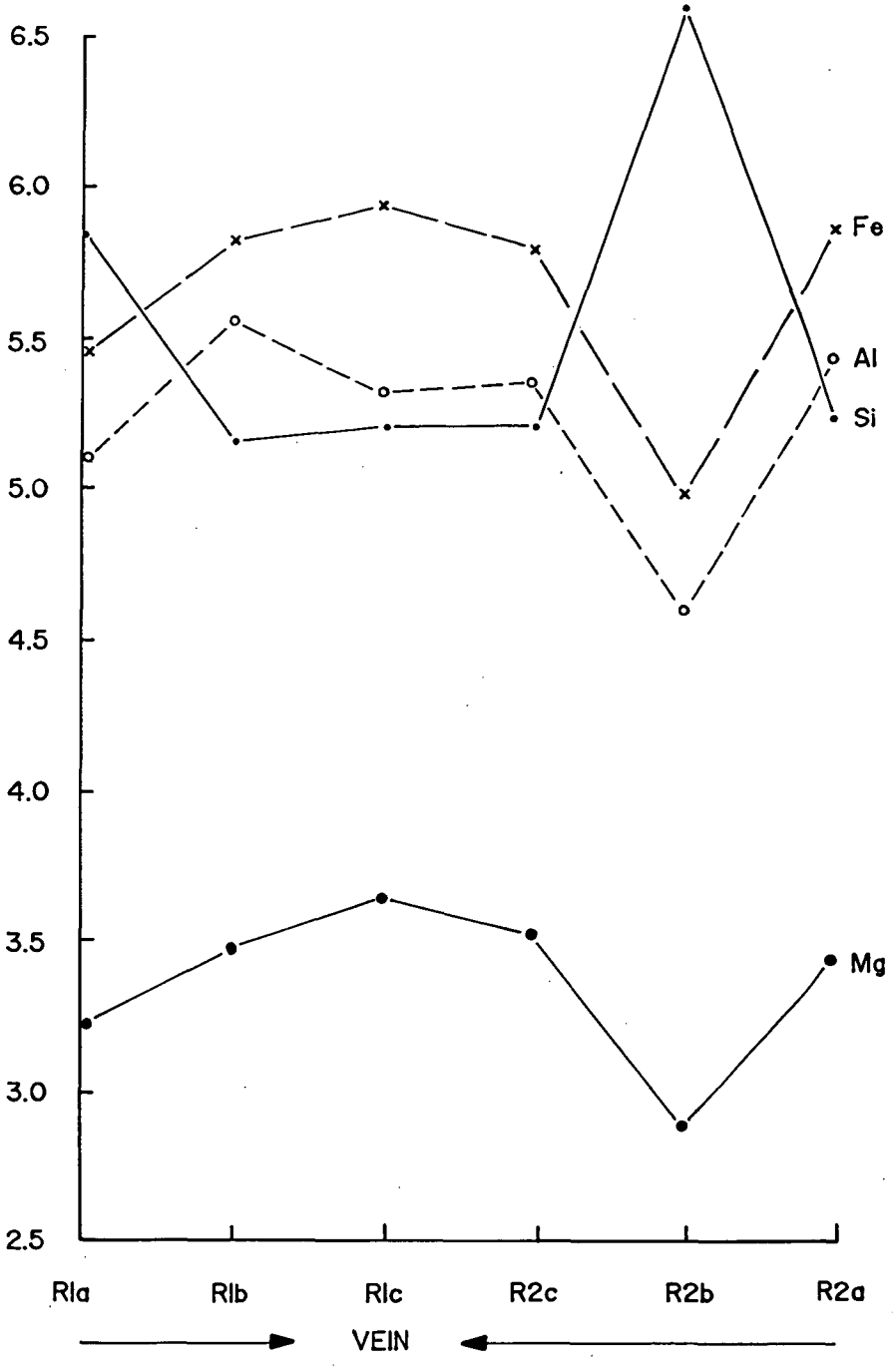

Figure 12 - VARIATION IN CHLORITE COMPOSITION
ACROSS QUARTZ-CHLORITE VEIN
SAMPLE M7544

shows that the Fe and Mg contents peak in the vein and that Si and Al occur in almost equal amounts. Away from the vein the Si and Al contents vary, dramatically in the case of sample R2b. The Fe and Mg content of sample R2b is significantly lower than the other samples, yet the Fe/Fe+Mg ratio is consistent. The variation results from a constant sum effect: the high concentration of Si excludes Mg, Fe and Al from the analysis. The R1a and R2b analyses may be composites of chlorite and quartz. The variations in Si and Al content in the other analysis is probably due substitution of Si for Al. Sample M7545(30,31) from a similar location and rock type to M7544, has similar Fe/Fe+Mg ratio of 62.

In sample M7553(32,33) coarse green chlorite occurs adjacent to fine purple chlorite in altered sediments with pyrite within the central part of the shear. Both chlorites are Mg rich, with a Fe/Fe+Mg ratio of 40. The green chlorite has slightly lower Fe and Si and higher Mg and Al content to the purple chlorite. This sample from 5135E has similarities with sample M7506 from the Pinter area stringer zone.

The chlorite in the altered sediments is generally Fe rich, except for M7553.

Talc

Within ironstones, adjacent to ore zones and within altered sediments alteration of Mg-chlorite to talc has taken place. Representative analyses are shown in Table 2.

During talc alteration the Si content almost doubled to 10 cations, the Mg content increases or decreases, depending upon the initial Mg content, to approximately 6 cations, the Fe content falls to approximately 1 cation and Al is almost completely removed. Thus during this process Al and Fe are released into, and Si removed from the hydrothermal fluid.

Samples M7559(36,37) and M7558(38,39) are of Mg chlorite partially altered to talc from the Pinter ironstone. The chlorites have similar composition to the chlorites in samples M7561, from the Pinter Ironstone, and M7405 from the Pinter ore zone. These compositions are consistent with the paragenetic interpretation that talc replaced chlorite within the Pinter Ironstone.

Sample M7552(40,41,42) from the magnetite-talc zone of the Deeps ironstone on 5135E contains purple and green Mg chlorite which has been altered to talc. The chlorite has a similar composition to the chlorite in the Deeps Ore sample, M7538.

Sample M7524(43,44) from the Lower West Lode area (4995E) contains very Mg rich chlorite altered to talc. This sample is separated from the orebodies by a quartz porphyry body and is associated with magnetite-talc and stringers. This sample is different from the others as the Lower West Lode ore is hosted by Fe rich chlorite, which does not have any associated talc.

Biotite

During the microprobe study several grains of biotite were observed within altered sediments. The analyses are shown in Table 2 and Appendix 1.

Only two of the 5 analyses were analysed using the biotite program on the microprobe, the other were analysed using the chlorite program. The biotites are low Ti, Na, high Al, Mg compared to the examples in Deer, Howie and Zussman (1989) and have similarities to the chlorites in the deposit. Huston (1991) noted the presence of hydrothermal biotite within quartz feldspar porphyry and the biotite in the altered sediments may also be hydrothermal.

Geothermometry

Chlorite geothermometry of the Los Azufres (Mexico) geothermal system was investigated by Cathelineau and Nieva (1985). They showed that there was a positive correlation between the Al^{iv} content of the chlorite and temperature (Fig 13, Cathelineau & Nieva,1985).

Kranidiotis and Maclean (1987) used the relationship derived by Cathelineau and Nieva (1985) to calculate the temperature of formation of chlorite at the Phelps

Dodge massive sulphide deposit at Matagami, Quebec. Kranidiotis and Maclean (1987) converted the formula of Cathelineau and Nieva (1985) to $8(Si+Al^{iv})$ and solved for T, yielding:

$$T^{o}C = 106Al^{iv} + 18$$

where Al^{iv} = 8-#Si cations.

A brief study of the temperatures of chlorite formation at White Devil was made using the above model. The results are shown in Figure 13 and 14, Table 1 and Appendix 1.

The Al vs T plot in figure 13 shows that the majority of the chlorites have a temperature range from 250 to 330°C. The four samples less than 200°C are from different samples and are probably erroneous. These analyses correspond to samples with anomalously high Si which may due to the chlorite containing minor quartz. The Si vs T plot in Figure 13 shows a negative relationship, which is to be expected. The Mg vs T plots shows some scattering of the data but shows a definite negative trend. The low temperature chlorites all contain low Mg. The Fe vs T plot shows a positive trend and the low temperature chlorites have a range of Fe values.

Figure 14 shows the temperature distribution of the different chlorites in detail. The formation temperature of chlorite within the orebodies are well grouped, but each orebody plots at a separate location on the graph, indicating a wide range of temperature of formation of ore mineralisation.

The green chlorite in a Pinter Lode (M7504) has similar temperature to chlorite associated with talc and chlorite in magnetite-quartz Pinter Ironstone and occurs at the low temperature end of the graph.

The two Deeps Ore chlorite analyses have temperatures of 275 and 282°C and have similar temperatures to higher temperature chlorite associated with talc and green and purple chlorite in the Stringer Zone and altered sediments.

The Pinter Lode (M7504) containing green low temperature chlorite is very rich in gold, similar to the Deeps, suggesting these two orebodies formed at similar times. This is in agreement with the model proposed by Huston et al (in press).

Figure 13
Temperature vs Al(iv), Si, Mg and Fe plots.

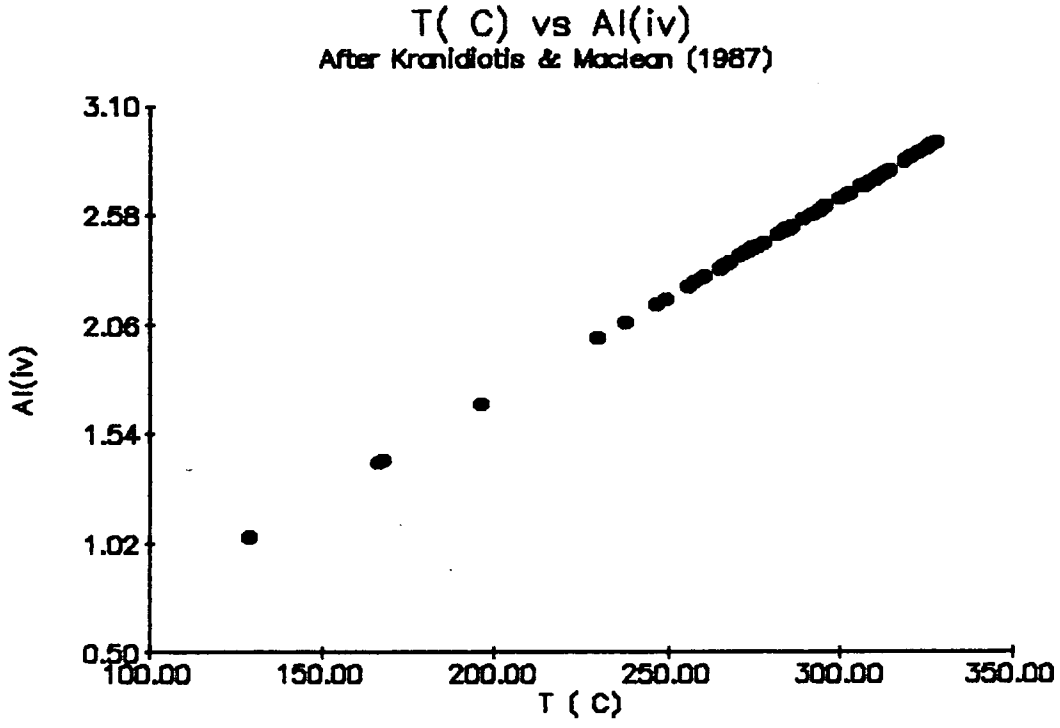

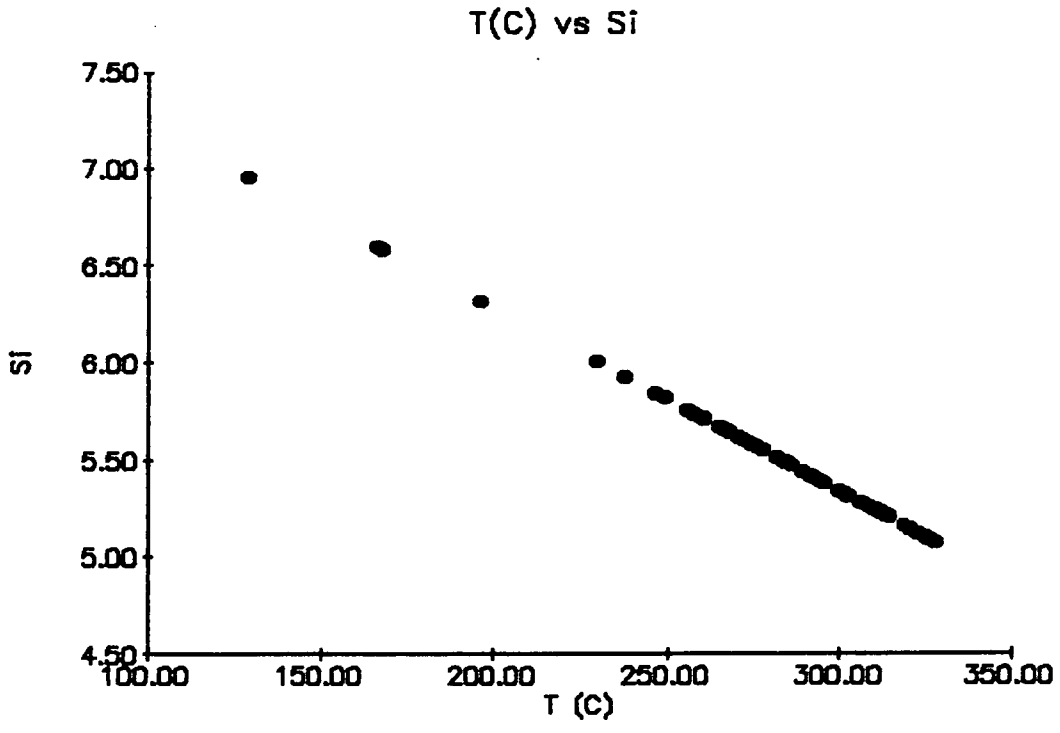

Figure 13 (cont.)

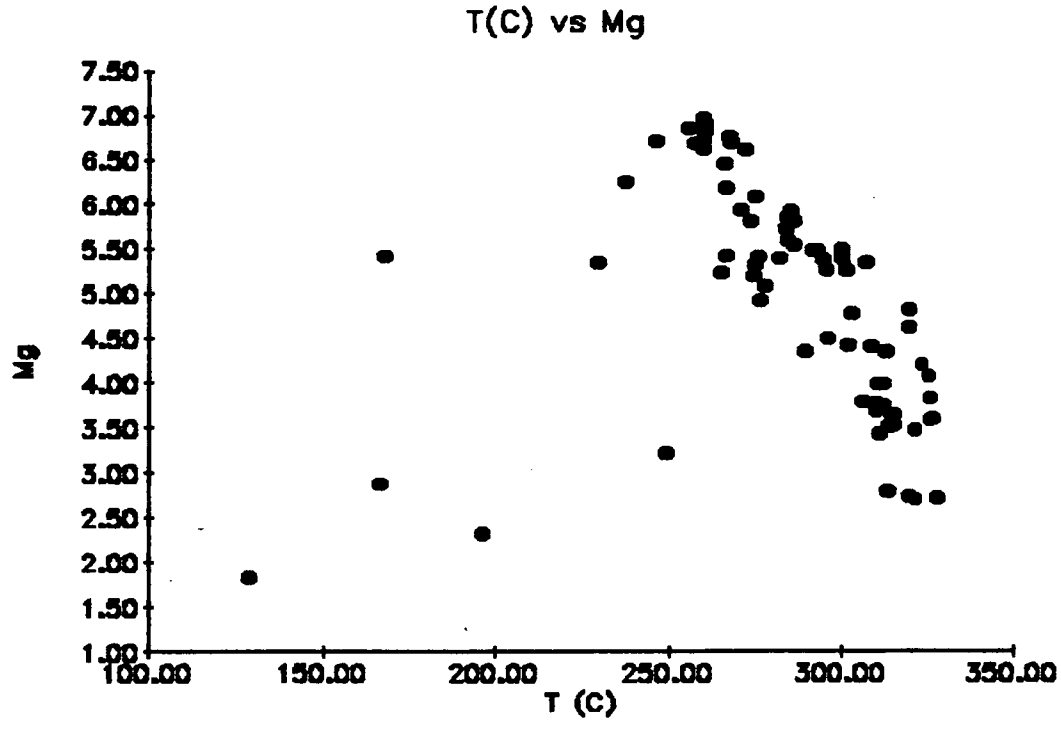

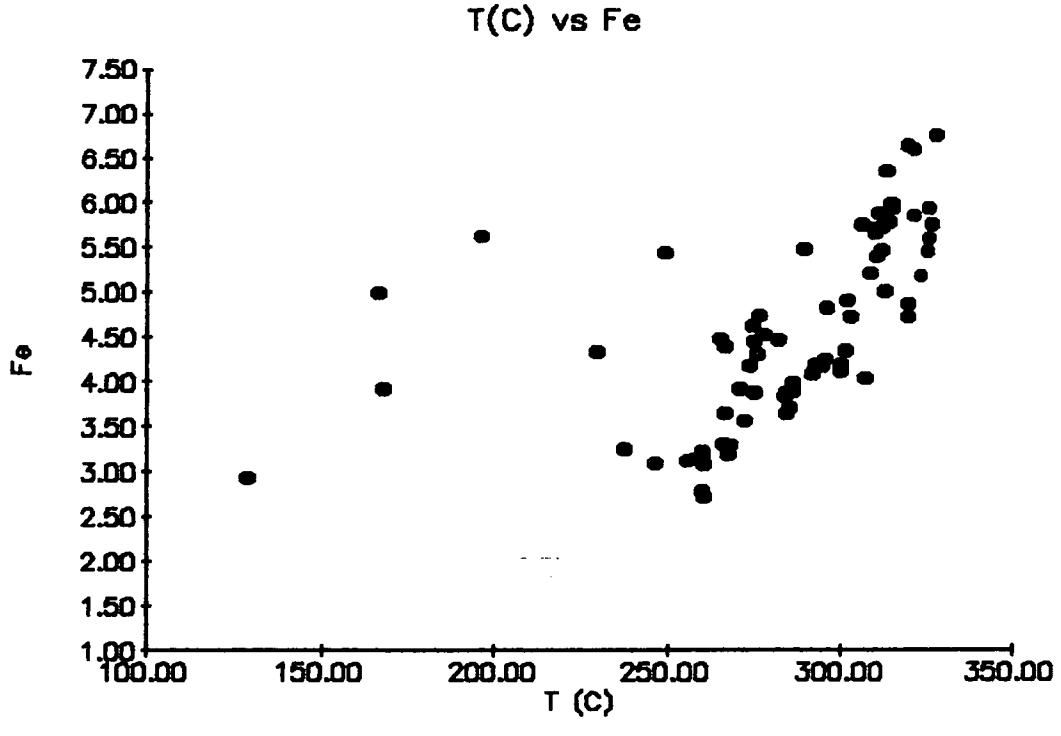

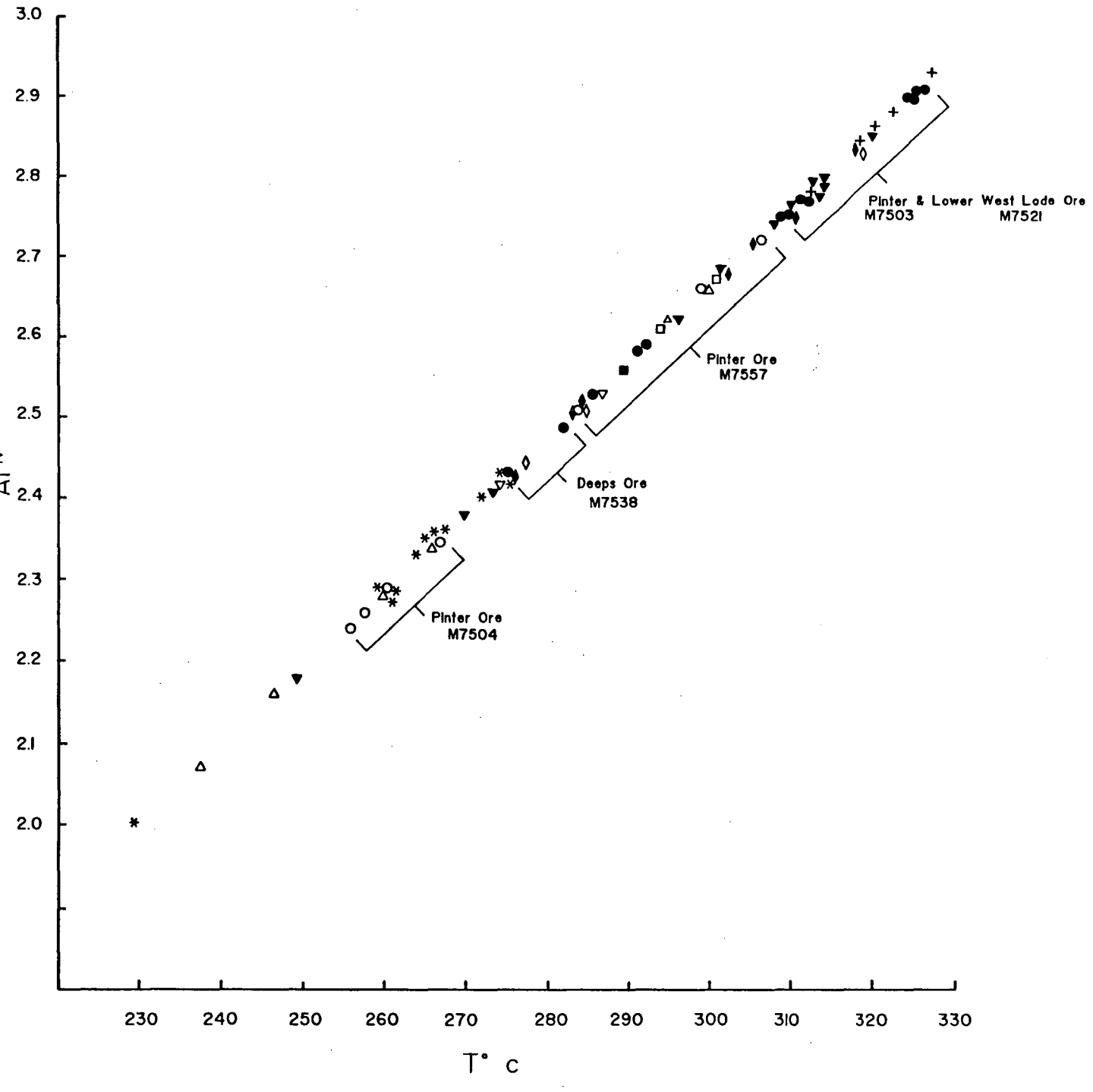

KEY

Chlorite

Purple	Green	
▲	△	MQ
●	○	Ore
■	□	Mag. - minor chlorite
♦	◊	AS/m, MAS
	*	Chlorite associated with talc
▼	▽	AS
+		Blue chlorite

POSEIDON EXPLORATION LIMITED

Detailed T°c vs Al iv
Showing temperatures of chlorite associated with ore & different rock types

Compiled	Date	Scale	Plan No.
G.J.Cozens	June, 1992	N.T.S.	Fig. 14

Higher temperature Pinter ore (M7557), 284 to 306°C, is associated with purple chlorite in magnetite-minor chlorite, green and purple chlorite in the Stringer Zone and chlorite in the Pinter Ironstone near the Stringer Zone contact. The wide range of chlorite temperatures in the ore indicates the ore was progressively deposited as the fluids heated up.

The high temperature Pinter and Lower West Lode ore has similar temperature to the blue chlorite in a quartz vein in altered sediment associated with the South Lower Main Zone orebody. These chlorites are also Fe rich. The Pinter and Lower West Lode chlorite have almost identical temperatures and distribution. Both samples contain chlorite between 310 and 315°C and 325 and 328°C, indicating chlorite deposited over a range of temperatures.

Within the Pinter ore lode system the temperatures of chlorite formation vary over a wide range, indicating several phases or an evolution of the mineralising fluids.

Only the low temperature chlorites have been altered to talc.

The temperatures calculated are lower than the temperatures from Type II fluid inclusions (Huston 1990a), which gave a temperature range from 325 to 350°C.

Within sample temperature variation occurs between the coarse and fine chlorite and green and purple (Table 1 and Appendix 1). In general in the altered sediments the coarse grained purple chlorite has a higher temperature than the fine purple and green chlorite. In the Stringer Zone, fine purple chlorite in the altered sediments has a higher temperature than coarse purple chlorite among magnetite. The coarse green chlorite has a higher temperature than fine purple. In the ore bodies the coarse green chlorite has a higher temperature than fine purple chlorite, but the coarse green has a lower temperature than fine green chlorite. Fine and coarse purple chlorite have similar temperatures. In sample M7517 the blue chlorite in the vein has a higher temperature than the fine chlorite in the altered sediment and the chlorite in the cross-cutting vein has a higher temperature than the earlier vein. Thus, in general the coarse grained chlorite formed at a higher temperature than the fine grained chlorite.

Conclusions

The chlorite within the deposit contains a range of Fe and Mg contents from very Fe rich to very Mg rich. The distribution and variation in Fe and Mg content of the chlorites is shown in Figure 15. The sections show the changes in Fe/Fe+Mg ratio within and between rock types.

The detailed Fe vs Mg plot (Figure 11) shows that there is a complete spectrum of chlorite compositions within the deposit rather than 2 distinct populations as suggested by Nguyen et al (1989) and Edwards et al (1990).

The chlorite associated with gold-bismuth-copper mineralisation ranges from Mg to Fe rich, even within the same lode system, as shown on section 5265E in Figure 15.

Where both purple and green chlorite occur together they essentially have the same composition and are generally Mg-chlorite. The green chlorites generally have higher Al and Mg and lower Si and Fe contents than the purple. The coarse and fine purple chlorite also vary slightly in composition, with the coarse being lower in Si but variable for Al, Mg and Fe. Generally the Mg and Fe contents are inversely related. The differences in composition may be due to the compositions of the different mediums the chlorite occurs in, or in the temperature of the hydrothermal fluids.

The green chlorites tend to be Mg-chlorite, the purple range from Mg to Fe rich and the blue are very Fe rich. This is consistent with the observations of Kranidiotis and Maclean (1987) in the Phelps Dodge massive sulphide deposit.

The chlorite altered to talc is Mg rich and has similar composition to associated orebodies indicating talc alteration post dated the mineralisation. The green chlorite within the Pinter ironstone is similar to the chlorite associated with talc near the Pinter Lodes, indicating that the Mg chlorite in the ironstone well away from mineralisation and now flooded with quartz, probably formed during the mineralising stage.

The chlorite in the altered sediments is generally Fe-chlorite and in the stringer zone ranges from Fe to Mg chlorite.

During talc alteration abundant Fe and Al were released into and Si and lesser Mg removed from the hydrothermal system.

The geothermometry showed that the majority of the chlorites formed between 250 and 330^{o}C and that ore deposition occurred over this temperature range. The green chlorites formed at the lower temperatures and blue at the high, with purple covering a wide range in between.

The hypothesis of Huston (1990a) that the presence of chlorite with anomalous blue birefringence was an indicator of mineralisation is still valid although the chlorite colour observed by Huston included both purple and blue at White Devil. The only blue chlorite observed in this study was in a quartz vein in altered sediment associated with the South Lower Main Zone orebody (M7517) and in a quartz vein in chloritic sediment within the shear (M7518), thin sections from which were not available prior to this study. The presence of coarse grained chlorite among magnetite may be an indicator of the presence of mineralisation.

Given the wide range of chlorite compositions throughout the deposit the observation by previous workers, that the ore is hosted by Mg-chlorite, has not been supported by this study. The ore is hosted by Mg-rich low temperature chlorite to Fe rich high temperature chlorite. The observation of Edwards et al (1990) that the chlorite in the altered sediment is relatively more Fe rich than that associated with the mineralisation is correct given that the only samples available at that time were from the Deeps Orebody, which is hosted by relatively Mg chlorite. This study has shown that mineralisation is hosted by Fe rich chlorite, with a Fe content greater than most of the altered sediment. The Fe chlorites are also the higher temperature chlorites, indicating they formed at the peak of the hydrothermal event. The chlorite in the sediments well outside the shear was not analysed in this study.

SECTION 4995E

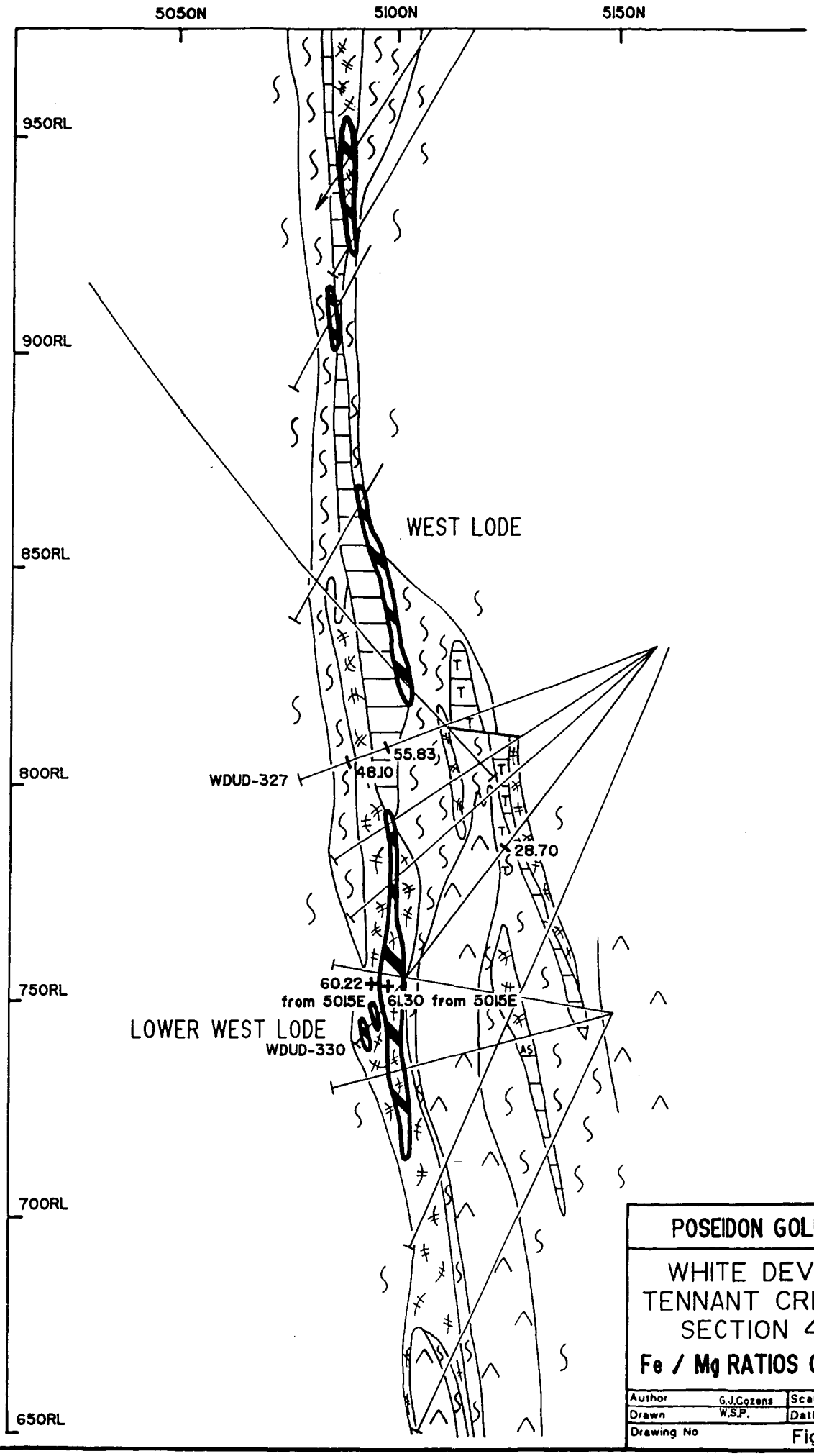

POSEIDON GOLD LIMITED

WHITE DEVIL MINE
TENNANT CREEK - N.T.
SECTION 4995E
Fe / Mg RATIOS OF CHLORITE

Author	G.J.Cozens	Scale	1 : 1250
Drawn	W.S.P.	Date	Feb. 1992
Drawing No		Figure 15 (i)	

SECTION 5155E

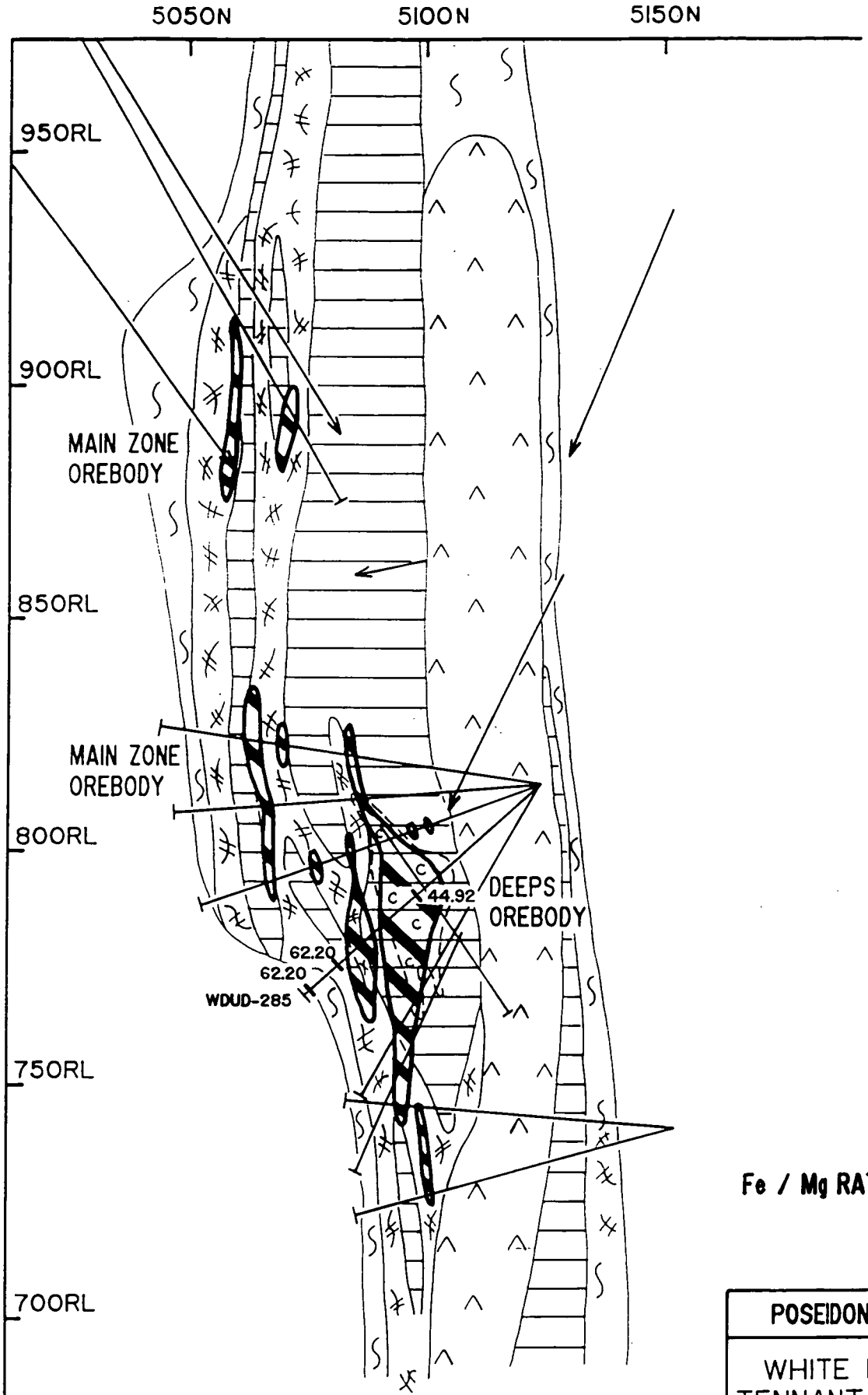

Fe / Mg RATIOS OF CHLORITE

POSEIDON GOLD LIMITED

WHITE DEVIL MINE
TENNANT CREEK - N.T.
SECTION 5155E

Compiled by G.J.COZENS - April, 1992
Drawn by W.S.P. - Scale 1 : 1250

Figure 15 (ii)

SECTION 5235E

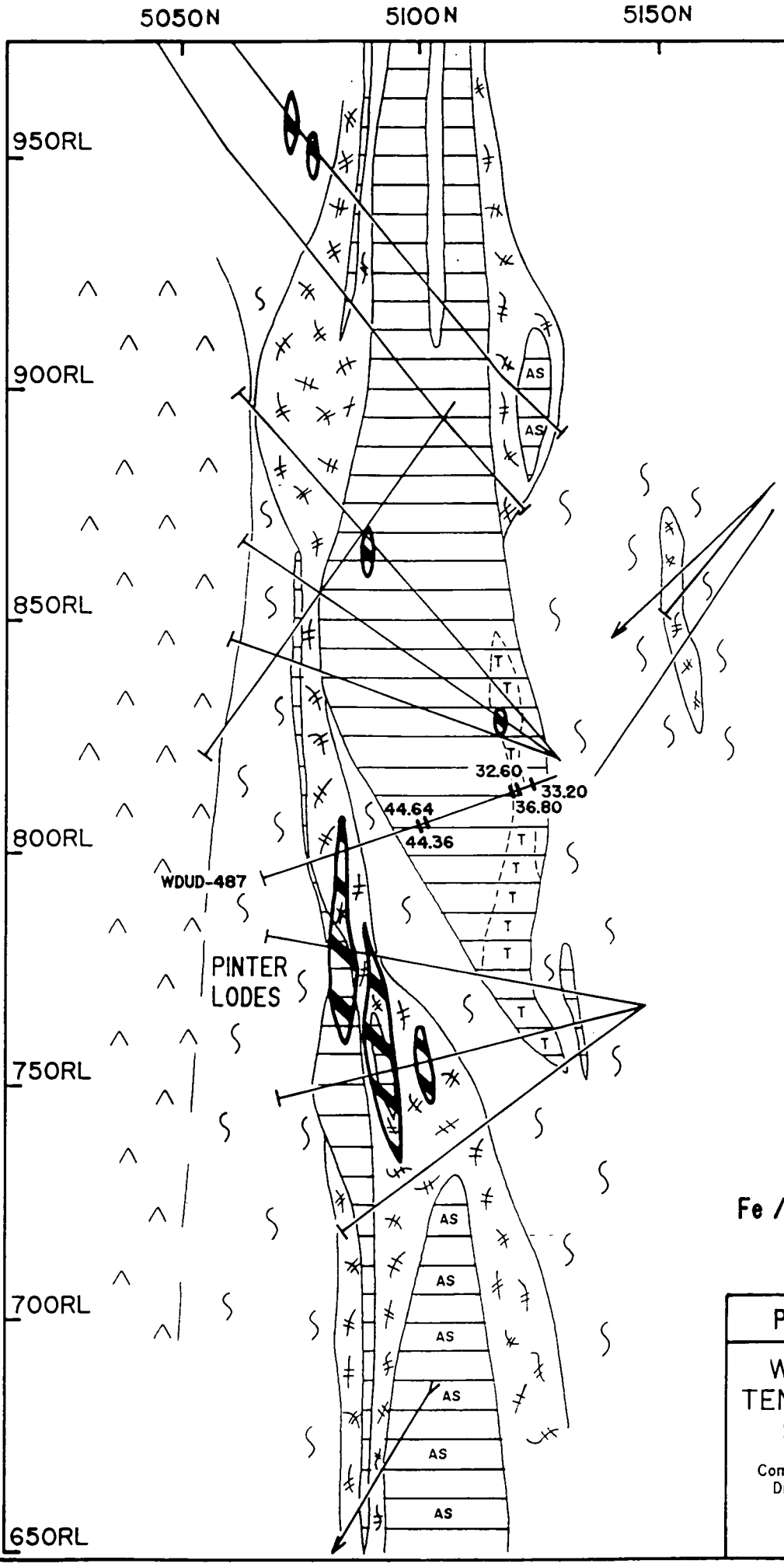

Fe / Mg RATIOS OF CHLORITE

POSEIDON GOLD LIMITED

WHITE DEVIL MINE
TENNANT CREEK - N.T.
SECTION 5235E

Compiled by G.J.COZENS - April, 1992
Drawn by W.S.P. - Scale 1 : 1250

Figure 15 (iii)

SECTION 5265E

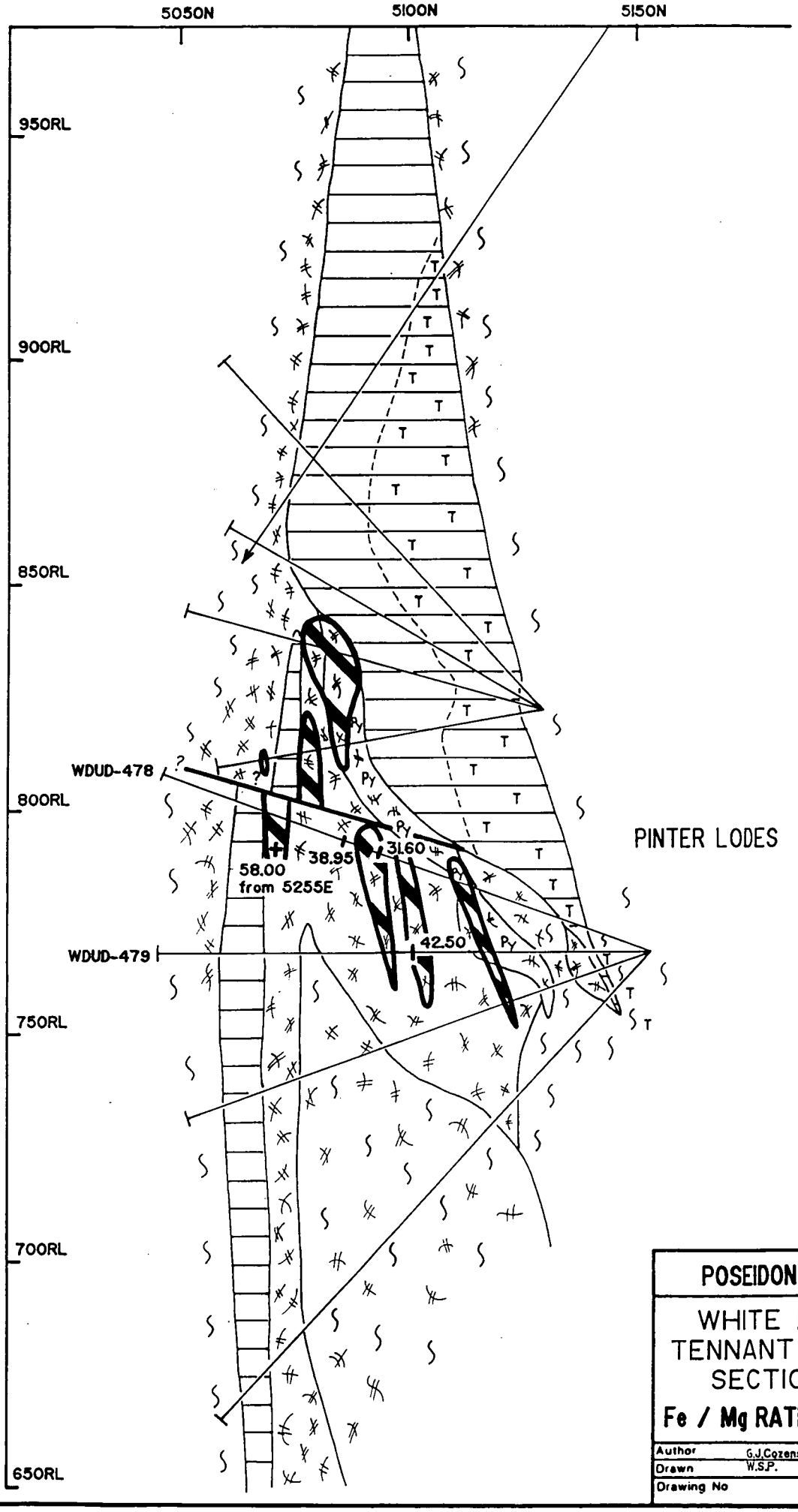

POSEIDON GOLD LIMITED

WHITE DEVIL MINE
TENNANT CREEK - N.T.
SECTION 5265E

Fe / Mg RATIOS OF CHLORITE

Author	G.J.Cozens	Scale	1 : 1250
Drawn	W.S.P.	Date	Feb. 1992
Drawing No		Figure	15 (iv)

7 PARAGENESIS AND MODEL

7.1 IRONSTONE FORMATION

There are two schools of thought amongst those who have worked on Tennant Creek deposits as to the formation of the ironstones. The replacement model (Large 1975, Wedekind et al 1989) infers that the ironstone formed by the interaction of and replacement of oxidised sediments by iron-rich reduced connate fluids. The alternative model of Wall and Valenta (1990) argues that the ironstone precipitated in dilation zones associated with regional deformation, from a mixture of high salinity connate and magmatic fluids.

The current model of Huston et al (in press) suggests that the ironstone formed at the contact between oxidised sediments with significant disseminated hematite and underlying reduced sediments with disseminated magnetite. Sulphur poor, reduced, low temperature connate fluids were focussed up along reverse faults or anticlinal hinges during regional greenschist facies metamorphism. The interaction with fluids in equilibrium with the oxidised sediments caused the precipitation of iron oxides and the formation of ironstones by a combination of open space filling (Wall & Valenta, 1990) and replacement of sediments (Large,1975; Wedekind et al.,1989).

At White Devil the ironstone is located within a shear near the hinge of an east-west anticline where open space filling could dominate.

Textural evidence from the ironstones suggests that the majority of the ironstone existed prior to the influx of reduced fluids and magnetite alteration. Evidence for this is the consistent lath like texture throughout the ironstone, including the stringers. Only small zones of primary magnetite were observed, towards the centre of the shear.

The proposed model is that oxidised fluids were channelled into the shear, which was already chloritised, and precipitated hematite within and near the major fluid channel which migrated towards the centre of the shear leaving behind a mass of

PLATE 29a

Start of ironstone. Single and interlocking laths within altered sediments. The original hematite grew within the sediments and was later altered to magnetite. Bright white rectangular laths are muscovite.
Thin section: M7508, WDUD 454, 56.8m, 5245E
FOV= 1.7mm

PLATE 29b

Skeletal/spongy texture developed in interlocking laths within altered sediments
Thin section: M7508, WDUD 454, 56.8m, 5245E
FOV=1.7mm

PLATE 29a

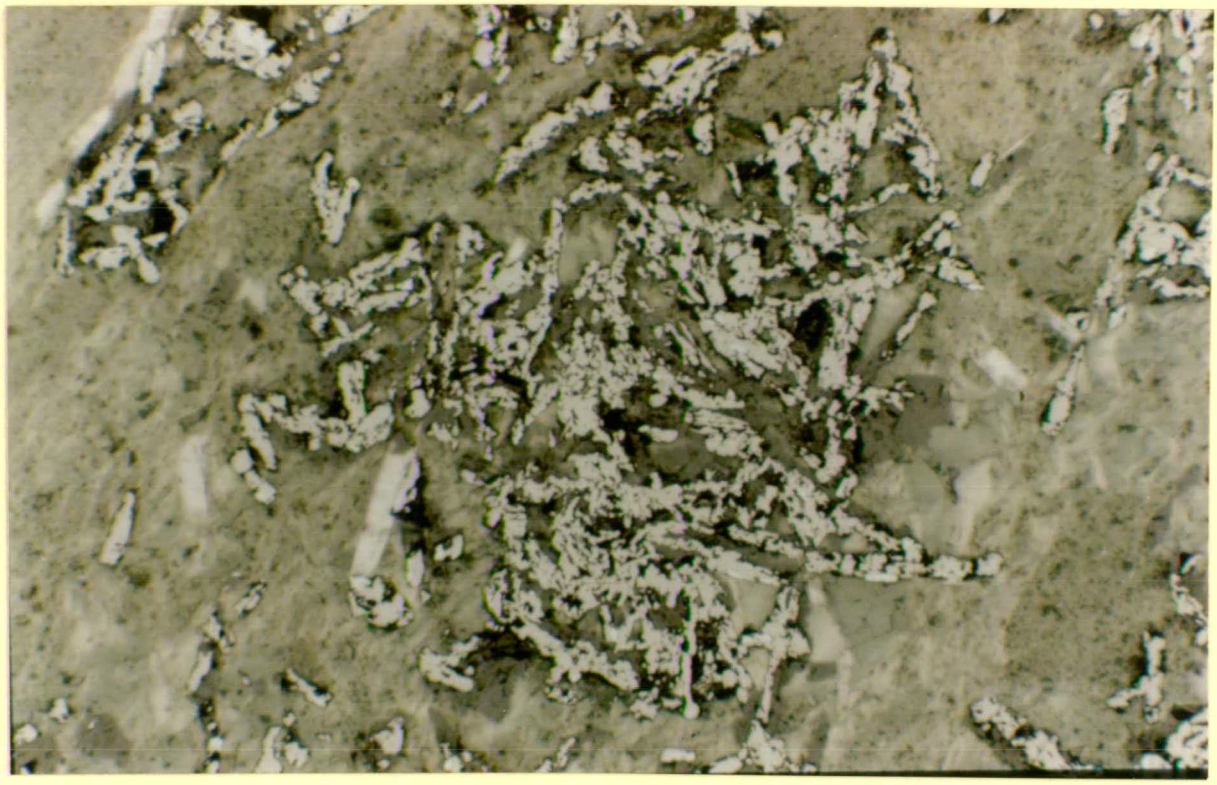

PLATE 29b

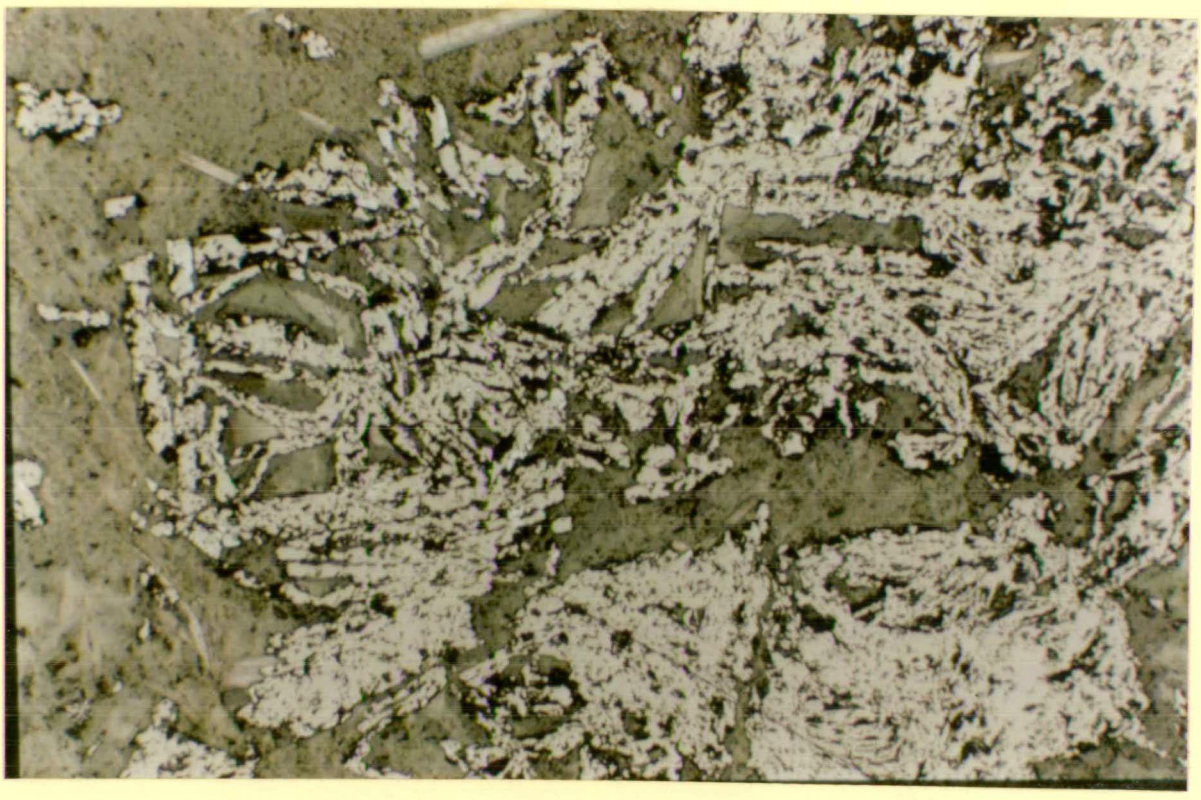

PLATE 29c

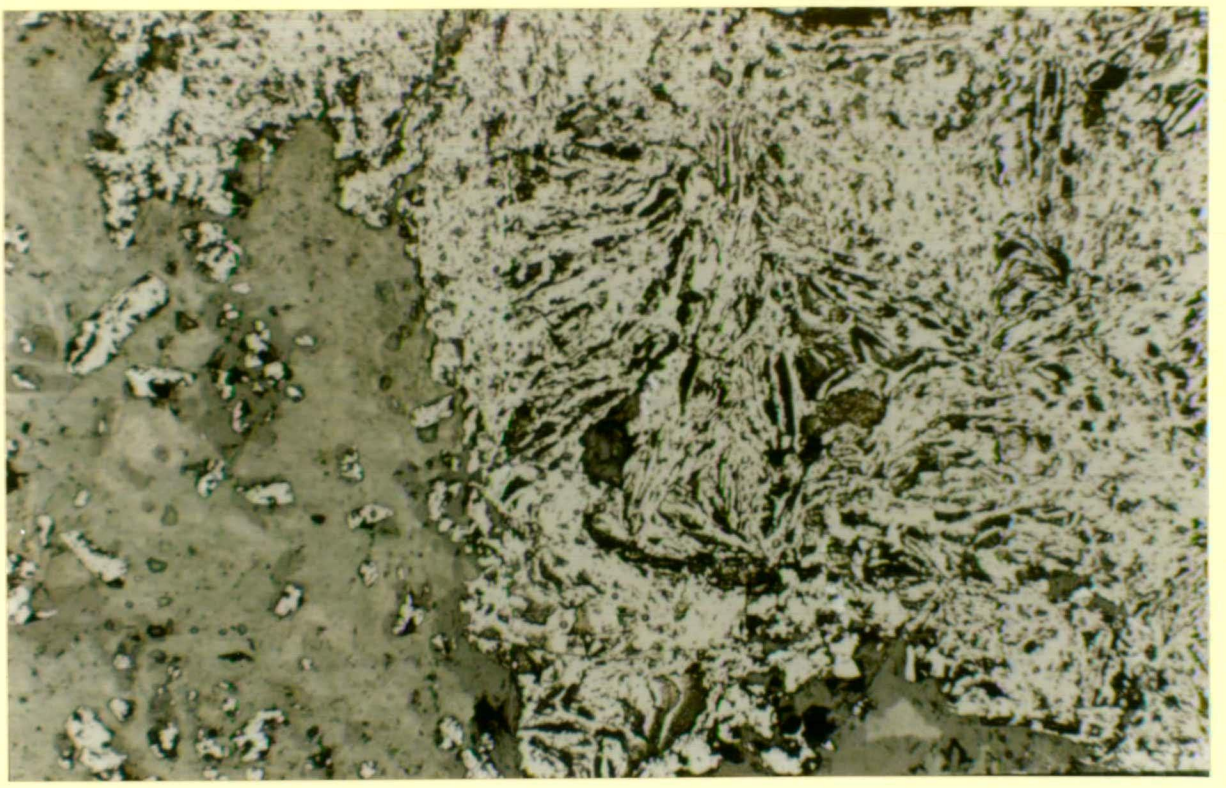

PLATE 29c

Skeletal/spongy ironstone with similar textures to the larger ironstones. The ironstone retains a very high porosity. The `density or massiveness' of the ironstone depends on the initial abundance and intergrowth of hematite. As can be seen in the photo, where the hematite grew as long individual laths the texture is very open but where the laths grew close together as a mass the texture has a more massive appearance.

Thin Section: M7508, WDUD 454, 56.8m, 5245E
FOV= 1.7mm

hematite laths in altered sediment. Later reduced, low sulphur fluids percolated through the spongy network of laths replacing the hematite with magnetite and depositing primary magnetite as overgrowths and subhedral grains. The pyrite was deposited during this event.

The formation of the ironstone is demonstrated in thin section M7508 (5245E), from the Pinter Lode area, but outside the ore zone (Plate 29). Plate 29a shows tabular laths, now magnetite, occurring as single or loosely interlocked grains, within chloritic sediment. Plate 29b shows a more coherent skeletal mass of magnetite laths and 29c what would be classed as "massive" ironstone, where the spongy, skeletal nature is preserved. This ironstone formed within the chloritic sediments, within the shear zone and has similar textures to the large and tabular ironstones. The abundance of initial hematite determined the size of the magnetite ironstone.

During the alteration of hematite to magnetite, rapid precipitation of magnetite occurred as indicated by the dendritic and spheroidal growth textures. Also during this alteration subhedral to euhedral magnetite grains grew along the edges of the laths and within altered sediments.

The fractured magnetite stringers in the altered sediments show that the second deformation event was under way prior to or early in the magnetite alteration event. Evidence for this is the sudhedral `clean' magnetite overgrowths within the fractures.

The M10 zone at Juno contains similar textures to White Devil, with skeletal masses of magnetite laths within quartz. In thin section 900/78-1086 within a mass of magnetite laths, incompletely replaced primary hematite laths can be seen, indicating the nature of the fluids changed and the ironstone was sealed by quartz before replacement was complete.

7.2 MINERALISING STAGE

The mineralising stage involved co-precipitation of gold, bismuth sulphosalts and chalcopyrite within magnetite chlorite of the Deeps and Pinter Ironstones, West

Lode and amongst the altered sediment-magnetite stringers in the Main Zone, Pinter Lodes and West Lodes. The mineralising fluids percolated through the porous portions of the large ironstone and deposited the ore minerals within chlorite and the magnetite laths. In the stringer zones the ore minerals were deposited in and around the magnetite stringers in coarse grained chlorite.

The mineralising stage began at relatively low temperatures with the deposition of a Pinter Lode and green Mg chlorite, associated with the ore and throughout the Pinter ironstone. As the temperature of the hydrothermal system began to increase the Deeps orebody, and purple chlorite was deposited. The Pinter Lode and Deeps orebodies are very rich in gold and contain only minor bismuth sulphosalts and chalcopyrite. This stage corresponds to the beginning of the sulphide stage of the model proposed by Huston et al (in press).

As the temperature increased, further mineralisation was deposited and the chlorite became relatively Fe rich and predominantly purple in colour. When the temperature climaxed, following the deposition of the Lower West Lode and a Pinter Lode and associated Fe rich chlorite the system began to cool. The blue Fe rich chlorite observed in a quartz vein in altered sediments associated with the South Lower Main Zone, was deposited at the peak temperature.

Gold, bismuth sulphosalts and chalcopyrite occur intergrown and as single elements in the same area indicating conditions of precipitation varied or several phases of mineralisation are present with the products related to the composition and geochemistry of the hydrothermal fluid.

As the system cooled the early Mg chlorite was altered to talc and quartz flooded through the Pinter Ironstone, but not the Deeps, Western or Tabular ironstones. In the Pinter Ironstone the quartz replaced the green Mg chlorite.

During the waning stages of the mineralising phase, martitisation of magnetite occurred, often in association with quartz veïns.

The relationships observed between gold, bismuth, chalcopyrite, ironstones and chlorite are consistent with the model proposed by Huston et al (in press). The model

proposes that oxidised, magmatic-hydrothermal mineralising fluids, interacted with the more reduced magnetite bodies causing the precipitation of gold with lesser bismuth sulphosalts and copper. Significant copper mineralisation did not occur until the fluids reached pyrite saturation (point B, Figure 7). Only minor gold precipitated with the copper (path B-C, Figure 7). Approaching point C the fluids were only capable of forming pyrite and hematite at the expense of magnetite (martitisation).

8 EXPLORATION IMPLICATIONS

This study has highlighted several features of ironstones and mineralisation which may have important implications in the exploration for Tennant Creek style deposits.

A feature of the White devil ironstones is the open lathlike texture which has allowed mineralising fluids to percolated through the ironstone and deposit metals and chlorite. The non or weakly mineralised portions of the ironstones have a dense intergrowth of laths which has inhibited fluid movement.

Deformation of the magnetite stringers prepared the stringer zone for mineralisation by forming low pressure zones for the metals and chlorite to deposit. The stringers acted as rigid bodies during deformation and developed low pressure zones, which acted as fluid pathways during mineralisation. The gold-bismuth-copper in the stringer orebodies occurs in coarse chlorite around the fractured magnetite stringers.

The presence of two phases of chlorite is considered indicative of mineralisation. The two phases indicates that hydrothermal fluids continued to flow through the ironstone and alteration zone. The colour of the chlorite is also important, as this indicates the temperature of the fluids. The presence of purple and blue chlorite indicates high temperature fluids and green lower temperature fluids. The size of the chlorite laths and growths indicates the conditions of formation of the chlorite. If the chlorite is fine grained and foliated, it has either replaced sediments of grown under the influence of deformation. If the chlorite is coarse grained it has grown in open spaces or in low strain zones. The ore at White Devil is associated with randomly orientated coarse grained chlorite around magnetite. The association of the coarse chlorite with magnetite is also important.

Gold mineralisation was not observed associated with strongly hematised ironstone, large volumes of quartz or talc, although gold has been reported in talc.

9 CONCLUSIONS AND SUMMARY

This study focussed on the textures within the ironstone and their relation to formation, the occurrence and relationships between the ore minerals and chlorite associated with them and throughout the deposit.

The study has shown that the ironstones and stringers consist of a skeletal or spongy mass of magnetite laths. The early hematite ironstone existed in entirety and was deformed prior to or early during magnetite alteration.

Gold, bismuth sulphosalts and chalcopyrite were deposited over a wide temperature range and the associated chlorite has a wide range of Fe/Fe+Mg values. The chlorite occurs in altered sediments, around magnetite stringers or between magnetite laths in the large ironstone. The coarse grained chlorite around the magnetite stringers and between the magnetite laths is intergrown with the mineralisation. The chlorite ranges in birefringence colour from green to purple and blue, which correlates with increasing Fe content and temperature.

The geothermometry showed that mineralisation occurred during the waxing of the hydrothermal event and talc and quartz alteration during the waning.

Several previous interpretations have been affected by this study, particularly the formation of the ironstone (Large 1975), the association of Mg chlorite with mineralisation (Large 1975, Wedekind et al 1989, Nguyen et al 1988 and Edwards et al 1990) and the role of structure in the preparation of the orebody site (Nguyen et al 1988, Edwards et al 1990).

This study has advanced the understanding of formation of the ironstones at White Devil, the different compositions of chlorite associated with mineralisation, the nature of the host to the mineralisation and the paragenesis of the deposit.

10 REFERENCES

Black, L.P., 1984, U-Pb zircon ages and a revised chronology for the Tennant Creek Inlier N.T. Australia. Aust. J. Earth Sci., v.31, p.123-131.

Bortnikov, N.S., Genkin A.D., Dobrovol'Skaya, M.G., Muravitskaya, G.N., Filimonova, A.A., 1991, The Nature of Chalcopyrite inclusions in sphalerite: Exsolution, Co precipitation or disease. Econ. Geol. v.86, p.1070.

Cathelineau, M., Nieva, D, 1985, A chlorite solid solution geothermometer The Los Azufres (Mexico) geothermal system. Contrib. Mineral. Petrol., 91:p 235-244

Deer, W.A., Howie, R.A., Zussman, J., 1989, An introduction to the Rock Forming Minerals, 16th Ed., Longman Scientific & Technical London, 528p.

Edwards G.C.,1987, Structural and Geochemical controls on alteration and mineralisation, Tennant Creek goldfield, Northern Territory, B.Sc. Hons Thesis (unPub) Monash Univ.

Edwards, G.C., Booth, S.A., Cozens, G.J., 1990: White Devil Gold Deposit. Tennant Creek, N.T. in Hughes (Ed) Geol. of the Mineral Deposits of Australia and Papua New Guinea, p.849-856. Aus I.M.M.,.

Henriquez, F. and Martin, R.F., 1978, Crystal Growth Textures in Magnetite flows and Feeder dykes, EL Laco Chile. Can Mineral Vol.16, p. 581-89.

Hey, M.H., 1954, A Review of Chlorites. Mineral Mag. v.30. p.277-292.

Huston, D., 1990 a., Paragenetic and fluid inclusion studies of the White Devil deposit and selected barren ironstones. Univ.Tas., CODES., Prot. Au-Cu Project Workshop Man.4.

Huston, D., 1990 b, Paragenetic & fluid inclusion studies of the Gecko K - 44 Deposit. Univ Tas. Prot. Au-Cu Project, Workshop Manual 4. p.127.

Huston, D., 1991, The timing of porphyry intrusion at White Devil: Petrological & geochemical evidence. Univ. Tas. Prot Au-Cu Project, Workshop Manual No.5, 1991.

Huston, D., Bolger, C., Cozens, G., Large R.R., 1992 (in press), A comparison of mineralisation at the Gecko K44 and White Devil deposits - implications of one genesis is the Tennant Creek district, N.T., Aust.

Huston D and Cozens G.J., (in press) The timing of porphyry intrusion at White Devil: petrological and geochemical evidence.

Hy, C., 1988, White Devil Mine, A structural interpretation. Poseidon Gold Company Report.

Kranidiotis, P and Maclean, W.H., 1987, Systematics of chlorite alteration at the Phelps Dodge Massive Sulfide Deposit, Matagami, Quebec. Econ Geol.,Vol 82: p 1898-1911.

Large, R.R., 1975, Zonation of hydrothermal minerals at the Juno Mine, Tennant Creek Goldfield. Econ.Geol. 70, p.1387-1413.

Le Messurier, P., Williams, B.T., Blake, D.H., 1990, Tennant Creek Inlier - Regional Geology and Mineralisation. in Hughes (Ed) Geol. of the Mineral Deposits of Australia and Papua New Guinea, p.829-838. Aus I.M.M.,.

McPhie, J., 1990, A Syn-sedimentary Rhyolitic sill with peperite margins: The Tennant Creek Porphyry, Early Proterozoic, N.T. Univ. Tas. CODES. Prot. Au-Cu Project Workshop Manual 4.

Nguyen, P.T., Booth, S.A., Both, R.A., James, P.R., 1989, The White Devil Gold Deposit, Tennant Creek, N.T.
in The Geology of Gold Deposits: The Perspective in 1988. Econ Geol Mon 6. p180-192.

Nyström, J.O. and Henriquez, F. , 1989, Dendritic Magnetite and miniature diapers - like concentrations of apatite: two magmatic features of the Kiirunavaara iron ore. Geologiska Foreningers; Stockholm Forhandlingar Vol.111., pt.1, p.53-64.

Rattenbury, M., 1990, The Mary Lane Shear and a Fold Thrust model for the deformation of the Tennant Creek Goldfield, N.T. Univ. Tas. CODES. Prot. Au-Cu Project. Workshop Manual No.4, p.93-109.

Ramdohr, P., 1980, The Ore Minerals and their intergrowths. 2nd Edition. Pergamon Press.

Wall, V.J. and Valenta, R.K., 1990, Ironstone related gold-copper mineralisation: Tennant Creek and elsewhere. In Pacific Rim 90 Congress Volume. P855-864.

Wedekind, M.R., Love, R.J., 1990, The Warrego Gold-Copper, Bismuth Mine, Tennant Creek, N.T. in Hughes (Ed) Geol. of the Mineral Deposits of Australia and Papua New Guinea, p.829-838. Aus I.M.M.

Wedekind, M.R., Large, R.R., Williams, B.T., 1989. Controls on high grade gold mineralisation at Tennant Creek, N.T. Australia, in The Geology of Gold Deposits: The Perspective in 1988. Econ Geol Mon 6. p168-179.

Williams, B.T., 1987, Exploration of the Tennant Creek Mineral Field, N.T. in Geology and Geochemistry of Au-Cu iron oxide systems. Tennant Creek & Starra Districts. Univ. Tas. CODES. Prot Au-Cu Project. Workshop Manual 1.

APPENDIX 1

CHLORITE MICROPROBE ANALYSES AND DESCRIPTIONS

WHITE DEVIL CHLORITE ANALYSES

SAMPNO	:M7561 R1a	M7561 R1b	M7561 R2a	M7561 R2b	M7564 R1a	M7564 R2a	M7533 R1a	M7563 R1a	M7563 R2a	M7557 R1a
EASTING	: 5235	5235	5235	5235	5235	5235	4995	5235	5235	5265
HOLE NO	: WDUD487	WDUD487	WDUD487	WDUD487	WDUD487	WDUD487	WDUD327	WDUD487	WDUD487	WDUD479
DEPTH	: 6.4m	6.4m	6.4m	6.4m	32.4m	32.4m	65.0m	32.1m	32.1m	52.6m
COLOUR	: GRN/BRN	GRN/BRN	GRN/BRN	GRN/BRN	GRN/BRN	GRN/BRN	PURPLE	GREEN	GREEN	GREEN
CRS/FINE	: COARSE	COARSE	COARSE	COARSE	COARSE	COARSE	COARSE	COARSE	COARSE	COARSE
SiO2	: 27.90	27.72	29.21	29.36	25.68	25.57	25.13	25.44	25.56	26.64
TiO2	: 0.06	0.05	0.00	0.03	0.02	0.00	0.00	0.02	0.00	0.06
Al2O3	: 19.14	18.31	18.39	18.56	20.95	20.63	19.00	20.75	20.45	20.62
Cr2O3	: 0.03	0.05	0.01	0.00	0.00	0.01	0.03	0.00	0.00	0.02
MgO	: 21.35	21.52	22.49	20.74	17.38	16.76	13.47	16.86	17.11	18.22
CaO	: 0.05	0.02	0.00	0.02	0.04	0.03	0.00	0.04	0.00	0.00
MnO	: 0.09	0.09	0.06	0.11	0.11	0.11	0.11	0.12	0.09	0.08
FeO	: 19.51	18.65	18.48	19.20	24.13	24.16	30.24	24.86	23.71	22.54
H2O	: 11.82	11.63	11.99	11.88	11.53	11.39	11.08	11.45	11.37	11.64
TOTAL	: 99.95	98.03	100.63	99.89	99.84	98.66	99.07	99.53	98.30	99.82
CATIONS										
Si	: 5.66	5.72	5.84	5.93	5.34	5.39	5.44	5.33	5.39	5.49
Ti	: 0.01	0.01	0.00	0.00	0.00	0.00	0.00	0.00	0.00	0.01
Al	: 4.58	4.45	4.34	4.42	5.13	5.12	4.85	5.12	5.09	5.01
Cr	: 0.00	0.01	0.00	0.00	0.00	0.00	0.01	0.00	0.00	0.00
Mg	: 6.45	6.62	6.71	6.24	5.39	5.26	4.35	5.27	5.38	5.59
Ca	: 0.01	0.00	0.00	0.00	0.01	0.01	0.00	0.01	0.00	0.00
Mn	: 0.02	0.02	0.01	0.02	0.02	0.02	0.02	0.02	0.02	0.01
Fe	: 3.31	3.22	3.09	3.24	4.20	4.26	5.47	4.36	4.18	3.88
TOTAL	: 20.04	20.04	19.99	19.86	20.09	20.05	20.13	20.11	20.06	20.00
(Fe+Mn)/ (Fe+Mn+Mg)	: 34.00	32.82	31.63	34.31	43.90	44.82	55.83	45.39	43.83	41.07
Al(IV)	: 2.34	2.28	2.16	2.07	2.66	2.62	2.56	2.67	2.61	2.51
T	: 266.03	259.81	246.57	237.55	299.83	295.19	289.37	301.10	294.24	284.28

WHITE DEVIL CHLORITE ANALYSES

SAMPNO	M7557 R1b	M7557 R2a	M7557 R2b	M7557 R3a	M7557 R3b	M7504 R1a	M7504 R1b	M7504 R2a	M7504 R2b	M7503 R1a
EASTING	5265	5265	5265	5265	5265	5265	5265	5265	5265	5255
HOLE NO	WDUD479	WDUD479	WDUD479	WDUD479	WDUD479	WDUD478	WDUD478	WDUD478	WDUD478	WDUD473
DEPTH	52.6m	52.6m	52.6m	52.6m	52.5m	62.7m	62.7m	62.7m	62.7m	72.4m
COLOUR	PURPLE	GREEN	PURPLE	GREEN	PURPLE	GREEN	GREEN	GREEN	GREEN	PURPLE
CRS/FINE	FINE	COARSE	FINE	COARSE	FINE	COARSE	COARSE	FINE	FINE	FINE
SiO2	25.60	25.22	25.44	25.26	26.44	28.04	28.19	27.35	27.60	23.43
TiO2	0.06	0.05	0.04	0.13	0.03	0.04	0.11	0.03	0.05	0.05
Al2O3	19.98	20.47	20.06	21.66	20.43	18.21	17.95	18.47	18.18	21.73
Cr2O3	0.03	0.05	0.03	0.04	0.05	0.00	0.00	0.00	0.00	0.00
MgO	17.39	17.41	17.24	17.18	17.94	22.75	22.48	21.91	21.57	11.81
CaO	0.04	0.00	0.03	0.00	0.02	0.03	0.00	0.03	0.01	0.00
MnO	0.07	0.08	0.08	0.06	0.09	0.06	0.04	0.04	0.02	0.09
FeO	23.76	23.25	22.93	23.10	23.08	18.08	18.26	18.45	18.03	30.75
H2O	11.36	11.33	11.26	11.48	11.59	11.77	11.74	11.61	11.54	11.03
TOTAL	98.33	97.85	97.11	98.92	99.67	98.98	98.77	97.89	97.00	98.89
CATIONS										
Si	5.41	5.34	5.42	5.28	5.47	5.71	5.76	5.65	5.74	5.10
Ti	0.01	0.01	0.01	0.02	0.01	0.01	0.02	0.01	0.01	0.01
Al	4.97	5.11	5.04	5.33	4.98	4.37	4.32	4.50	4.45	5.57
Cr	0.01	0.01	0.01	0.01	0.01	0.00	0.00	0.00	0.00	0.00
Mg	5.47	5.49	5.47	5.35	5.54	6.91	6.84	6.75	6.69	3.83
Ca	0.01	0.00	0.01	0.00	0.01	0.01	0.00	0.01	0.00	0.00
Mn	0.01	0.01	0.01	0.01	0.02	0.01	0.01	0.01	0.00	0.02
Fe	4.20	4.12	4.09	4.04	4.00	3.08	3.12	3.19	3.14	5.59
TOTAL	20.09	20.09	20.05	20.03	20.02	20.10	20.07	20.10	20.03	20.11
(Fe+Mn)/ (Fe+Mn+Mg)	43.46	42.93	42.83	43.07	42.01	30.91	31.35	32.13	31.94	59.44
Al(IV)	2.59	2.66	2.58	2.72	2.53	2.29	2.24	2.35	2.26	2.90
T	292.37	299.96	291.44	306.68	285.76	260.44	255.75	267.14	257.77	325.88

WHITE DEVIL CHLORITE ANALYSES

SAMPNO	:M7503 R1b	M7503 R1c	M7503 R2a	M7521 R1a	M7521 R2a	M7521 R2b	M7521 R3a	M7538 R1a	M7538 R2a	M7517 R1a
EASTING	: 5255	5255	5255	5015	5015	5015	5015	5155	5155	5075
HOLE NO	: WDUD473	WDUD473	WDUD473	WDUD339	WDUD339	WDUD339	WDUD339	WDUD285	WDUD285	WDUD366
DEPTH	: 72.4m	72.4m	72.4m	102.25m	102.25m	102.25m	102.25m	36.1m	36.1m	28.0m
COLOUR	: PURPLE	PURPLE	PURPLE	PURPLE	PURPLE	PURPLE	PURPLE	PURPLE	PURPLE	BLUE
CRS/FINE	: FINE	COARSE	COARSE	COARSE	FINE	FINE	COARSE	FINE	FINE	COARSE
SiO2	: 23.80	23.23	24.57	23.26	24.38	24.56	23.53	26.05	26.92	23.51
TiO2	: 0.05	0.06	0.08	0.04	0.05	0.07	0.03	0.00	0.04	0.09
Al2O3	: 20.64	21.19	21.41	21.27	21.22	21.33	22.05	18.99	19.43	21.28
Cr2O3	: 0.02	0.02	0.02	0.02	0.00	0.00	0.00	0.01	0.01	0.01
MgO	: 12.21	12.47	12.53	11.02	11.72	11.58	11.20	17.09	17.54	8.35
CaO	: 0.04	0.01	0.00	0.02	0.03	0.01	0.09	0.02	0.01	0.01
MnO	: 0.12	0.08	0.09	0.09	0.06	0.11	0.09	0.14	0.13	0.10
FeO	: 29.77	26.67	30.00	32.37	31.89	31.97	31.79	25.22	24.85	36.17
H2O	: 10.91	10.92	11.24	10.95	11.19	11.23	11.10	11.34	11.59	10.93
TOTAL	: 97.55	97.65	100.14	99.02	100.53	100.86	99.89	98.86	100.54	100.43
CATIONS										
Si	: 5.23	5.10	5.25	5.10	5.23	5.25	5.09	5.51	5.57	5.16
Ti	: 0.01	0.01	0.01	0.01	0.01	0.01	0.01	0.00	0.01	0.02
Al	: 5.35	5.49	5.39	5.49	5.36	5.37	5.62	4.73	4.74	5.50
Cr	: 0.00	0.00	0.00	0.00	0.00	0.00	0.00	0.00	0.00	0.00
Mg	: 4.00	4.08	3.99	3.60	3.74	3.69	3.61	5.39	5.41	2.73
Ca	: 0.01	0.00	0.00	0.00	0.01	0.00	0.02	0.00	0.00	0.00
Mn	: 0.02	0.01	0.02	0.02	0.01	0.02	0.02	0.03	0.02	0.02
Fe	: 5.47	5.45	5.39	5.93	5.72	5.71	5.75	4.46	4.30	6.64
TOTAL	: 20.09	20.15	20.05	20.15	20.08	20.05	20.10	20.12	20.05	20.07
(Fe+Mn)/ (Fe+Mn+Mg):	57.87	57.23	57.56	62.30	60.48	60.84	61.49	45.43	44.42	70.91
Al(IV)	: 2.77	2.90	2.75	2.90	2.77	2.75	2.91	2.49	2.43	2.84
T	: 311.49	325.35	309.90	325.71	311.69	309.71	326.88	281.90	275.54	319.01

WHITE DEVIL CHLORITE ANALYSES

SAMPNO	:M7517 R2a	M7517 R2b	M7517 R2c	M7517 R3a	M7509 R1a	M7509 R2a	M7509 R2b	M7506 R1a	M7506 R1b	M7506 R1c
EASTING	: 5075	5075	5075	5075	5225	5225	5225	5265	5265	5265
HOLE NO	: WDUD366	WDUD366	WDUD366	WDUD366	WDD392	WDD392	WDD392	WDUD478	WDUD478	WDUD478
DEPTH	: 28.0m	28.0m	28.0m	28.0m	274m	274m	274m	71.5m	71.5m	71.5m
COLOUR	: BLUE	BLUE	BLUE	BLUE	PURPLE	GREEN	PURPLE	PURPLE	PURPLE	GREEN
CRS/FINE	: FINE	COARSE	COARSE	COARSE	FINE	COARSE	FINE	COARSE	COARSE	COARSE
SiO2	: 30.35	23.92	23.29	22.49	23.25	24.46	25.31	27.13	26.85	26.80
TiO2	: 0.06	0.05	0.03	0.00	0.03	0.04	0.04	0.06	0.04	0.09
Al2O3	: 20.03	21.77	21.51	20.97	20.29	22.26	21.09	20.73	20.75	30.35
Cr2O3	: 0.00	0.03	0.00	0.00	0.01	0.00	0.01	0.00	0.03	0.05
MgO	: 7.48	8.60	8.21	8.07	14.56	14.69	15.25	18.96	19.20	19.40
CaO	: 0.01	0.01	0.00	0.04	0.00	0.03	0.03	0.02	0.00	0.00
MnO	: 0.12	0.08	0.10	0.14	0.09	0.09	0.11	0.05	0.05	0.07
FeO	: 32.30	34.80	35.69	35.76	26.20	26.72	26.86	22.65	21.31	21.66
H2O	: 11.52	11.00	10.86	10.64	10.80	11.37	11.42	11.84	11.73	11.72
TOTAL	: 101.86	100.26	99.70	98.11	95.23	99.67	100.12	101.44	99.97	100.14
CATIONS										
Si	: 6.32	5.22	5.14	5.07	5.16	5.16	5.32	5.49	5.49	5.48
Ti	: 0.01	0.01	0.01	0.00	0.01	0.01	0.01	0.01	0.01	0.01
Al	: 4.92	5.59	5.60	5.57	5.31	5.54	5.22	4.95	5.00	4.91
Cr	: 0.00	0.00	0.00	0.00	0.00	0.00	0.00	0.00	0.00	0.01
Mg	: 2.32	2.79	2.70	2.71	4.82	4.62	4.78	5.72	5.85	5.92
Ca	: 0.00	0.00	0.00	0.01	0.00	0.01	0.01	0.00	0.00	0.00
Mn	: 0.02	0.02	0.02	0.03	0.02	0.02	0.02	0.01	0.01	0.01
Fe	: 5.62	6.34	6.59	6.75	4.86	4.72	4.72	3.84	3.64	3.71
TOTAL	: 19.21	19.98	20.05	20.14	20.18	20.06	20.07	20.02	20.00	20.04
(Fe+Mn)/ (Fe+Mn+Mg)	: 70.86	69.48	70.99	71.40	50.32	50.59	49.80	40.19	38.43	38.59
Al(IV)	: 1.68	2.78	2.86	2.93	2.84	2.84	2.68	2.51	2.51	2.52
T	: 196.19	313.10	320.94	328.29	318.75	318.94	302.57	283.66	284.19	284.79

WHITE DEVIL CHLORITE ANALYSES

SAMPNO	M7522 R1a	M7522 R2a	M7534 R1a	M7534 R1b	M7518 R1a	M7519 R1a	M7519 R1b	M7519 R2a	M7519 R2b	M7544 R1a
EASTING	5015	5015	4995	4995	5075	5075	5075	5075	5075	5155
HOLE NO	WDUD339	WDUD339	WDUD327	WDUD327	WDUD366	WDUD366	WDUD366	WDUD366	WDUD366	WDUD285
DEPTH	104.4m	104.4m	70.5m	70.5m	14.8m	20.9m	20.9m	20.9m	20.9m	56.6m
COLOUR	PURPLE	PURPLE	PURPLE	GREEN	BLUE	PURPLE	PURPLE	PURPLE	PURPLE	PURPLE
CRS/FINE	FINE	COARSE	FINE	COARSE	COARSE	FINE	COARSE	FINE	COARSE	FINE
SiO2	23.97	24.29	26.64	26.41	23.58	25.20	24.38	25.39	24.62	27.35
TiO2	0.06	0.07	0.12	0.04	0.02	0.06	0.00	0.05	0.09	0.06
Al2O3	20.71	20.45	19.36	19.55	21.78	21.35	20.53	21.06	21.76	20.33
Cr2O3	0.05	0.00	0.00	0.00	0.00	0.05	0.00	0.01	0.00	0.00
MgO	11.56	11.69	15.82	16.02	13.02	14.05	13.69	14.22	13.74	10.17
CaO	0.01	0.01	0.04	0.06	0.00	0.04	0.05	0.03	0.01	0.02
MnO	0.16	0.07	0.06	0.06	0.06	0.06	0.06	0.09	0.07	0.12
FeO	30.89	31.62	27.06	25.74	28.50	27.82	28.88	27.23	28.23	30.86
H2O	10.96	11.03	11.48	11.41	11.05	11.36	11.11	11.32	11.31	11.27
TOTAL	98.39	99.22	100.58	99.47	98.01	99.98	98.69	99.41	99.83	99.87
CATIONS										
Si	5.25	5.28	5.57	5.55	5.12	5.32	5.26	5.38	5.22	5.82
Ti	0.01	0.01	0.02	0.01	0.00	0.01	0.00	0.01	0.01	0.01
Al	5.34	5.24	4.77	4.84	5.57	5.31	5.22	5.26	5.44	5.10
Cr	0.01	0.00	0.00	0.00	0.00	0.01	0.00	0.00	0.00	0.00
Mg	3.77	3.79	4.93	5.08	4.21	4.42	4.41	4.49	4.35	3.22
Ca	0.00	0.00	0.01	0.01	0.00	0.01	0.01	0.01	0.00	0.00
Mn	0.03	0.01	0.01	0.01	0.01	0.01	0.01	0.02	0.01	0.02
Fe	5.65	5.75	4.73	4.52	5.17	4.91	5.21	4.82	5.01	5.44
TOTAL	20.07	20.09	20.03	20.02	20.09	20.01	20.13	19.98	20.04	19.62
(Fe+Mn)/ (Fe+Mn+Mg)	60.11	60.33	49.04	47.17	55.18	52.69	54.24	51.89	53.61	62.88
Al(IV)	2.75	2.72	2.43	2.45	2.88	2.68	2.74	2.62	2.78	2.18
T	309.81	306.09	275.95	277.66	323.33	301.87	308.19	295.82	312.53	249.06

WHITE DEVIL CHLORITE ANALYSES

SAMPNO	M7544 R1b	M7544 R1c	M7544 R2a	M7544 R2b	M7544 R2c	M7545 R1a	M7545 R2a	M7553 R1a	M7553 R1b	M7553 R2a
EASTING	5155	5155	5155	5155	5155	5155	5155	5135	5135	5135
HOLE NO	WDUD285	WDUD285	WDUD285	WDUD285	WDUD285	WDUD285	WDUD285	WDUD273	WDUD273	WDUD273
DEPTH	56.6m	56.6m	56.6m	56.6m	56.6m	66.0m	66.0m	52.2m	52.2m	52.2m
COLOUR	PURPLE	PURPLE	PURPLE	PURPLE	PURPLE	PURPLE	PURPLE	PURPLE	GREEN	PURPLE
CRS/FINE	FINE	COARSE	FINE	FINE	FINE	FINE	COARSE	FINE	COARSE	FINE
SiO2	23.78	23.99	23.98	32.42	23.99	35.51	23.82	26.81	26.42	26.57
TiO2	0.06	0.03	0.06	0.06	0.63	0.15	0.04	0.04	0.04	0.03
Al2O3	21.86	20.79	21.13	19.14	20.96	26.75	20.79	18.43	20.05	18.41
Cr2O3	0.00	0.01	0.04	0.03	0.01	0.05	0.06	0.00	0.01	0.03
MgO	10.77	11.29	10.53	9.48	10.86	6.30	10.84	18.69	18.80	18.84
CaO	0.01	0.00	0.03	0.00	0.01	0.01	0.00	0.03	0.01	0.01
MnO	0.05	0.09	0.10	0.14	0.08	0.03	0.10	0.09	0.02	0.06
FeO	32.30	32.69	32.13	29.34	31.85	17.88	32.69	23.94	22.44	22.20
H2O	11.08	11.06	10.98	11.79	11.04	12.25	10.98	11.50	11.58	11.35
TOTAL	99.90	99.96	98.97	102.40	99.43	98.93	99.32	99.54	99.37	97.51
CATIONS										
Si	5.15	5.21	5.24	6.60	5.21	6.95	5.21	5.59	5.47	5.62
Ti	0.01	0.01	0.01	0.01	0.01	0.02	0.01	0.01	0.01	0.01
Al	5.57	5.32	5.44	4.59	5.37	6.18	5.36	4.53	4.89	4.59
Cr	0.00	0.00	0.01	0.00	0.00	0.01	0.01	0.00	0.00	0.00
Mg	3.47	3.65	3.43	2.87	3.52	1.84	3.53	5.81	5.80	5.94
Ca	0.00	0.00	0.01	0.00	0.00	0.00	0.00	0.01	0.00	0.00
Mn	0.01	0.02	0.02	0.02	0.01	0.01	0.02	0.02	0.00	0.01
Fe	5.85	5.93	5.87	4.99	5.79	2.93	5.97	4.17	3.89	3.92
TOTAL	20.06	20.13	20.03	19.10	20.00	17.93	20.10	20.14	20.07	20.08
(Fe+Mn)/ (Fe+Mn+Mg):	62.77	61.96	63.20	63.58	62.27	61.47	62.93	41.90	40.14	39.87
Al(IV)	2.85	2.79	2.76	1.40	2.79	1.05	2.79	2.41	2.53	2.38
T	320.57	314.21	310.60	166.65	313.50	128.96	314.07	273.30	285.86	270.77

WHITE DEVIL CHLORITE ANALYSES

SAMPNO	:M7553 R2b	M7513 R1a	M7513 R1b	M7559 R1a	M7559 R1b	M7559 R2a	M7558 R1a	M7558 R2a	M7558 R2b	M7552 R1a
EASTING :	5135	5095	5095	5235	5235	5235	5235	5235	5235	5135
HOLE NO :	WDUD273	WDUD359	WDUD359	WDUD487	WDUD487	WDUD487	WDUD487	WDUD487	WDUD487	WDUD273
DEPTH :	52.2m	4.4m	4.4m	8.0m	8.0m	8.0m	8.0m	8.0m	8.0m	51.1m
COLOUR :	GREEN	GREEN	TALC	TALC			TALC		TALC	PURPLE
CRS/FINE :	COARSE	COARSE			COARSE	COARSE		COARSE		COARSE
SiO2 :	26.58	27.32	60.27	60.79	27.77	27.50	58.40	27.30	59.81	27.14
TiO2 :	0.10	0.04	0.00	0.01	0.00	0.00	0.00	0.00	0.01	0.00
Al2O3 :	18.49	18.56	0.18	0.22	18.19	18.45	0.26	18.99	0.15	18.72
Cr2O3 :	0.00	0.03	0.00	0.03	0.09	0.04	0.04	0.00	0.07	0.03
MgO :	19.42	20.04	26.20	26.68	21.89	21.88	26.04	20.62	26.43	16.80
CaO :	0.00	0.02	0.03	0.00	0.00	0.00	0.06	0.02	0.03	0.06
MnO :	0.01	0.15	0.02	0.01	0.11	0.06	0.00	0.09	0.00	0.08
FeO :	22.06	21.11	7.51	6.92	18.49	19.21	6.98	20.78	7.46	25.58
H2O :	11.43	11.58	14.24	14.36	11.65	11.68	13.88	11.68	14.19	11.48
TOTAL :	98.08	98.86	108.44	109.01	98.19	98.83	105.66	99.48	108.15	99.89
CATIONS										
Si :	5.58	5.66	10.15	10.16	5.72	5.65	10.09	5.60	10.02	5.67
Ti :	0.02	0.01	0.00	0.00	0.00	0.00	0.00	0.00	0.00	0.00
Al :	4.57	4.53	0.04	0.04	4.41	4.46	0.05	4.60	0.03	4.61
Cr :	0.00	0.00	0.00	0.00	0.01	0.01	0.01	0.00	0.01	0.00
Mg :	6.08	6.18	6.58	6.65	6.72	6.69	6.71	6.61	6.66	5.23
Ca :	0.00	0.01	0.01	0.00	0.00	0.00	0.01	0.00	0.01	0.01
Mn :	0.00	0.03	0.00	0.00	0.02	0.01	0.00	0.02	0.00	0.01
Fe :	3.87	3.66	1.06	0.97	3.18	3.30	1.01	3.57	1.05	4.47
TOTAL :	20.12	20.07	17.83	17.82	20.07	20.12	17.88	20.10	17.87	20.02
(Fe+Mn)/ : (Fe+Mn+Mg):	38.94	37.31	13.88	12.71	32.28	33.08	13.07	36.22	13.67	46.14
Al(IV) :	2.42	2.34			2.28	2.36		2.40		2.33
T :	274.62	266.26			259.94	267.63		271.92		264.81

WHITE DEVIL CHLORITE ANALYSES

SAMPNO	:M7552 R1b	M7552 R1c	M7552 R1d	M7552 R2a	M7552 R2b	M7552 R3a	M7552 R4a	M7524 R1a	M7524 R1b	M7524 R2a
EASTING	: 5135	5135	5135	5135	5135	5135	5135	4995	4995	4995
HOLE NO	: WDUD273	WDUD273	WDUD273	WDUD273	WDUD273	WDUD273	WDUD273	WDUD330	WDUD330	WDUD330
DEPTH	: 51.1m	51.1m	51.1m	51.1m	51.1m	51.1m	51.1m	52.4m	52.4m	52.4m
COLOUR	: PURPLE	TALC	GREEN	PURPLE	GREEN	TALC	GREEN			TALC
CRS/FINE	: COARSE		COARSE	FINE	FINE		COARSE	COARSE	COARSE	
SiO2	: 26.59	59.96	26.95	26.29	31.63	57.45	28.87	28.57	28.42	61.08
TiO2	: 0.03	0.03	0.00	0.01	0.03	0.02	0.09	0.00	0.00	0.00
Al2O3	: 19.00	0.35	18.51	18.70	14.83	0.14	16.99	19.17	19.68	0.43
Cr2O3	: 0.00	0.00	0.00	0.00	0.00	0.00	0.01	0.04	0.00	0.01
MgO	: 17.00	24.27	17.32	16.43	17.47	23.44	17.26	23.32	22.76	26.67
CaO	: 0.04	0.03	0.03	0.01	0.05	0.03	0.05	0.00	0.04	0.00
MnO	: 0.05	0.00	0.00	0.01	0.03	0.02	0.05	0.22	0.19	0.00
FeO	: 25.40	10.28	25.07	25.99	22.56	10.20	24.95	16.59	16.18	6.27
H2O	: 11.43	14.17	11.43	11.30	11.52	13.59	11.53	11.98	11.93	14.39
TOTAL	: 99.54	109.08	99.31	98.75	98.12	104.89	99.80	99.90	99.21	108.84
CATIONS										
Si	: 5.58	10.15	5.65	5.58	6.58	10.14	6.00	5.72	5.71	10.18
Ti	: 0.00	0.00	0.00	0.00	0.00	0.00	0.01	0.00	0.00	0.00
Al	: 4.70	0.07	4.58	4.68	3.64	0.03	4.16	4.52	4.66	0.09
Cr	: 0.00	0.00	0.00	0.00	0.00	0.00	0.00	0.01	0.00	0.00
Mg	: 5.32	6.12	5.42	5.20	5.42	6.16	5.35	6.96	6.82	6.63
Ca	: 0.01	0.00	0.01	0.00	0.01	0.01	0.01	0.00	0.01	0.00
Mn	: 0.01	0.00	0.00	0.00	0.00	0.00	0.01	0.04	0.03	0.00
Fe	: 4.46	1.46	4.40	4.61	3.93	1.51	4.34	2.78	2.72	0.87
TOTAL	: 20.07	17.81	20.06	20.08	19.59	17.85	19.90	20.02	19.96	17.77
(Fe+Mn)/ (Fe+Mn+Mg)	: 45.65	19.21	44.81	47.04	42.04	19.65	44.82	28.80	28.77	11.66
Al(IV)	: 2.42		2.35	2.42	1.42		2.00	2.28	2.29	
T	: 274.84		266.60	274.52	168.03		229.49	259.97	260.46	

WHITE DEVIL CHLORITE ANALYSES

BIOTITE

	M7518	M7524 R1a	M7524 R1c	M7545 R1	M7545 R2
SiO2	35.35	40.18	40.48	35.46	31.74
TiO2	0.22	0.48	0.44	0.14	0.10
Al2O3	28.82	13.77	14.02	26.68	22.06
CR2O3	0.01	0.00	0.00		
MgO	6.56	19.75	18.83	6.43	9.46
CaO	0.01	0.07	0.00	0.03	0.04
MnO	0.05	0.03	0.10	0.18	0.11
FeO	15.42	13.81	14.00	17.88	27.06
Na2O				0.12	0.05
K2O				4.98	1.21
H2O	12.40	12.55	12.53	3.86	3.77
F				0.28	0.11
Cl				0.00	0.03
TOTAL	98.84	100.64	100.41	96.05	95.74
O=F				-0.12	-0.04
O=Cl				0.00	-0.01
TOTAL	98.84	100.64	100.41	95.93	95.68
CATIONS					
Si	6.84	7.68	7.75	5.33	4.98
Ti	0.03	0.07	0.06	0.02	0.01
Al	6.57	3.10	3.16	4.73	4.08
CR	0.00	0.00	0.00		
Mg	1.89	5.63	5.37	1.44	2.21
Ca	0.00	0.01	0.00	0.01	0.01
Mn	0.01	0.00	0.02	0.02	0.01
Fe	2.49	2.21	2.24	2.25	3.55
Na				0.04	0.01
K				0.96	0.24
TOTAL	17.84	18.70	18.61	14.78	15.10
Fe/Mg	56.94	28.23	29.60	61.69	61.70

DESCRIPTION OF MICROPROBE SAMPLES

M7561, 5235E. Chlorite in magnetite quartz Pinter ironstone
R1a: Coarse grained green/brown chlorite in quartz
R1b: Finer grained chlorite in quartz
R2a: Coarse grained green/brown chlorite in quartz
R2b: Coarse grained green/brown chlorite in quartz

M7564, 5235E. Chlorite in magnetite quartz Pinter ironstone
R1a: Coarse grained green/brown chlorite in quartz
R2a: Coarse grained green/brown chlorite in quartz

M7563, 5235E. Magnetite-minor chlorite Pinter ironstone
R1a: Coarse grained green chlorite amongst magnetite
R2a: Coarse grained green chlorite amongst magnetite

M7533, 4995E. Magnetite-minor chlorite ironstone
R1a: Coarse grained purple chlorite

M7557, 5265E. Magnetite-chlorite rock, Pinter ore
R1a: Apple green coarse grained chlorite
R1b: Foliated fine grained purple chlorite
R2a: Apple green coarse grained chlorite adjacent to magnetite
R2b: Foliated fine grained purple chlorite
R3a: Coarse grained green chlorite adjacent to magnetite
R3b: Foliated fine grained purple chlorite

M7504, 5265E. Pinter Lode stringer ore
R1a: Coarse grained green chlorite amongst magnetite
R1b: Coarse grained green chlorite amongst magnetite
R2a: Fine grained foliated green chlorite in altered sediment
R2b: Fine grained foliated green chlorite in altered sediment

M7503, 5255E. Pinter Lode stringer ore
R1a: Fine grained foliated green chlorite in altered sediment
R1b: Fine grained foliated green chlorite in altered sediment
R1c: Coarse grained purple chlorite amongst magnetite laths
R2a: Coarse grained purple chlorite amongst magnetite laths

M7521, 5015E. Magnetite-chlorite-bismuth rock, Lower West Lode ore
R1a: Coarse grained purple chlorite amongst quartz and bismuthinite. Chlorite contains bismuthinite
R2a: Fine grained purple chlorite near quartz and hematite grains
R2b: Fine grained purple chlorite near quartz and hematite grains
R3a: Coarse grained purple chlorite associated with magnetite

M7538, 5155E. Magnetite-chlorite-altered sediment- bismuth rock, Deeps ore
R1a: Fine grained foliated purple chlorite in altered sediment
R2a: Fine grained foliated purple chlorite in altered sediment

M7509, 5255E. Altered sediment-magnetite stringer-pyrite rock
R1a: Fine grained foliated purple chlorite and small magnetite grains in altered sediment
R2a; Coarse grained chlorite amongst magnetite grains and laths
R2b: Fine grained foliated purple groundmass chlorite

M7506, 5265E. Altered sediments-minor magnetite and pyrite, outside ore zone
R1a: coarse grained purple chlorite in fracture
R1b: coarse grained green chlorite
R1c: coarse grained green chlorite

M7522, 5015E. Magnetite-altered sediment rock
R1a: Fine grained foliated purple chlorite in altered sediment
R2a: Coarse grained purple chlorite with magnetite

M7534, 4995E. Magnetite-altered sediment-chalcopyrite rock
R1a: Fine grained foliated purple chlorite in altered sediment
R1b: Coarse grained green chlorite in vein in altered sediment

M7517, 5075E. Chloritic sediments + quartz-chlorite vein
R1a: Blue chlorite in vein
R2a: Fine grained foliated groundmass chlorite
R2b: Blue chlorite in vein
R2c: Blue chlorite in vein, crosscutting R2b vein
R3a: Blue chlorite in vein with minor pyrite

M7518, 5075E. Chloritic sediments + small chlorite vein
R1a: Blue coarse grained chlorite vein in fine grained chloritic sediments

M7519, 5075E. Altered sediments
R1a: Fine grained foliated purple groundmass chlorite
R1b: Coarse grained purple chlorite between sediment clasts
R2a: Fine grained foliated purple groundmass chlorite
R2b: Coarse grained purple chlorite between sediment clasts

M7544, 5155E, Altered sediment + quartz chlorite vein
R1a: Fine grained purple chlorite in altered sediment
R1b: Fine grained purple chlorite on vein contact
R1c: Coarse grained purple chlorite in vein
R2a: Fine grained purple chlorite in altered sediment
R2b: Fine grained purple chlorite in altered sediment closer to vein
R2c: Fine grained purple chlorite in altered sediment next to vein

M7545, 5155. Chloritic sediments on edge of shear
R1a: Groundmass chlorite
R2a: Coarse grained purple chlorite in vein

M7553, 5135E. Altered sediment + pyrite
R1a: Fine grained purple chlorite adjacent to pyrite
R1b: Coarse green chlorite adjacent to fine purple chlorite
R2a: Fine grained purple chlorite
R2b: Coarse green chlorite

M7513, 5095E: Remnant green chlorite in talc
R1a: Coarse grained green chlorite
R1b: Talc with chalcopyrite and magnetite

M7559, 5235E. Magnetite-quartz Pinter ironstone with minor chlorite altered to talc
R1a: Coarse grained talc
R1b: Coarse grained chlorite
R2a: Coarse grained chlorite

M7558, 5235E. Magnetite-talc Pinter ironstone
R1a: Talc
R2a: Remnant coarse chlorite grain
R2b: Talc

M7552, 5135E. Magnetite-talc-minor chlorite rock
Traverse across chlorite-talc contact
R1a: Purple chlorite well within grain
R1b: Purple chlorite close to grain edge
R1c: Talc near chlorite grain
R1d: Small chlorite grain in talc
R2a: Purple chlorite within talc
R2b: Purple chlorite within talc
R3a: Talc
R4a: Talc/chlorite near minor magnetite

M7524, 4995E. Talcose altered sediment
R1a: Coarse grained chlorite in altered sediment.
Biotite present in altered sediment
R1b: Coarse grained chlorite in altered sediment.
R2a: Talc in talc-quartz

BIOTITE ANALYSES

M7518, 5075E. Chloritic sediments with minor biotite

M7524, 4995E. Talcose altered sediment
R1a: Biotite in altered sediment
R1c: Biotite in altered sediment

M7545, 5155E. Chloritic sediments on edge of shear
R1: Biotite in chloritic sediment
R2: Biotite in chloritic sediment